AD NUMBER

ADB084462

NEW LIMITATION CHANGE

TO

Approved for public release, distribution unlimited

FROM

Distribution limited to U.S. Gov't. agencies only; Test and Evaluation; Jun 84. Other requests must be referred to Commanding Officer, Naval Research Lab., Washington, DC 20375.

AUTHORITY

NRL ltr, 9 Feb 2004

NRL Memorandum Report 5335

White-Water Wake Characteristics of Surface Vessels

R. D. PELTZER

Fluid Dynamics Branch
Marine Technology Division

June 5, 1984

NAVAL RESEARCH LABORATORY
Washington, D.C.

SECURITY CLASSIFICATION OF THIS PAGE

REPORT DOCUMENTATION PAGE

1a. REPORT SECURITY CLASSIFICATION UNCLASSIFIED	1b. RESTRICTIVE MARKINGS
2a. SECURITY CLASSIFICATION AUTHORITY	3. DISTRIBUTION/AVAILABILITY OF REPORT
2b. DECLASSIFICATION/DOWNGRADING SCHEDULE	(See page ii)
4. PERFORMING ORGANIZATION REPORT NUMBER(S) NRL Memorandum Report 5335	5. MONITORING ORGANIZATION REPORT NUMBER(S)
6a. NAME OF PERFORMING ORGANIZATION Naval Research Laboratory 6b. OFFICE SYMBOL (If applicable) Code 5841	7a. NAME OF MONITORING ORGANIZATION
6c. ADDRESS (City, State and ZIP Code) Washington, DC 20375	7b. ADDRESS (City, State and ZIP Code)
8a. NAME OF FUNDING/SPONSORING ORGANIZATION Office of Naval Research 8b. OFFICE SYMBOL (If applicable)	9. PROCUREMENT INSTRUMENT IDENTIFICATION NUMBER
8c. ADDRESS (City, State and ZIP Code) Arlington, VA 22217	10. SOURCE OF FUNDING NOS. PROGRAM ELEMENT NO.: 61153N PROJECT NO.: RR023-01-41 TASK NO: WORK UNIT NO.: EX280-250
11. TITLE (Include Security Classification) White-Water Wake Characteristics of Surface Vessels	
12. PERSONAL AUTHOR(S) Peltzer, R.D.	
13a. TYPE OF REPORT Interim 13b. TIME COVERED FROM TO	14. DATE OF REPORT (Yr., Mo., Day) June 5, 1984 15. PAGE COUNT 108
16. SUPPLEMENTARY NOTATION	
17. COSATI CODES FIELD / GROUP / SUB GR.	18. SUBJECT TERMS (Continue on reverse if necessary and identify by block number) Ship wakes; Ship hydrodynamics White-water; Marine hydrodynamics

19. ABSTRACT (Continue on reverse if necessary and identify by block number)

The visible white-water wake generated by a vessel underway is a streak of foamy, aerated turbulent water. Aerial photographs showing the white-water wakes generated by vessels underway were examined in order to study the wake characteristics of these surface vessels. Both visual and dimensional analyses of the data contained within the photographs were performed.

The major variables that influence the production, geometry, persistence and visibility of the foamy white-water in the wake generated by surface vessels moving through a body of water were identified and discussed. In a majority of the nondimensional plots involving these variables, the data appeared to collapse onto curves unique to each vessel class, with the propeller tip to surface clearance of each vessel class determining the relative location of these curves on the plots. Vessels with minimal tip to surface clearance had longer, stronger and wider white-water wakes than those with significantly deeper propellers.

(Continues)

20. DISTRIBUTION/AVAILABILITY OF ABSTRACT UNCLASSIFIED/UNLIMITED ☐ SAME AS RPT ☒ DTIC USERS ☐	21. ABSTRACT SECURITY CLASSIFICATION UNCLASSIFIED
22a. NAME OF RESPONSIBLE INDIVIDUAL R. D. Peltzer	22b. TELEPHONE NUMBER (Include Area Code) (202) 767-1021 22c. OFFICE SYMBOL Code 5841

DD FORM 1473, 83 APR EDITION OF 1 JAN 73 IS OBSOLETE

SECURITY CLASSIFICATION OF THIS PAGE

3. DISTRIBUTION/AVAILABILITY OF REPORT

Distribution limited to U.S. Government agencies only; test and evaluation; June 1984. Other requests for this document must be referred to the Commanding Officer, Naval Research Laboratory, Washington, DC 20375.

19. ABSTRACT (Continued)

The white-water wake length data appeared to collapse, within an order of magnitude, onto four different curves. The best of these curves revealed that the maximum length of the visible white-water wake was proportional to a ratio of the vessel's speed raised to a power divided by the vessel's propeller revolutions per second raised to a different power. The equation was $L_{ww} = 13.7\ V_s^{1.68}/n^{0.32}$. The data scattered no more than a factor of three below the curve.

The width of the turbulent boundary layer and bow wave portions of the overall wake and the length of the initial spreading region and far wake region of the propeller wake all increase as the speed of the vessel increases. The wake geometry and characteristics of a single class of vessels may exhibit some type of similarity.

CONTENTS

NOMENCLATURE

a	wave amplitude
ak	wave steepness parameter
B_{wl}	vessel's waterline beam
C_f	frictional resistance coefficient
C_r	residuary resistance coefficient
C_T	total resistance coefficient
D_T	depth of propeller tips below the surface
D_p	propeller diameter
D_{wl}	vessel's waterline draft
EHP	vessel's effective horsepower
F_r	Froude number
g	gravitational acceleration
k	$(2\pi/L)$ wave number
L	wavelength
L_{HL}	horizontal aft location in the wake
L_{OA}	vessel's overall length
L_{wl}	vessel's waterline length
L_{ww}	white-water wake length
n	propeller revolutions per second
Re	Reynolds number
R_f	frictional resistance
R_r	residuary resistance
R_t	total resistance
rps	propeller revolutions per second
S	vessel's watted surface area
SHP	vessel's shaft horsepower

V_s	vessel's velocity
W	width of the white-water wake
∇	vessel's displacement
ΔC_f	roughness allowance
ρ	mass density of seawater
η_p	propulsive efficiency
μ	absolute viscosity of seawater
ν	kinematic viscosity of seawater

WHITE-WATER WAKE CHARACTERISTICS OF SURFACE VESSELS

INTRODUCTION

The visible white-water wake generated by a vessel underway is a streak of foamy, aerated turbulent water. The purpose of this report is to study the white-water wake characteristics of vessels by examining aerial photographs of vessels underway (mainly World War II Navy Ships). Both visual and dimensional analyses of the available data (white-water wake characteristics, ship parameters) are performed.

Most of the major research on the structure and physical constitution of white-water wakes was performed during World War II, and the results were presented in a National Defense Research Committee Report entitled "Part IV-Acoustic Properties of Wakes"[6]. Aside from a few more recent and relevant reports on the subject of acoustic wakes, the 1946 NDRC report remains the most comprehensive, authoritative study on ship wakes. Rather than summarizing the major points of interest contained in the NDRC study at this point in the paper, they will be presented in the paper when they are applicable to the ongoing discussion.

BACKGROUND

A. Variables Effecting White-Water Generation, Spread, Persistence and Visibility

There are numerous variables (1a) affecting the generation, spread, persistence and visibility of the white-water wake behind a vessel moving through the water. They can be grouped such that they fall into three gross categories:

1) Method of Detection and/or Observation;

2) Sea and Weather Conditions;

3) Vessel and Vessel Class Characteristics.

The variables contained within these categories will be listed and discussed presently.

There are many methods that are currently employed to study, observe and/or detect the presence of the white-water wake generated by a vessel moving through the water. Some of these methods are visual (eye), photographic (camera), radar (microwave, synthetic aperature) and infared radiometry. In the present study, the eye and photography were the principal investigative tools used to examine the white-water wake. The quality of a

Manuscript approved March 12, 1984.

photograph and the amount of relevant visible detail that it contains will depend upon a variety of factors, some of which are listed below:

1) Weather conditions - sun glitter, haze, fog, clouds, rain darkness;
2) Distance, altitude and angle of the camera relative to the vessel, task force or convoy;
3) Camera specifications, settings, lenses and filter systems employed;
4) Photographic film - ASA no. (speed), black and white or color, amount of contrast, light sensitivity.

Sun glitter from the surface of the ocean, and/or the presence of fog, rain, clouds, or haze in the atmosphere located between the camera or eye and the surface can render photographic or visual study of the white-water wake generated by a vessel totally useless because each of these conditions can hide the normally visible wake. Some of these factors had only a minor influence on a small portion of the data.

The distance, altitude and angle of the camera (or eye) relative to the vessel, task force or convoy will greatly influence the resolution and amount of visible detail pertaining to the white-water wakes(s) in the photograph. Photographs that are taken when the camera is directly overhead the subject at altitudes ranging between 500 and 5000 feet contain more accurate and detailed information than those taken at oblique angles four to six miles away. The wake geometry will be greatly distorted and the measured values of L_{ww}/L_{wl} (white-water wake length/vessel waterline length) will generally be less in these high altitude, oblique photographs than those values obtained from the overhead photographs. Measured values of the white-water wake length were obtained from both types of photographs.

When all other variables except camera location are equivalent on the nondimensional plots presented later in the paper, the white-water wake length data will plot within a maximum (overhead) to minimum (high altitude, oblique) range on these plots. The same type of range will be present when the data values obtained in the foreground of these high altitude photographs are compared with those measured in the background of the photographs.

The quality and specifications of the camera, lenses, filters and film that are used to photograph the subject determine the amount and type of

details that are present in the processed photograph. If the photographic system was designed properly, the details of interest pertaining to the subject would have been clearly recorded on the film when the photograph was taken. Some problems created by improper design of the photographic system can be partially corrected with some type of image processing.

A measured value of the visible length of the white-water wake generated by a vessel underway was the main physical quantity of interest in the present study. The physical end of the visible white-water wake will be defined as that astern location in the vessel's wake where no more visible foamy patches can be observed on the water surface. The wake remains thermally visible to IR detection and there are still many acoustically visible bubbles left in the wake long past the end of the foamy white-water region [6]. There is also a visible deadening of the sea surface in the wake long past the end of the foamy region.

Sea and weather conditions will measurably influence the generation, spread, persistence and visibility of the white-water wake. The most important of these influencing variables are:

1) Sea state - wave height, direction, spectrum;
2) Wind velocity and direction;
3) Surface chemistry and condition - presence of surfactants, pollutants, living organisms (plankton), particulate matter;
4) Water depth.

The optimum conditions under which a vessel can be powered through the water most efficiently are when the water surface is calm (flat), the wind velocity is negligible and the water depth is much greater than the vessel's draft. Winds, (dead ahead or incident at an angle) whose velocity ranges between one and two times the speed of the vessel, can increase the total resistance of the vessel by ten to thirty percent. If high winds are striking the ship at an angle there can be an additional increase in resistance if the rudder is needed to keep the ship on a straight course. Rough weather and a rough high sea state can increase the residuary resistance of the vessel by as much as 500 percent. These increases in resistance mandate an accompanying increase in horsepower and propeller rps over those values used to power the vessel through the water at the same velocity under optimum conditions. The white-water wake characteristics will be altered by the presence of strong

winds and high seas. More production of white-water can be expected because of the higher rps values. The wake will also dissipate more rapidly (foam will not persist as long) due to the increased roughness of the surface [9].

The added presence of particulate matter and plankton in the upper surface layer of the water has been shown to increase the time that the wake is acoustically visible, i.e. they increase the lifetime of the smaller bubbles. They may also contribute to the persistence of the foamy white-water. Surfactants, diesel oils and other exhaust products dampen the amplitude of the capillary waves on the surface in the wake. At the present time it is not known whether these surfactants and exhaust products will effect the production and persistence of the foamy white-water.

The residuary resistance of a vessel in shallow water increases up to a certain critical speed because the wave heights are increased. These increased wave heights are created by the increased water velocities and pressures found around the submerged hull because the water flow around the hull is restricted by the shallow depth. After this critical speed, which depends on the vessel's length and velocity and the depth of the water, is reached the increase in shallow water resistance diminishes towards zero and the vessel may actually encounter less resistance in shallow water than in deep water. The powering requirements will be increased (or decreased above the critical velocity) and the white-water wake characteristics will be changed. If the vessel is travelling in a canal or river where the water is restricted laterally, the effects are further exaggerated. There is also an accompanying increase in trim and sinkage in shallow or laterally restricted water. The wave pattern generated by the vessel changes as the vessel passes from deep to shallow water.

An important group of variables that will influence the white-water wake characteristics fall into the vessel and vessel class characteristics categories. These variables are:

1) Vessel dimensions;
2) Type and shape of the hull;
3) Speed of the vessel;
4) Bow and stern shape;
5) Loading of the vessel;
6) Propulsion system;

7) Fouling of the hull;

8) Turning and/or acceleration of the vessel.

The vessels that travel and patrol today's waterways have many different hull shapes and characteristics that can be grouped into four major categories according to their method of support in the water.

Aerostatically supported craft are commonly called surface effect ships (SES), of which air cushion vehicles (ACV) and captured air bubble craft (CAB) are two examples. These types of craft literally travel on a cushion of air over the water surface. The speed of these types of craft is presently on the order of 75 to 100 knots.

Hydrodynamically supported craft apply the theories of Bernoulli's law and can be grouped into two categories: hydrofoils and planing hulls. Hydrofoil craft can presently attain maximum speeds between 40 and 60 knots depending upon the size and weight of the vessel. The hull of the hydrofoil craft is supported clear of the water surface by the hydrodynamic lift of the surface piercing or submerged foils. Planing hulls can obtain maximum speeds between 25 and 40 knots. The bottoms are shallow V section surfaces which give vertical lift and provide directional stability. Planing hulls operate best in flat water. Craft of these type operate at speed to length ratios greater than 2.0.

Hydrostatically supported displacement craft apply mainly the theory of Archimedes' law and operate at speed to length ratios less than 2.0. There are two categories of displacement craft: the conventional displacement type, examples of which include fast cargo ships, destroyers, cruisers and aircraft carriers; and the special displacement types which include catamarans, multi-hull small waterplane area craft and deep displacement supertanker type craft. High speed military displacement craft usually rely on some form of hydrodynamic support (Bernoulli's law) as well as the hydrostatic support, hence the larger maximum speed to length ratios, up to 2.0. Typical displacement hulls have maximum speed to length ratios around 1.4. These hydrostatically supported craft have a maximum speed range between 15 knots (supertankers) and 36 knots (military craft).

The final class of displacement vessels are those designed for completely submerged operation applying the theory of Archimedes' law. When operating

submerged, these bodies of revolution have negligible wave making resistance and are not influenced by sea and weather conditions. When these vessels operate on the surface, they do so very inefficiently.

There were two types of hulls for which data points were available in the present study. Only conventional monohull displacement type craft and submersible craft operating on the surface will be considered.

There are five classifications of marine power plants in use in the four categories of vessels previously discussed. The type of power plant used to propel a certain vessel depends upon many factors, among which include the vessel's size, hull characteristics, speed and mission requirements. Each of the five types of power plants provides a specific horsepower range and operates under a different basic thermodynamic cycle.

The steam turbine provides 35,000 to 120,000+ shaft horsepower (SHP) using the Rankine steam cycle. For gas turbine power plants, the Brayton cycle is the basic cycle that provides 500 to 40,000 SHP to the vessel. Diesel cycle engines provide 25 to 25,000 SHP and can be grouped into low speed rps (less than 1000 SHP) and high speed rps (greater than 1000 SHP) engines. Otto cycle engines are the internal combustion reciprocating gasoline engines found in smaller craft requiring between 10 and 500 SHP. The aircraft type turbojet engines can provide up to 3500 SHP to a vessel.

The angle of the shaft(s) connecting the power plant to the propeller(s), the number and direction of rotation of the propellers, and the characteristics of the propellers, i.e. rps, diameter, number of blades, pitch, fully or partially cavitating, distance between the tips and the surface, etc., all will influence the white-water wake characteristics.

Fouling of the wetted surface by sea growth is dependent upon the environment that the vessel operates in and the type of antifouling paint used on the hull. Fouling can increase the frictional resistance by as much as 50 percent over the clean-hull value. The value, $\Delta C_f = 0.0004$, was used in the present analysis to try and account for the increase in frictional resistance due to hull fouling.

Changes in the loading of the vessel will vary the trim, wetted surface, displacement and underwater hull form. Insufficient trim by the stern can result in a decrease in propulsive efficiency because the tips are too close

to the surface, forcing the blades to draw in air in smooth water or break the surface and race in rough seas. Variations in the wetted surface will cause the frictional resistance to change. The vessels in the present study were all assumed to be fully loaded.

The design of the hull form will influence the white-water wake characteristics. The resistance is predominately frictional for displacement ships that run at low speed-to-length ratios and in order to keep the wetted surface small (minimize C_f) the hull shape must be short and full. Wave making resistance predominates for ships that operate at high speed to length ratios, so the vessel must be increased in length and fineness to minimize the wave drag as the speed to length ratio increases. The bow of the vessel must be designed to avoid slamming, allow the hull to enter the water smoothly when pitching and provide a minimal amount of wave making resistance as the hull moves through the water in both a calm or sustained sea.

A dramatic example of the changes in the white-water wake characteristics resulting from variations in the underwater hull form at the bow of a vessel is shown in Figure 1. Two high speed passenger sister ships (L_{wl} = 83.6m), the Kurenai Maru (top) and the Murasaki Maru, are shown running abreast at the same velocity, V_s = 17.6 knots. The Froude number, $Fr = V_s/(L_{wl}g)^{1/2}$, is 0.316. The Kurenai Maru has a large bulb at the bow while the Muraski Maru has a conventional bulb. The width of the Kurenai Maru's white-water wake is measurably narrower than the Murasaki Maru's wake and there is a noticable difference in the Kelvin wave patterns. The larger bulb reduced the wave resistance by reducing the wave-breaking or turbulent motion at the bow and also by smoothing the flow around the bow [10].

The geometry of the hull will influence the size, growth and separation of the boundary layer as well as the form resistance. Other elements of ship form that should be considered are the distribution of the displacement along the length (shape of the cross-sectional area curves), shape of the load waterline and transverse sections, the type of stern (raised counter, transom, cruiser, etc.) and the midship-section area coefficient.

Turning and acceleration of a vessel will influence the white-water wake characteristics. As the ship turns, the foam on the curved section of the path along the outer edge is visually much denser than the straight line portion laid before the turn. When the ship accelerates on a straight course

the visual density is again increased, and knuckles of foam are left on the surface in the wake.

It was assumed that the geometry, strength and persistence of the white-water wake generated by vessels moving horizontally through the surface of a body of water could be related by some nondimensional group of unrelated variables. The following is a brief development of the dimensional analysis procedure that was used to find those groups which might collapse the data onto a unique curve. The significant variables that were available for the present analysis are listed and defined below:

1) L_{ww} White-water wake length
2) L_{wl} Vessel waterline length
3) B_{wl} Midsection beam at the waterline
4) D_{wl} Midsection draft
5) S Wetted surface area
6) ∇ Displacement volume
7) D_p Propeller diameter
8) D_T Depth of the propeller tips below the surface
9) V_s Vessel velocity
10) n Propeller revolutions per second
11) EHP Vessel effective horsepower
12) R_T Total resistance
13) η_p Propulsive efficiency
14) g Gravitational acceleration
15) μ Absolute viscosity of seawater
16) ρ Mass density of seawater.

The visible white-water wake lengths were measured directly from individual aerial photographs of a vessel, convoy or task force. These photographs were obtained from the Navy photographic section of the National Archives in Washington, DC. The speed of the vessel, convoy or task force was obtained directly from the photograph description or from the original ships' deck logs also available from the Archives.

The total resistance R_T is equal to $550EHP/V_s$ and can be broken into two parts, the frictional resistance R_f and the residuary resistance R_r, where $R_T = 0.5\ (C_f + C_r)\ \rho V_s^2 S$. The smooth hull frictional resistance coefficient

C_f can be calculated using the ITTC model-ship correlation line, $C_f = 0.075/(\log_{10}Re - 2)^2$. The roughness allowance $\Delta C_f = 0.0004$ is then added to the smooth hull value to obtain the total rough hull frictional resistance coefficient. The total resistance was separated into the frictional and residuary resistances to try and isolate the unknown contribution to the residuary resistance and EHP from the sea state. This was done because the EHP values available in the present analysis were based on smooth water model test data obtained from the David Taylor Naval Ship Research and Development Center (DTNSRDC). The numerical values for the remaining parameters pertaining to the vessels' dimensions and propulsion system were also obtained from DTNSRDC model test data.

The gravitational acceleration was assumed to be constant, $g = 32.2$ ft/sec^2. The density, absolute viscosity and kinematic viscosity of sea water were assumed to be constant, $\rho(59°F) = 1.9905$ slugs/ft^3, $\mu(59°F) = 2.5512 \times 10^{-5}$ slugs/ ft sec and $\nu(59°F) = 1.2817 \times 10^{-5}$ ft^2/sec.

Eighteen major groups of functional relationships were established by the dimensional analysis. These groupings are detailed in Appendix A and their derivation is given in Appendix B.

RESULTS AND DISCUSSION

A. Production of White-Water

There are three major sources that contribute to the production of the foamy white-water as a displacement ship moves through a body of water. They are:

1) Breaking or folding over of the bow wave;
2) Entrainment of air into the vessels turbulent hull boundary layer at the surface;
3) Propeller rotation - drawing in air from the surface, racing in a rough seaway, cavitation.

Considering all ship classes, other contributors to the white-water wake are:

4) Aeration of water under the skirt of an ACV or SES;
5) Hull slap of a planing hull or a displacement hull in a rough seaway;
6) Ventilation of the flow around foils and foil struts on the hydrofoil craft;

7) Cavitation of the foil and foil struts on hydrofoil craft;

8) Aeration of the water in and behind a waterjet propulsion system;

9) Wave slap against a vessel's hull;

10) Kelvin wave breaking;

11) Hull cavitation.

Contributions from each of these sources will depend mainly on the vessel class and speed.

Figure 2 illustrates the three major sources of white-water production from displacement type vessels and defines some of the terminology that will be used throughout the remainder of the paper. The aerated white-water created by the bow wave as it folds over is the first visible contributor to the overall white-water wake. The propeller wake can be divided into two regions, an initial region of high divergence directly behind the stern called the initial spreading region and the far wake where the white-water spreads at a small angle on the order of one degree. The bow wave white water merges with the propeller wake in the initial spreading region of the propeller wake. Adjacent to the vessel's hull is the turbulent, air entraining boundary layer. The width of the turbulent boundary layer white-water region just aft of the stern is on the order of one and a half to two times the ship's beam. The boundary layer white-water also merges with the propeller wake in the initial spreading region.

Figure 3, a photograph of the USS Calahann, DD 658, presents an excellent example of the turbulent boundary layer entrainment of air along the hull of a displacement vessel underway. The boundary layer white-water merges into the initial spreading region of the propeller wake. The visual density of the boundary layer white-water is much less than the visual white-water density in the initial spread region. One can also observe breaking (spilling type) of portions of the divergent Kelvin wave system on the port and starboard sides of the hull.

Figure 4 is a close-up photograph of the initial spreading region aft of the USS Augusta, CA 31, traveling at a risk 28 knots speed. The edges of the ISR appear to be a breaking wave which loses amplitude as it diverges from the stern. When the amplitude of the breaking wave becomes negligible, the wake then starts spreading at a small angle on the order of one degree. In this far wake region the visual effect is one of painting the sea surface with a

large white band. The visual density of both the boundary layer and propeller wakes are equivalent. In the fully loaded condition, the tips of the four twelve-foot diameter propellers on the Augusta are less than six feet from the surface of the water which causes the blades to drew in air from the surface. This drawing-in of air from the surface results in a large production of foamy turbulent white water in the propeller wake.

Figure 5 is a photograph of the USS Sampson, DD 394, underway. It is presented mainly to illustrate breaking (spilling type) divergent Kelvin waves, shown by arrows superimposed upon the photograph. Waves will break when the steepness parameter, ak, where a is the wave amplitude and k is the wave number, ($k = 2\pi/L$, L is the wavelength) is greater than some constant value. Theoretically this constant was found to be equal to 0.44, and experimentally the constant was 0.30 or 0.31 [3], a value significantly less than the theoretical limit. There are two major reasons that explain whey the Kelvin waves in the photograph are breaking. The first is that enough energy has been input into the Kelvin wave system by the vessel's movement through the water to cause the steepness parameter, ak, to be greater than 0.30 or 0.31, which therefore causes the waves to break. The second is that the addition of the Kelvin waves and the random sea state waves causes the steepness parameter to increase to a value greater than 0.30 or 0.31 and the waves then break. Examples of both types of breaking are present in the photograph. Directly perpendicular to the midsection on the port and starboard sides of the Sampson are examples of breaking divergent Kelvin waves. On the starboard side of the far wake is an example of a breaking wave caused by the addition of one of the divergent Kelvin waves with the random sea waves.

Figure 6 shows the bow, boundary layer and a portion of the propeller wake generated by the USS Lexington, CV2, during a full power run at approximately 34 knots. Figure 7 shows the stern and far wake region of the USS Saratoga, CV3, moving at 22 knots. The fully developed bow wave wake alongside the Lexington is measurably wider than the propeller wake and contributes a significant quantity of white-water to the total visible wake. Both the carriers exhibit similar boundary layer and propeller wakes. The bow wave alongside the Saratoga is not wider than the propeller wake, as it was on the Lexington, and merges into it. The differences in the width and strength

between the two carrier wakes is related to the difference in speed between the two vessels.

When the width-to-beam ratios of the initial spreading and far wake regions of the two carrier wakes are compared with those behind the cruiser (Figure 4), destroyer (Figure 5) and submarine (Figure 8), one notes that the carrier wake width-to-beam ratios are generally two to three times smaller than the others. The carriers each have four 14.8 ft diameter propellers, the cruiser four 12 ft diameter propellers, the submarine two 7.8 ft diameter propellers and the destroyer two 11.5 ft diameter propellers. The depth of the propeller tips below the surface is significantly larger for the carriers, D_T = 11.5 ft, when compared to the cruiser, D_T = 5.8 ft, destroyer, D_T = 6.3 ft, and submarine, D_T = 5.3 ft. Because the carrier's propeller tips are two times deeper below the surface than the three other vessels, they do not draw significantly large quantities of air in from the surface whereas the three other vessels' propellers do. The breaking wave at the surface in the ISR region of the carrier wake is significantly smaller than those produced by the cruiser, destroyer and submarine because the energy input into the breaking wave was decreased by the added depth. The proximity of the propeller tips to the surface is therefore a significant parameter governing the production of white-water, and the geometry and length of the white-water wake.

Figure 8 shows a closeup of the bow, turbulent boundary layer and initial spreading regions of the wake generated by the submarine USS Barbero, SS 317, underway. Since submarines were not designed to operate on the surface, they generate a very pronounced, wide, visible white-water wake. The bow wave extends to a width of one to two ship beams on either side of the hull. The boundary layer wake is also very wide and pronounced.

The wake generated by a two-masted sailing vessel under full wind power is shown in Figure 9. There is a conspicuous absence of white-water and only a deadening (flattening) of the sea surface in the stern wake. There are basically three contributors of white-water to the visible white-water wake; folding over of the bow wave, wave slap on the forward portion of the bow and air entrainment into the turbulent boundary layer along the vessels hull. The visible foamy white-water wake generated by the sailing vessel is substantially less than that generated by a propeller-driven displacement

vessel, emphasizing that a majority of the white-water in the wake of a propeller-driven displacement vessel is produced by the propellers.

Figure 10 presents an aerial view of four PT boats and their foamy white-water wakes. The white water in the bow wake of the planing hull is produced by the bow wave folding over, slapping of the hull surface onto the water as it passes over waves and the aeration of the water at the hull water interface as the hull planes through the water. The bow wake is as strong and persistent as the screw wake which spreads initially at a large divergent angle for several boat lengths immediately behind the stern. The initial spreading region of the propeller wake is again outlined by a breaking wave which loses amplitude as the distance aft of the stern increases. There is a region of visually denser white-water in the center of the propeller wake which persists (remains visible) longer than the remainder of the wake in the far wake region. There is a significant difference in the character of the wakes generated by a planing hull and those generated by displacement hulls.

An aerial view of the stern wake and a closeup starboard view of the strut and foil wakes laid by the Tucumcari, PCH 2, a water jet propelled Navy hydrofoil are shown in Figurec 11 and 12. White-water is generated by venting and cavitation of the struts supporting the foils and the foils themselves, and spray from the struts. The waterjet propulsion system generates a strong white-water stern wake due to the violent mixing of the air and water after the jet is expelled to power the vessel through the water. The water may also be highly aerated as it enters the intake scoop into the water jet propulsion system, and therefore will be expelled in that aerated condition. The foam in the far wake visually appears very dense and there is no observable initial speading region at the start of the stern wake. For hydrofoils that are propeller-driven, cavitation of the propellers and the drawing-in of air from the surface by the propellers are be the significant contributors of white-water to the stern wake.

A closeup photograph of the white-water wake generated by the USNS Hayes, a multihull catamaran vessel, is shown in Figure 13. Clearly visible are the initial spreading regions in the propeller wakes behind each hull, the turbulent boundary layers around each hull and the bow waves from each hull. Each of these sources appears to contribute equal quantities of foamy white-water to the overall wake.

The final two examples of wakes generated by different vessels are shown in Figures 14 and 15. Both are surface effect ships. Figure 14 is a closeup photograph of an air cushion vehicle which is supported on a cushion of low pressure air supplied by ducted internal fan and propelled by turbine driven water jets. The second, Figure 15, is a captured air bubble vehicle which is supported on a cushion of air screened at the sides by a rigid side structure. The primary sources contributing white-water to the wakes of these vehicles are aeration of the air-water interface by the fans under the skirt or beneath the the cushion, the propulsion system and spray generated as the skirt or rigid side structure contacts the water.

The purpose of this white-water production section was to illustrate the white-water production sources and wake geometries that exist for the many varied ship types and hull configurations found in today's waterways.

B. Dimensional Analysis

In this section the non-dimensional parameters that were formed from the dimensional analysis will be used to try and collapse the available data onto some type of curve. Sixty five complete (1 - 65), and two partial data sets (66, 67) were available to be used in the present study. They are listed below in Table 1 according to the number of the data points per ship class in the numerical order they will appear on the non-dimensional plots. The actual individual data sets are listed in Appendix C. The columns containing the missing data values in sets 66 and 67 have been filled in with the value .100E+01.

Figures 16-19 present examples of four photographs used to obtain the numerical values of white-water wake length and the class of the vessel generating the wake for 18 of the 67 data sets. Knowing the speed and vessel class from the photograph, one could then obtain the remaining numerical values of the parameters used in the dimensional analysis from DTNSRDC model test data and numerical calculations.

Table 1

Ship Data Employed In the White-Water Study

Ship Type	Abbreviation	Data pt. number(s)
Aircraft Carrier	CV	1 - 6
Heavy Cruiser	CA	7
Light Cruiser	CL	8 - 11
Battleship	BB	12 - 13
Destroyer	DD	14 - 25
Attack Cargo Ship	AKA	26 - 29
Ammunition Ship	AE	30
Oiler	AO	31 - 32
Submarine	SS	33 - 38
Infantry Landing Craft	LCI	39 - 52
Tank Landing Ship	LST	53 - 61
Motor Minesweeper	YMS	62
Submarine Chaser	SC	63 - 64
Utility Landing Craft	LCU	65
Ferry Boat, Uncatena	FER	66 (partial)
German Submarine	SS	67 (partial)

Figure 16 shows the white-water and Kelvin wakes behind a 107 ft sub chaser (SC) underway at 10 knots, 16(1), and 15 knots, 16(2), and a 369 ft destroyer (DD) under way at 20 knots, 16 (3,4). Figure 17 shows two different altitude views of a 400 ft German Narvik class destroyer (DD) moving at an approximate speed of 25 knots. The cusp line of the Kelvin wake is indicated by arrows. Figure 18 is a high altitude oblique photograph of Task Force 58.1 underway at an approximate speed of 22.5 knots. There are four ship classes represented in the photograph; CV, BB, CL, and DD. The loss of detail in this high altitude, oblique photograph is quite apparent when one compares the destroyer wakes in the foreground of the photograph with those destroyer wakes in the background. Figure 19 shows the white-water and Kelvin wakes generated by six 130-foot motor minesweepers (YMS) underway at a speed of 8 knots. The minesweepers are each towing two paravanes which generate their own white-water wakes.

The next sixteen figures (20-35) present the dimensional and nondimensional plots that are required to summarize the major results of the white-water wake study. In each figure, 12 data bands, representing identical ships at identical speeds, appear. The spread between the individual numerical values of the points on the Y axis will be indicated by bared

vertical lines. The spread between points 1 and 2 (CV) was due solely to the fact that the second carrier in the high altitude, oblique photograph was in the background of the photo, whereas the first was in the foreground where the wake detail was much more visually distinct. The spread between points 8-11(CL), 12-13(BB), 17-21(DD), 23-24(DD), 26-29(AKA), 31-32(AO), 39-52(LCI) and 53-61(LST) was also due to the fact that in each of the high altitude oblique photographs of conveys or task forces from which each of the individual data points were obtained, more white-water wake detail could be observed behind the ships in the foreground than those in the background of the photograph. The ranges between points 34 and 38 (SS at 20 knots), 36 and 37 (SS at 10 knots) and 16 and 22 (DD at 25 knots), where each data point was obtained from an individual overhead photograph, could be attributed to variations in the sea and weather conditions, vessel trim or loading, the presence of surfactants in the water or differences in the surface chemistry of the water. These factors can result in the creation of different amounts of foam. The quality of the photograph with respect to the resolution of the white-water wake detail depends upon the type and quality of the camera, lenses and film, the absence or presence of more or less wake detail, or the possibility that the numerical value of the speed of the vessel used in the calculations could have been in error.

In Figure 20 the lengths of the white-water wakes (L_{ww}) generated by the 67 vessels are plotted versus the vessels' speed (V_s). The important feature to note is that the white-water length increased with speed for all ship classes. Data pertaining to the individual ship classes appeared to plot onto their own unique curves. When the white-water length values are nondimensionalized by the vessels' displacement to the one-third power ($\nabla^{1/3}$), and again plotted versus the speed in Figure 21, the data again appear to plot onto individul curves. The data for the vessels with their propeller tips in close proximity to the surface ($< 1/2D_p$) plotted onto curves whose numerical values were greater than those curves associated with vessels whose propeller tips were further from the surface ($\approx 1.0D_p$). This behavior also supports the observation noted in the white-water production section, i.e. that the white-water wake generated by a vessel whose propeller tips are in close proximity to the surface is spatially longer, stronger and persists longer in time than the wake behind a vessel whose propeller tips are further from the surface.

This is because the amount of air drawn in from the surface by the propeller rotation is much greater.

The white-water length over the vessels' displacement to the one-third power is plotted versus the vessels' propeller revolutions per second in Figure 22. The length of the visible white-water region for the individual vessel classes increases with the revolutions per second, a behaviour consistent with the velocity versus white-water length plot. More air is drawn in from the surface and the propeller cavitation increases as the propeller revolutions are increased to power the ship at higher velocities, thereby resulting in the increased wake length.

The white-water length decreased with an increase in the frictional coefficient, C_f (decrease in Reynolds number $V_s L/\nu$), in Figure 23. The data for each vessel class appears to plot onto an individual curve, rather than collapse onto a single curve. The same type of behavior was exhibited by the plots of L_{ww} vs. R_f, R_T and C_T and $L_{ww}/\nabla^{1/3}$ vs. C_f, C_T, R_f and R_T.

The white-water wake length, and the white-water wake length non-dimensionalized by the vessel displacement to the one-third power are plotted versus the displacement Reynolds number ($Re_\nabla = V_s \nabla^{1/3}/\nu$) in Figures 24 and 25. The data showed no signs of collapsing onto any single curve, and again plot onto individual ship class curves. The data for those ship classes with tip to surface clearances around one propeller diameter (CV,BB) again fall on those curves whose numerical values are less than those vessel classes (SC,DD,SS) with tip to surface clearances around one-half a propeller diameter. The white-water lengths increase with Reynolds number.

Figure 26 shows a plot of the white-water wake length non-dimensionalized by the displacement to the one-third power versus the displacement Froude number ($Fr_\nabla = V_s/(g\nabla^{1/3})^{1/2}$). The data collapse onto individual ship class curves and the white-water length increases with Froude number.

The data in the next three sets of figures (x-y and ln-ln plots of the complete (65) data sets) collapse, within an order of magnitude, onto a single curve. Two linear curves were drawn such that they formed an upper and lower boundary that enclosed all the data points. Figures 27 and 28 show the x-y

and logarithmic plots of $L_{ww}C_f V_s{}^3 S/\nu^3$ versus $C_f V_s{}^3 S^{3/2}/\nu^3$. The equation describing the upper boundary to the data is:

$$L_{ww} = 0.036 C_f{}^{0.128} V_s{}^{0.384} S^{0.692} \nu^{-0.384}.$$

The white-water wake length generated by a vessel underway appears to be related to a product of the vessel's frictional resistance coefficient, velocity and wetted surface area, each raised to some individual power.

Figures 29 and 30 show the x-y and logarithmic plots of $L_{ww}C_f V_s{}^3 S/\nu^3$ versus $C_f V_s{}^2 S/\nu^2$. The equation describing the upper boundary to the data is:

$$L_{ww} = 0.393 C_f{}^{0.727} V_s{}^{0.454} S^{0.727} \nu^{-0.454}.$$

The white-water wake length is again related to a product of the vessel's frictional resistance coefficient, velocity and wetted surface area. Both this and the previous equation numerically describe the length of the white-water wake equally well.

Figures 31 and 32 show the x-y and logarithmic plots of $L_{ww}C_f V_s{}^3 S/\nu^3$ versus $C_f V_s{}^3 S/\nu^{2.5} n^{0.5}$. The equation describing the upper boundary to the data is:

$$L_{ww} = 0.427 C_f{}^{0.370} V_s{}^{1.110} S^{0.370} \nu^{-0.425} n^{-0.685}.$$

The length of the white-water wake is related to a product of the vessel's frictional resistance coefficient, velocity, wetted surface area and propeller revolutions per second, each raised to an individual power.

The final two figures (33 and 34) plot the ratios $L_{ww}n^2/g$ versus $V_s n/g$ and $\ln[L_{ww}n^2/g]$ versus $\ln[V_s n/g]$ for the 67 data sets. The log plot is the most informative and shows that the data collapse, within a band, onto a single curve. The position of the individual ship class curves on the plots is not dependent upon the propeller tip to surface clearance. Much of the spread between the upper and lower straight line boundaries enclosing the data in this figure, as well as the data in the previous six figures, is due to the loss of wake detail in the background of the high altitude oblique photographs, differences in the sea and weather conditions when individual

photographs were taken, differences in the vessels trim or loading, the presence of surfactants on the surface or differences in the surface chemistry of the surface water, differences in the resolution of wake details because of differences in the photographic film, camera and lenses used to obtain the photographs, or the possibility that the speed (and consequently the rps value) of the vessel(s) might have been in error. The equations describing the upper and lower boundary curves are:

$$\underline{\text{upper}} \qquad L_{ww} = 145.0[V_s n/g]^{1.68} g/n^2$$

$$\text{or} \qquad L_{ww} = 13.7\ V_s^{1.68}/n^{0.32}$$

$$\underline{\text{lower}} \qquad L_{ww} = 47.0[V_s n/g]^{1.68} g/n^2$$

$$\text{or} \qquad L_{ww} = 4.44\ V_s^{1.68}/n^{0.32}.$$

The lower curve is a factor of three less than the upper curve (the data falls within ± 50 percent of a mean curve). The white-water wake length behind a vessel underway appears to be directly related to a ratio of the vessel's speed raised to some power divided by the propeller revolutions per second raised to a different power. Again it must be stressed that this relationship is valid only for displacement and submersible vessels operating on the surface. Based on the available data, one can state with a fair amount of confidence that for a given displacement ship speed and rps combination, the length of the white-water wake will not be longer than that length calculated using the equation

$$L_{ww} = 13.7\ V_s^{1.68}/n^{0.32}\ .$$

C. White-Water Wake Geometry and Spreading

The three major contributors of white-water to the foamy wake created by a displacement vessel moving through the water are the rotating propellers, the entrainment of air into the turbulent boundary layer along the vessel's hull and the folding over (breaking) of the bow wave created by the vessel. These have been discussed previously. The purpose of this section of the report is to examine some of the visual and geometric characteristics of the

bow wave white-water wake, turbulent boundary layer white-water wake and the initial spreading and far wake regions of the propeller wake.

A close-up aerial photograph of the bow, boundary layer and initial spread regions of the white-water wake generated by the USS Moale, DD 693, moving through the water is shown in Figure 35. Figures 36-41 will present six high altitude, overhead photographs of the white-water wake generated by a destroyer (four photos are of the Moale) moving at four different speeds, along with a graphical representation of the wake. The horizontal axis of the graph will represent the location in the wake nondimensionalized by the overall vessel length, starting from the bow where $L_{HL}/L_{OA} = 0$ and measuring aft positive L_{HL}/L_{OA}. The vertical axis will represent the width of the various white-water wake regions nondimensionalized by the overall length of the vessel, W/L_{OA}. The centerline of the ship corresponds to the line $W/L_{OA} = 0$, with positive W/L_{OA} starboard and negative W/L_{OA} to the port.

Figure 36 shows the overhead aerial photographic (2500 ft altitude) and graphical representations of the white-water wake generated by the USS Moale as it moves through the water at 16 knots. Only the propeller wake contributes significantly to the overall white-water wake at this low speed. The angle of spread of the white-water in the intial spreading region (ISR) of the propeller wake is approximately 60 degrees. The length of the ISR is 69 feet or $L_{HL}/L_{OA} = 0.183$. The far wake, aft of the ISR, spreads at an angle of 1.57 degrees. The propeller wake has strongly defined edges and a dense core along the centerline for a distance of one to two vessel lengths astern. Further astern, the edge remains well defined and the inner wake breaks into an orderly streaked, foamy pattern.

Figure 37 presents the photographic (2500 ft altitude) and graphic representations of the white-water wake generated by the Moale at 20 knots speed. The bow and boundary layer wakes now contribute significant amounts of white-water to the overall wake, as well as the propeller wake. The initial angle of spread of the white-water in the propeller wake is approximately 40 degrees, twenty degrees less than the angle measured when the ship was moving at 16 knots. The length of the ISR is 138 ft, $L_{HL}/L_{OA} = 0.367$, or double that at 16 knots speed (69 feet, $L_{HL}/L_{OA} = 0.183$). The far wake spreads at an angle of 1.0 degrees, compared to 1.57 degrees at 16 knots. The wake again has strongly defined edges and a dense core for distances up to two vessel

lengths astern. The edges remain dense and the wake breaks up into an orderly streaked foamy pattern further astern.

Figure 38 shows the wake of a destroyer (in the same vessel class as the Moale) as it moves through the water at 20 knots. The quality of the photograph with regard to the white-water wake details is not nearly as good as the Moale photograph because of the high altitude (15,000 feet) from which it was taken, so that the information yielded by this photograph may not be as accurate. The far wake spreads at an angle of approximately 1.40 degrees (1.0 degrees, Moale). The propeller wake spreads initially at an angle of approximately 34 degrees and is approximately 142 feet, L_{HL}/L_{OA} = 0.375 (40 degrees, 138 feet, Moale). These values compared reasonably well with the Moale values measured at 20 knots. The wake widths at similar astern locations are slightly smaller than the Moale values. The edge of the far wake region remains well defined and visible on the port side significantly longer than on the starboard side.

The graphic and photographic (3000 feet) representations of the white-water wake generated by the Moale at 25 knots are shown in Figure 39. The propeller wake spreads initially at an angle of approximately 38 degrees for 231 feet, L_{HL}/L_{OA} = 0.614. For four ship lengths aft of the ISR, the far wake spreads at an angle of 1.67 degrees, and further astern of that region the far wake spreads at an angle of 0.65 degrees. It is not clear whether this difference in the spreading angle of the far wake is a natural occurrence or a photographically induced variation because of the distance and angle between the camera and vessel wake. The dense core and well defined edges are present in the wake for two to three vessel lengths aft of the ISR, and further along the wake breaks up to form an orderly streaked foamy pattern with visible edges. The bow and boundary layer generated white-water contributions are more significant at 25 knots than they were at 16 and 20 knots.

The graphic and photographic representations of the wake generated by a German Narvik-class destroyer moving at 25 knots are shown in Figure 40. The ISR is 184 feet long, L_{HL}/L_{OA} = 0.45, and spreads at an approximate angle of 38 degrees, the same angle that the ISR of the Moale propeller wake generated at 25 knots spread at. The far wake then spread at an approximate angle of 1.80 degrees, similar to 1.67 degree spread of the Moale far wake at comparable astern locations.

Figure 41, the final in this series of photographic and graphic representations of individual destroyer wakes, shows the wake generated by the Moale moving at 33 knots. The propeller wake spreads initially at an approximate angle of 36 degrees for 311 feet, $L_{HL}/L_{OA} = 0.826$. The far wake spreads at an angle of 1.24 degrees. The wake edges are defined by a visually dense line and the inner wake core is completely turbulent (edges and core mixed thoroughly) for a distance of four to five vessel lengths astern before the wake starts to break up into the orderly streaky foamy pattern. The bow and boundary layer wakes are fully developed, highly visible and contribute a significant quantity of white-water to the total wake.

The only significant variable that changed during the analysis of the four individual Moale wakes was the speed of the vessel. Any changes in white-water production and wake geometry can then be considered velocity related. Figure 42 is a plot of the four Moale wakes generated at 16, 20, 25 and 33 knots, the similar class destroyer wake generated at 20 knots and the Narvik wake generated at 25 knots superimposed. The plot is presented to help visualize and summarize the changes in the white-water wake characteristics that are solely velocity related. The width of the boundary layer, bow and propeller wakes increased with speed as well as the length of the initial spreading region of the propellor wake. Except for the initial 60 degree angle of spread of the Moale propeller wake region at 16 knots, the remainder of the propeller wakes spread initially at an angle of about 38 degrees. Generally the far wakes spread at an angle of about 1.50 degrees.

There appears to be a reasonably constant increase in the width of the far propeller wake with speed, suggesting the possibility that some type of similarity solution may exist to describe the spread and width of the far wake generated by a moving destroyer. A simple attempt has been made to ascertain whether a similarity solution may exist. The wake width values were multiplied by the constant,

$$1.0 + \sum_{n=2}^{10} \left(\frac{V_{MAX} - V_s}{V_{MAX}} \right)^n ,$$

and plotted in Figure 43. Since the velocity to rps ratio is fairly constant over a wide range of speeds, the wake width values also can be multiplied by the constant,

$$1.0 + \sum_{n=2}^{10} \left(\frac{RPS_{MAX} - RPS_s}{RPS_{MAX}} \right)^n .$$

These values are plotted in Figure 44. Both plots were nearly identical. Four of the six individual wake plots collapse onto a single curve, with the two remaining plots collapsing within plus (Moale at 20 Kt) and minus (DD at 20 Kt) ten percent of the curve. This apparent collapse of the data onto a single curve stengthens the supposition that some type of similarity solution may indeed exist. A more complete analysis to find the correct formula to determine the appropriate constant needs to be performed and a larger data set needs to be examined before pursuing the idea of wake similarity any further.

The graphic and photographic representations of the white-water wake produced by the USS Saratoga, CV3, moving through the water at 22 knots are shown in Figure 45. The clearance between the carrier's propeller tips and the water surface is twice that normally found between the Moale's propeller tips and the water surface. Consequently the width of the carrier wake is significantly smaller than the destoyer wake. The carrier's ISR is shorter and not as easily indentifiable as the destroyer ISR. The far wake spreads at an approximate angle of 1.48 degrees and the white-water decays much more quickly than the destroyer white-water.

The wake produced by the ferry boat, Uncatena, that travels between Woods Hole and Martha's Vineyard, Mass. at a nominal speed of 15.5 knots, is shown in Figure 46. The bow wave and propeller wakes contribute significant quantities of white-water to the highly structured total wake. The initial spreading region of the propeller wake is barely visible. The Uncatena's hull shape is significantly different than the Moale's hull shape and the propeller rpss are six to eight times greater. The differences in the wake characteristics between the Moale and Uncatena are quite evident and can be directly related to the differences between the two vessels.

SUMMARY

The major variables that influence the production, geometry, persistence and visibility of the foamy white-water wake generated by different classes of vessels moving in a body of water have been identified and discussed throughout this report. The white-water wake is an extremely complex phenomenon, influenced by many variables. A dimensional analysis involving some of these variables was performed to try and collapse the white-water wake length data onto a single unique curve. The data appears to collapse onto curves unique to each vessel class on a majority of the non-dimensional plots. The propeller tip-to-surface clearance of each vessel class seemed to determine the relative location of the curves on the non-dimensional plots. Those vessels with minimal tip-to-surface clearance have longer, stronger and wider white-water wakes than those vessels with significantly deeper propellers.

The best result obtained from the dimensional analysis is that the maximum length of the white-water wake generated by a vessel underway is proportional to a ratio of the vessel's speed raised to a power divided by the vessel's propeller revolutions per second raised to a different power. The actual equation is

$$L_{ww} = 13.7\ V_s^{1.68}/n^{0.32}.$$

The data scattered no more than a factor of three below this curve. The reasons for this scatter were discussed previously. Based on the available data, one can state with a reasonable amount of confidence that for a given combination of vessel displacement, vessel speed and propeller revolutions per minute, the length of the white-water wake will not be longer than that calculated using the above equation.

Six graphic representations of the high altitude overhead photographs of six destoyer wakes generated at four different speeds have been superimposed in order to analyze the changes in wake characteristics that can be directly related to changes in the speed of the vessel. The width of the turbulent boundary layer, bow wave and propeller wakes all increased with speed as well as the length of the initial spreading region. The propeller wake appears to spread initially at an angle of 38 degrees, and the far propeller wake spreads at an average angle of approximatley 1.50 degrees. Because there appears to

be a constant increase in the width of the far wake region with speed, a simple attempt has been made to ascertain whether some type of far wake similarity may exist. The six wake plots appear to collapse onto a single curve (taking the uncertainty of the data into account). When they are multiplied by two constants based on the difference in velocity or rps. The wake geometry and characteristics of different class vessels may exhibit similarity by individual vessel class, as did the destroyer data. However, because of the differences in hull geometry, hydrodynamic support and propulsion systems between vessel classes, it will be very difficult to determine whether any type of similarity exists between all vessels.

ACKNOWLEDGMENTS

This study was conducted as part of the Advanced Marine Technology Program at the Naval Research Laboratory. The data pertaining to vessel class characteristics listed in Appendix C was provided by Ruth S. Goldberg and Seth Hawkins of the David Taylor Naval Ship R & D Center.

REFERENCES

1. Hiller, A.J., Caldwell, J.H., and Klee, C.W., "Ship Wake Research," Naval Research Laboratory Memorandum Report 2117, June 1970. AD876 251L

2. Gillmer, Thomas C., Modern Ship Design, Second Edition, Naval Institute Press, Annapolis, Maryland, 1975.

3. Griffin, O.M., "The Breaking of Ocean Surface Waves," Naval Research Laboratory Memorandum Report 5337, June 1984.

4. Newman, J.N., "Recent Research on Ship Wakes", Eighth Symposium on Naval Hydrodynamics: Hydrodynamics in the Ocean Environment, Office of Naval Research, Department of the Navy, Aug. 24-28, 1970, pp. 519-545. ACR-179

5. Lang, Thomas G., "Hydrodynamic Design of an S^3 Semi-Submerged Ship," Ninth Symposium on Naval Hydrodynamics: Unconventional Ships, Ocean Engineering, Office of Naval Research, Department of the Navy, Aug. 20-25, 1972, Vol. 1, pp. 549-580. ACR-203

6. Physics of Sound in the Sea, Part IV - Acoustic Properties of Wakes, National Defense Research Committee Division 6, Summary of Technical Report Volume 8, 1946, reprinted in 1969 as NAVMAT Report P-9675.

7. Principles of Naval Architecture, Published by the Society of Naval Architects and Marine Engineers, Fourth Printing, August 1977.

8. Williams, K.G., and Thomas, T.M., "Optical Detection of Kelvin Waves," Naval Research Laboratory Report 6610, Feb. 8, 1968. AD388 440L

9. Holter, N.J., "The Geometry of Surface Wakes and Experiments on Artificial Wakes," U.S. Navy Radio and Sound Laboratory Report No. S-10, May 22, 1943. AD 495851

10. Takahei, Tetsuo, "Appraisal of Flow Visualisation For Development of Ship Hydrodynamics", Proceedings of the Third International Symposium on Flow Visualization, Ann Arbor, USA, Sept, 1983, pp. 529 - 538.

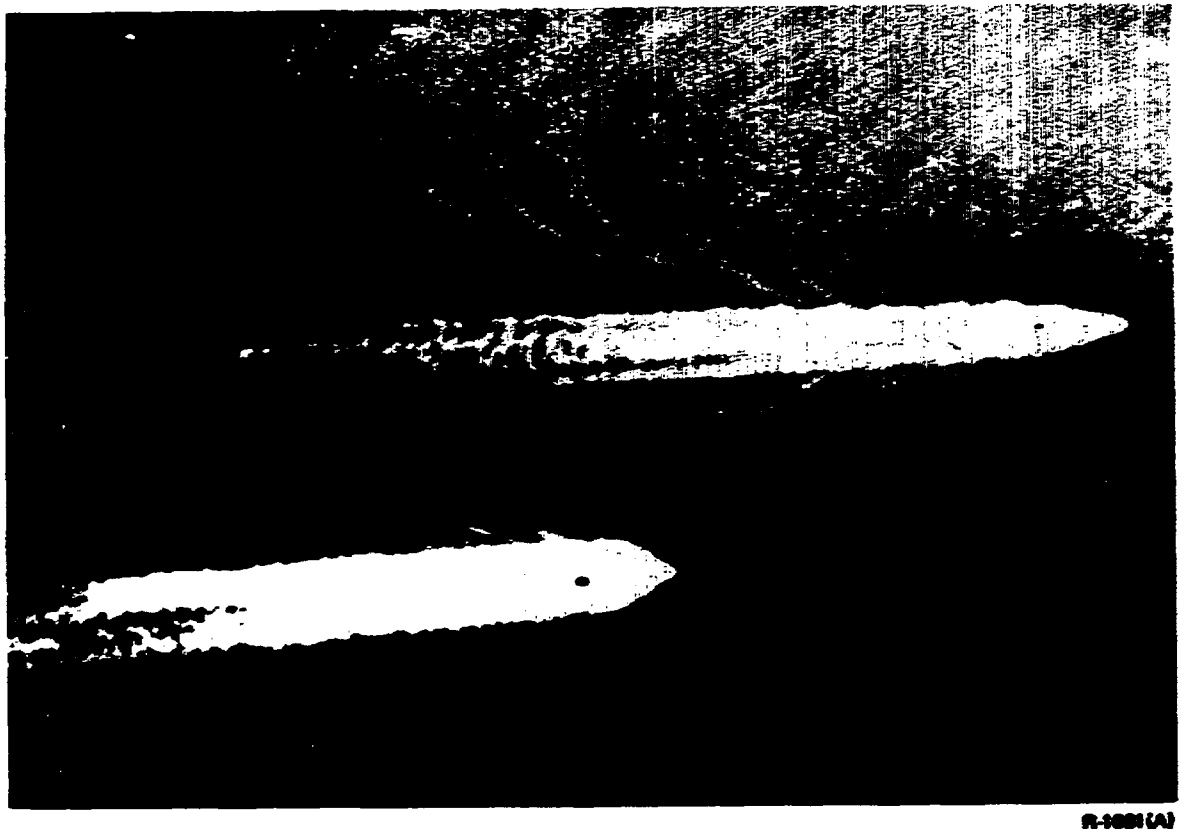

R-1628(A)

Figure 1 Changes in the white-water wake characteristics resulting from variations in the underwater hull form at the bow.

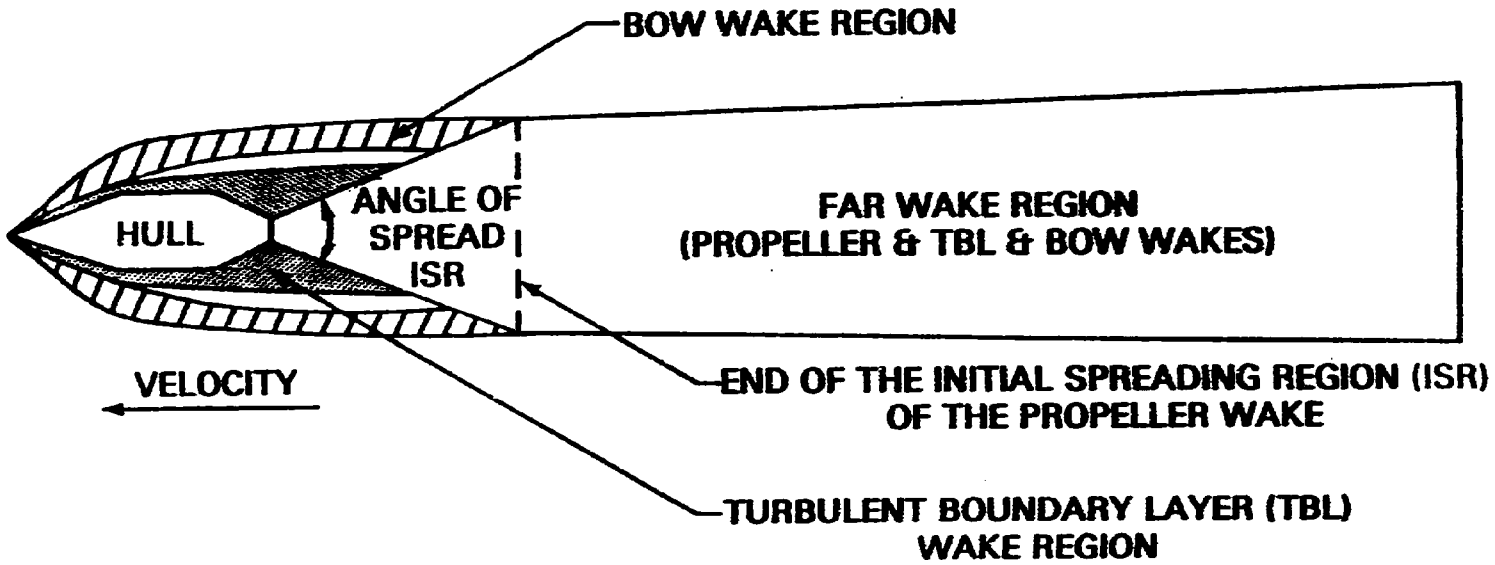

Figure 2 Three major sources of white-water production from displacement vessels.

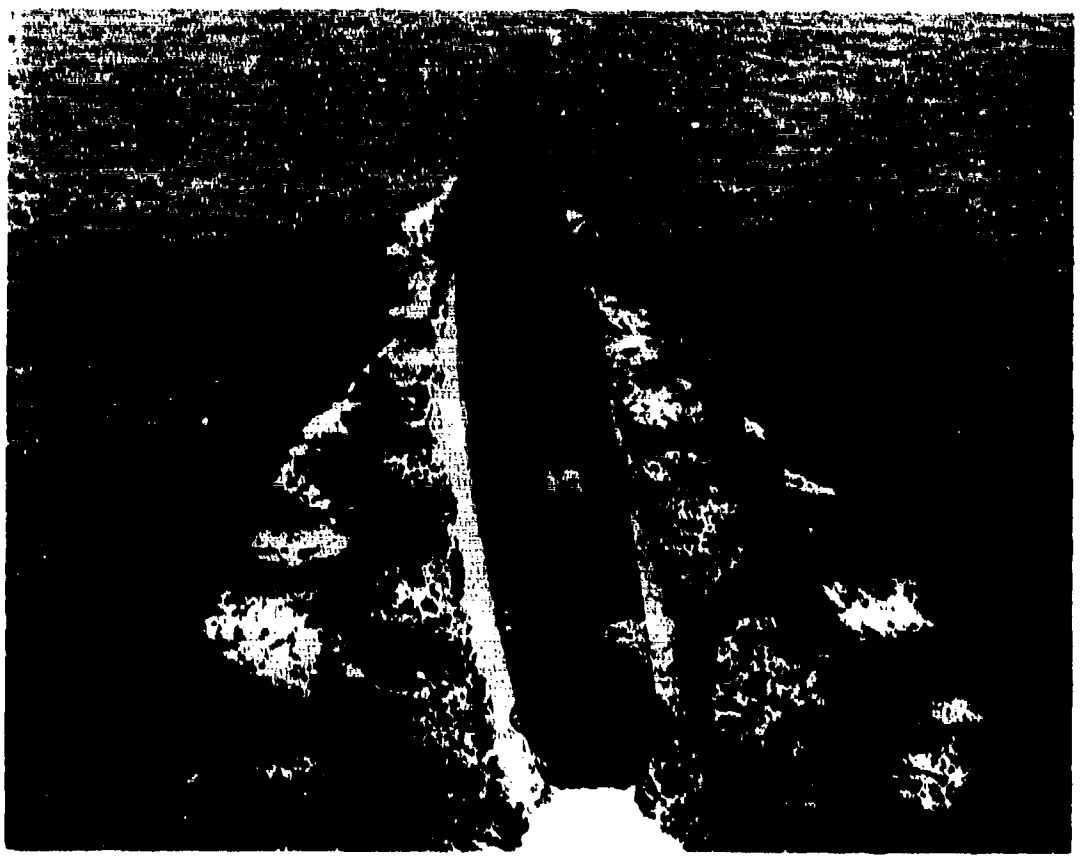

R-1062(A)

Figure 3 Closeup photograph of the turbulent boundary layer white-water wake.

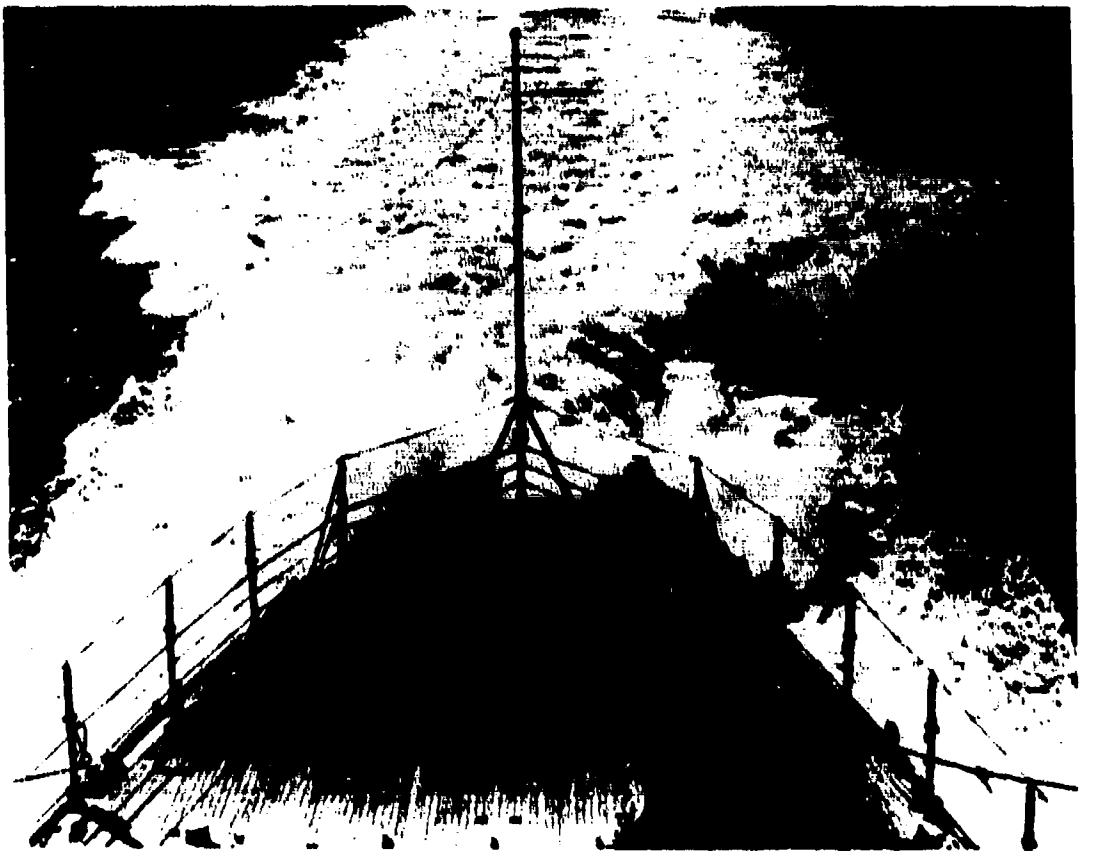

R-1057(A)

Figure 4 Closeup photograph of the initial spreading region of the propeller wake.

R-1068(A)

Figure 5 White-water production by breaking Kelvin waves.

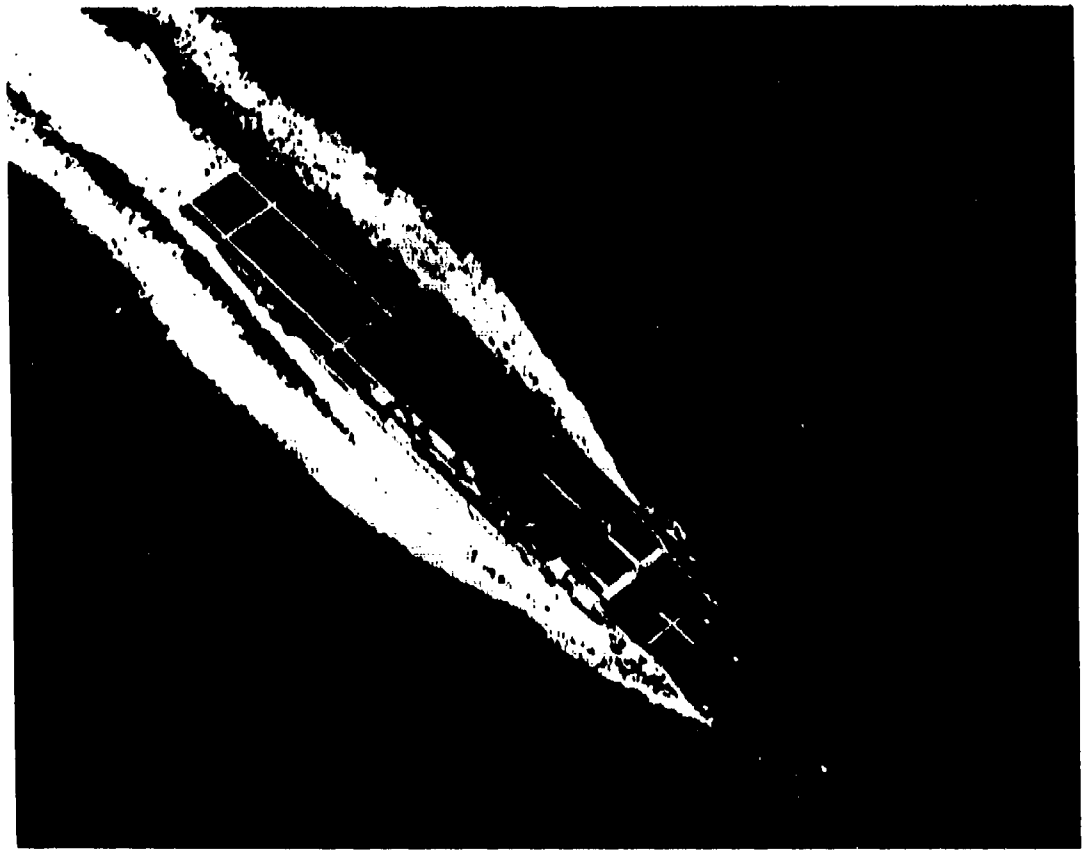

R-1059(A)

Figure 6 Overhead view of the white-water wake generated by the USS Lexington during a full power run (34 knots).

R-1080

Figure 7 Overhead view of the white-water wake generated by the USS Saratoga at 22 knots.

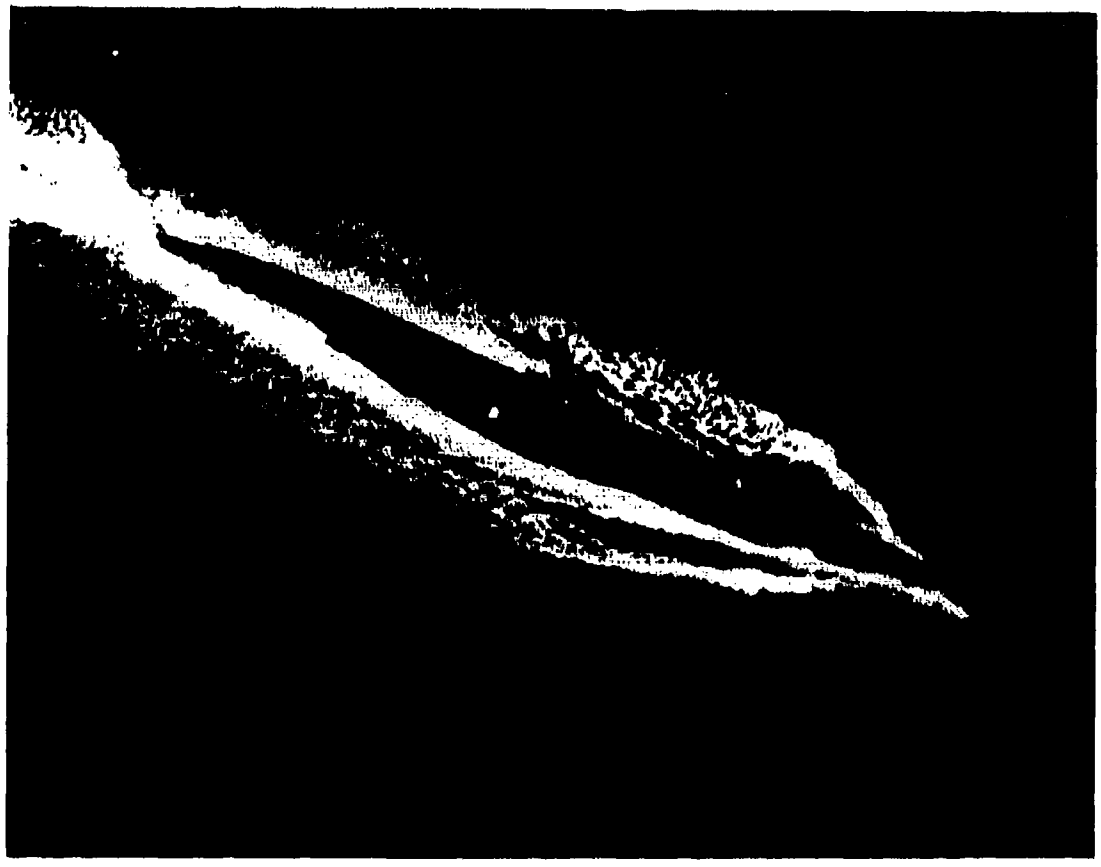

R-1083(A)

Figure 8 White-water wake generated by a submersible vessel operating on the surface.

R-1060(A)

Figure 9 White-water wake generated by a sailing vessel.

R-1059(B)

Figure 10 White-water wakes generated by planing hulls.

R-1057(C)

Figure 11 Aerial view of the white-water wake generated by the Tucumcari, a waterjet propelled Navy hydrofoil.

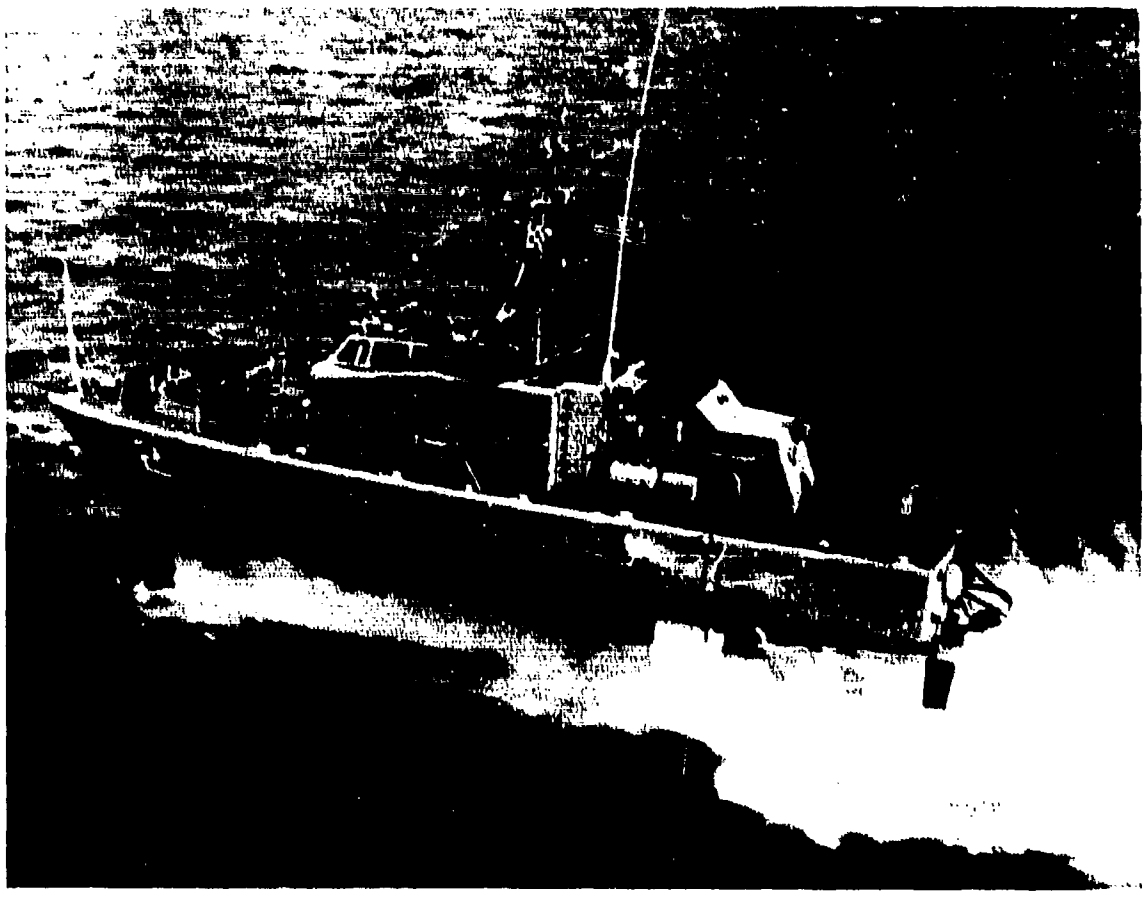

R-1068(B)

Figure 12 Close-up photograph of the white-water wake generated by the Tucumcari.

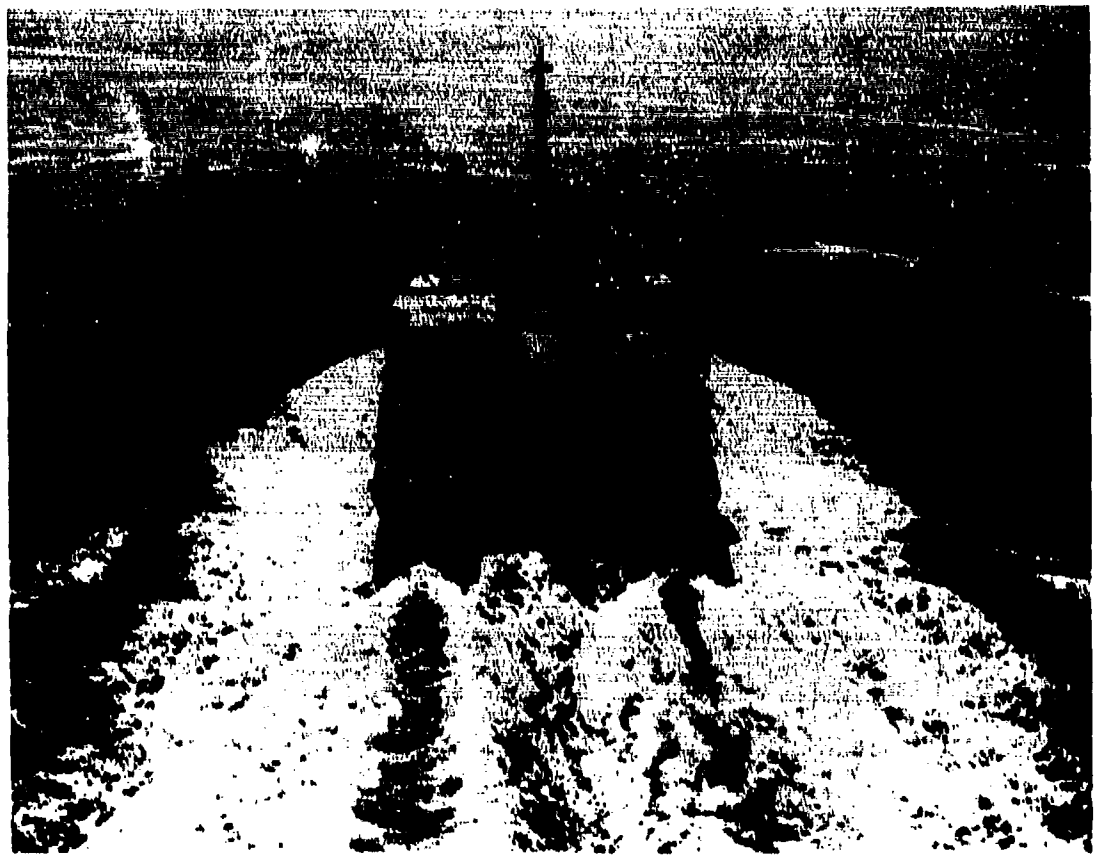

R-1061(B)

Figure 13 White-water wake generated by a catamaran vessel, the USNS Hayes.

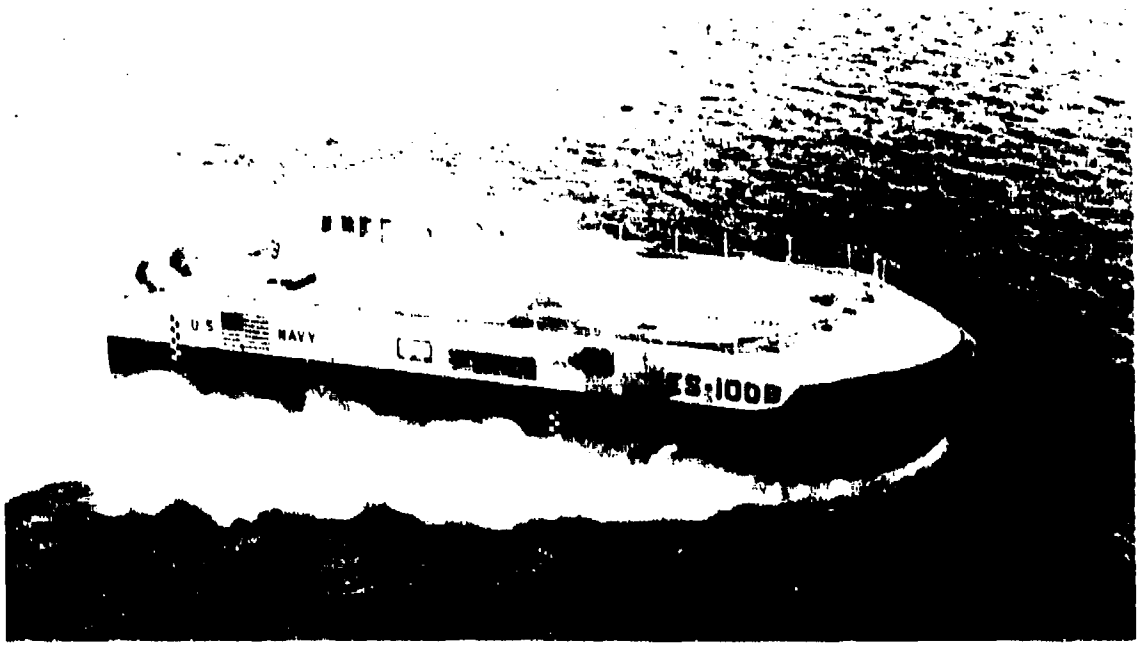

R-1067(B)

Figure 14 Closeup photograph of an Air Cushion Vehicle's white-water wake.

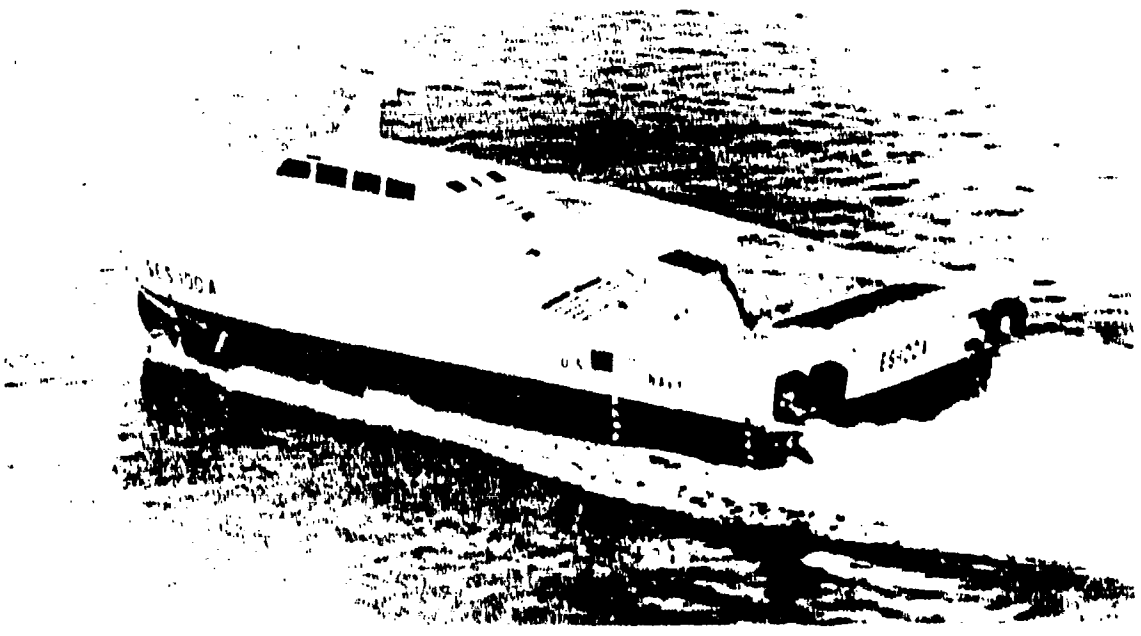

R-1062(B)

Figure 15 Closeup photograph of a Captured Air Bubble craft's white-water wake.

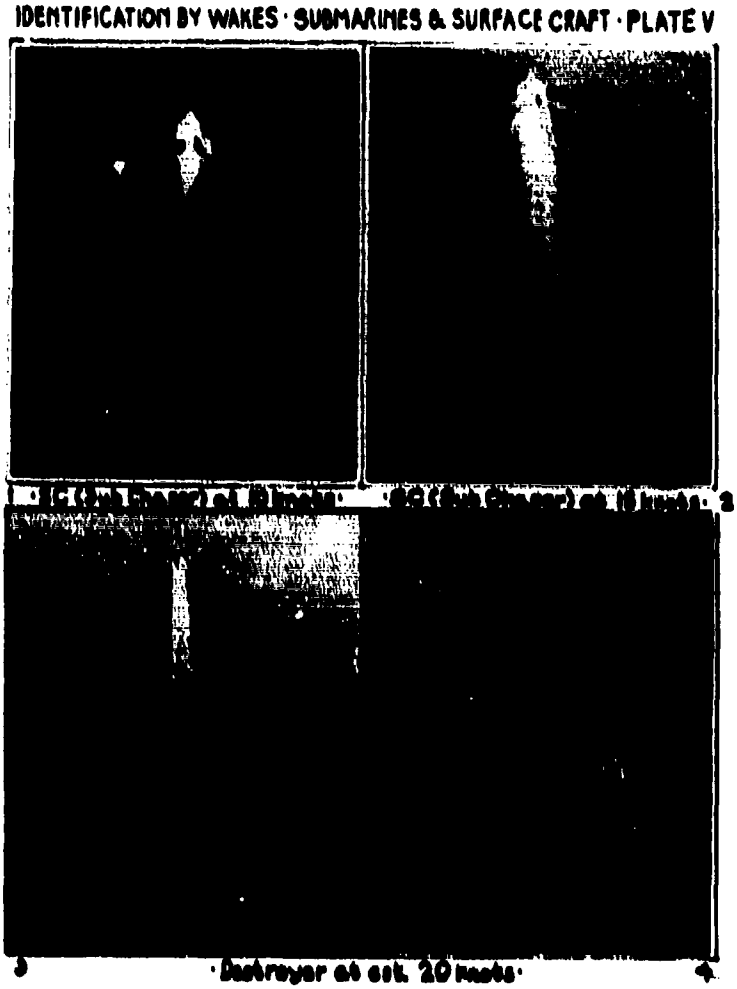

Figure 16 Overhead aerial views of the white-water wakes generated by a Sub Chaser at 10 and 15 knots (1,2) and a Destroyer at 20 knots (3,4).

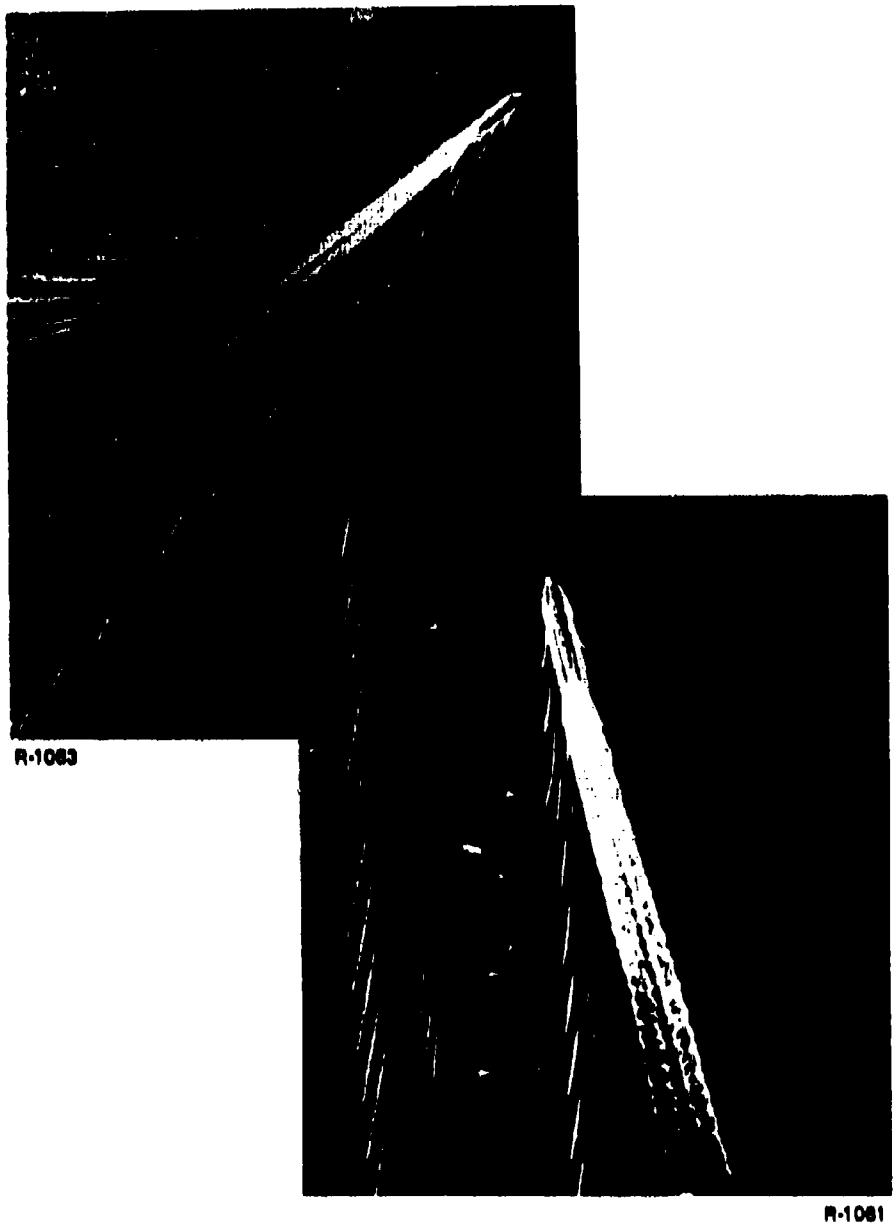

Figure 17 Overhead aerial views of the white-water wake generated by a German Narvik class destroyer at 25 knots.

R-1084(B)

Figure 18 Oblique aerial view of Task Force 58.1 underway at 22.5 knots.

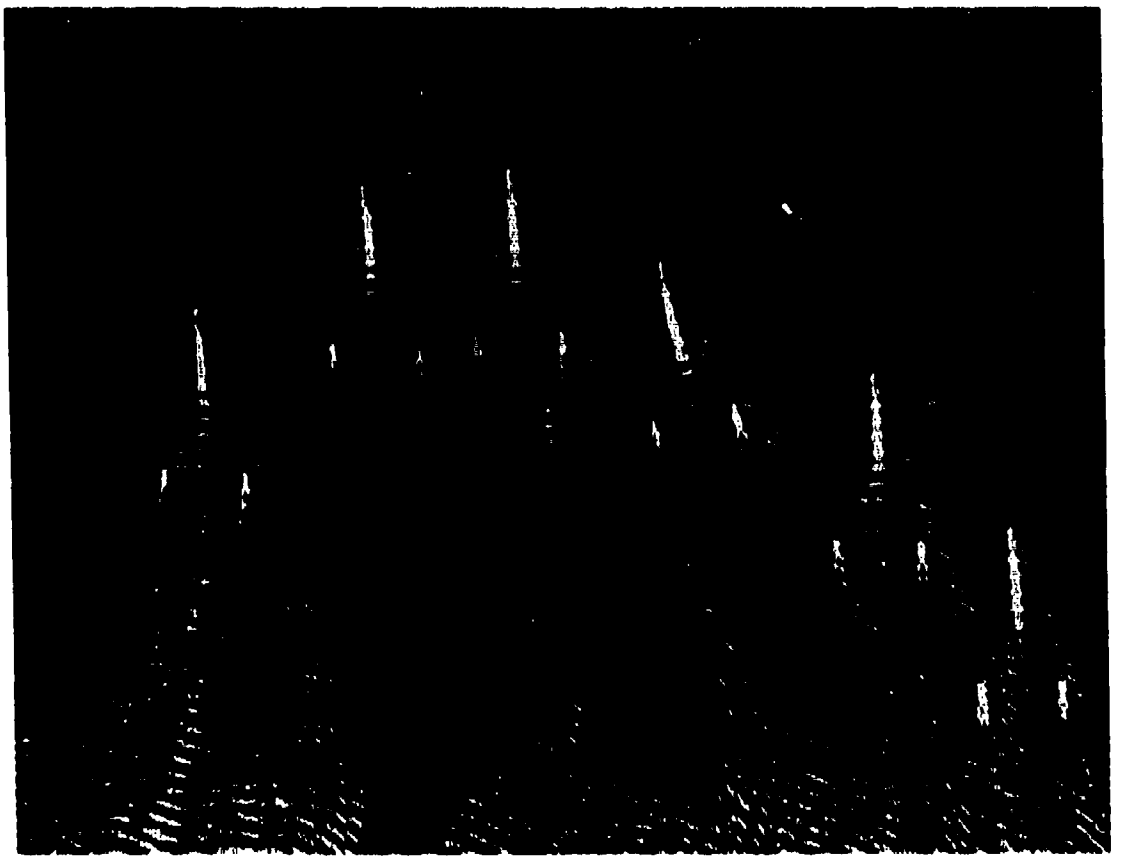

R-1063(8)

Figure 19 High altitude, overhead view of the white-water wakes generated by six Motor Minesweepers.

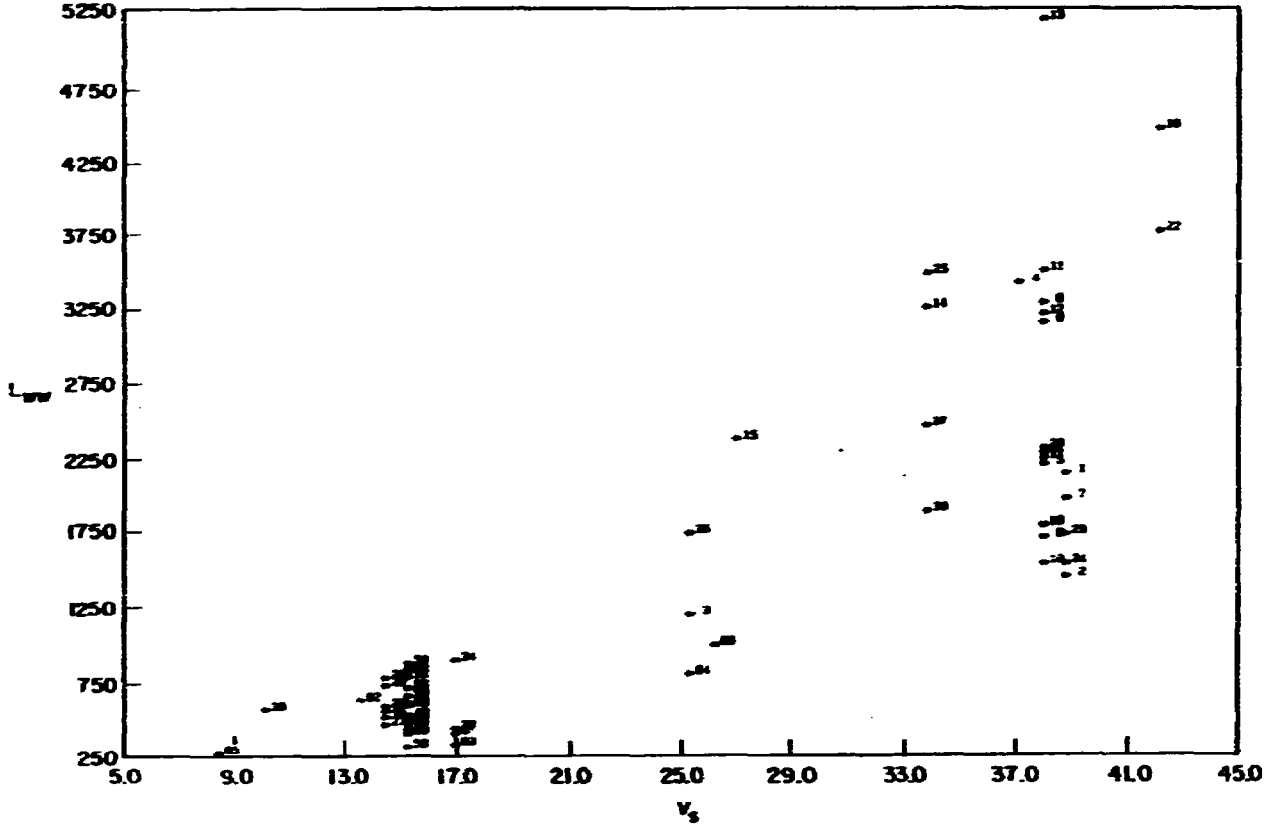

Figure 20 White-water wake length (L_{ww}) vs. vessel velocity (V_s).

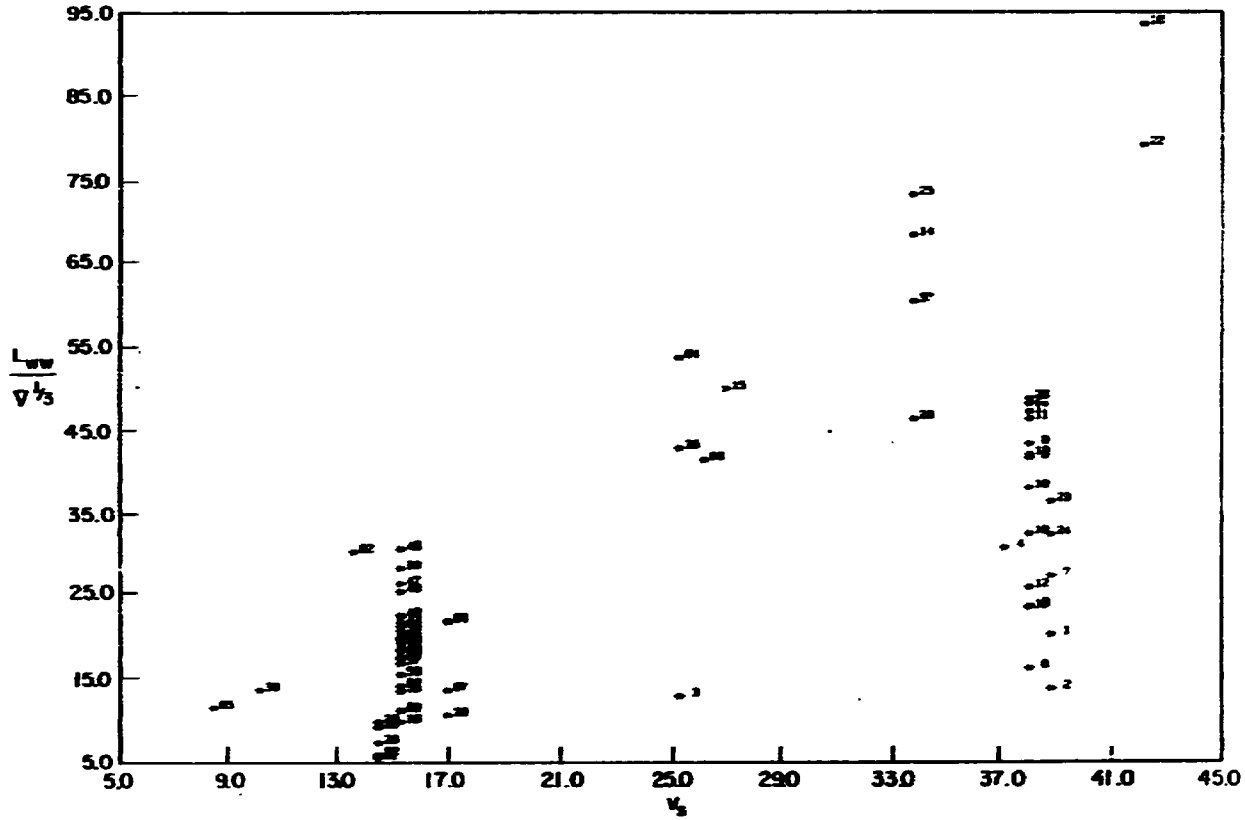

Figure 21 White-water wake length divided by the vessel displacement ($L_{ww}/\nabla^{1/3}$) vs vessel velocity (V_s).

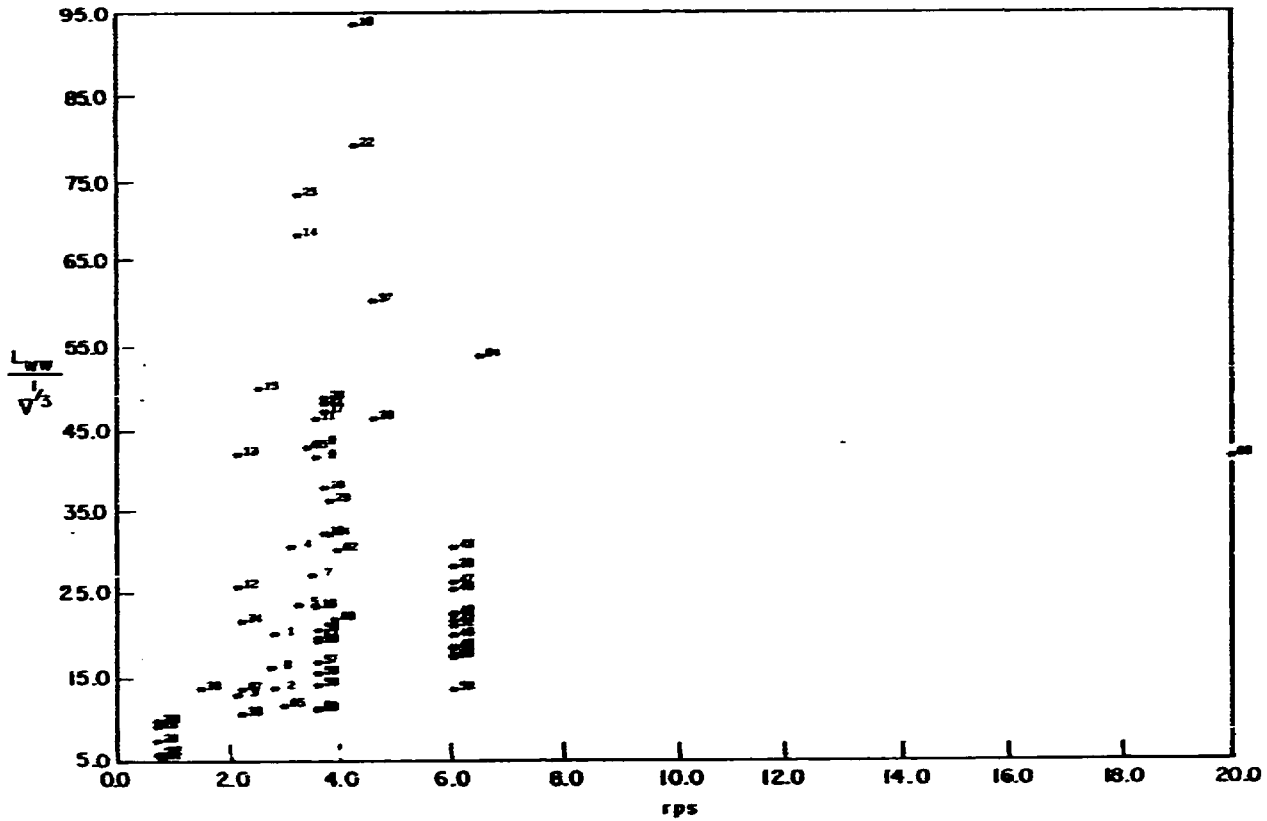

Figure 22 White-water wake length divided by the vessel displacement ($L_{ww}/\nabla^{1/3}$) vs propeller revolutions per second (rps).

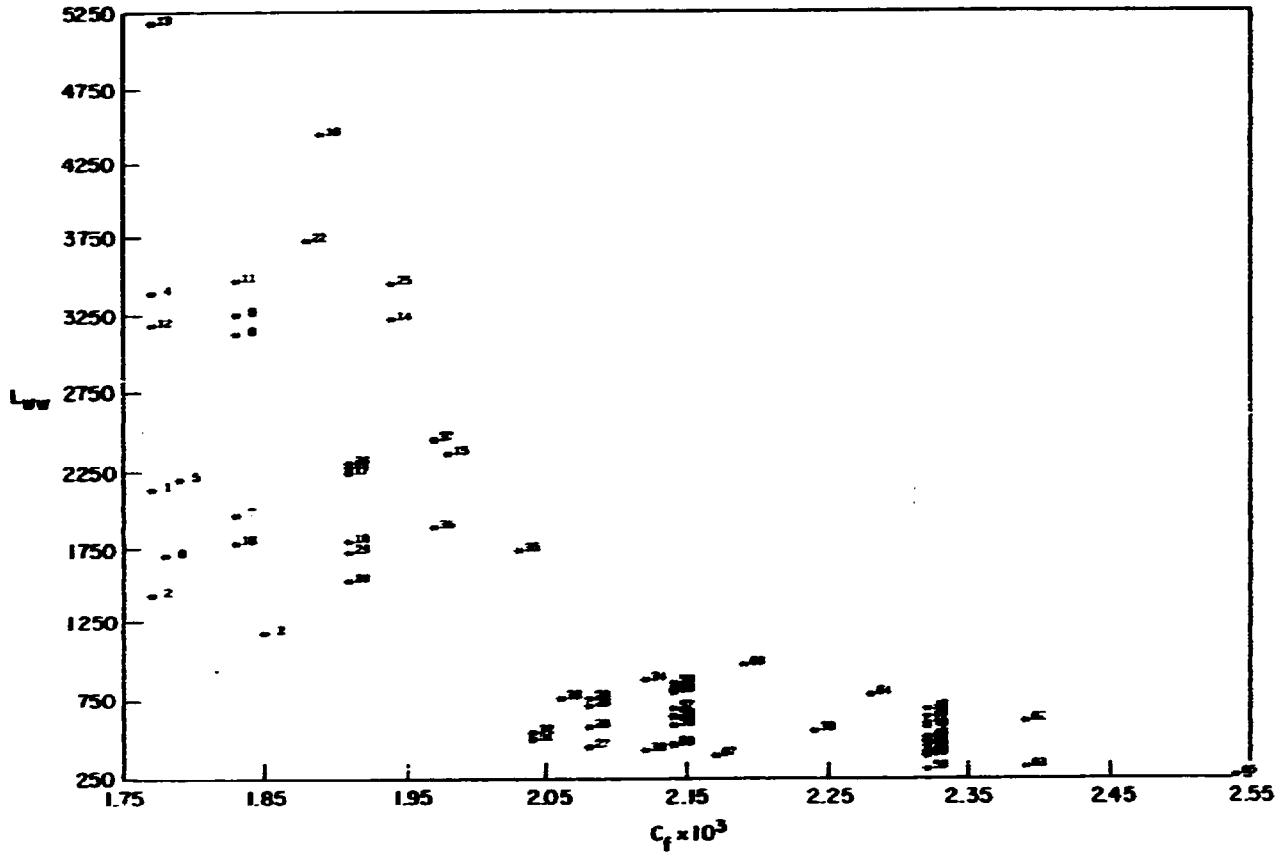

Figure 23 White-water wake length (L_{ww}) vs frictional resistance coefficient (C_f).

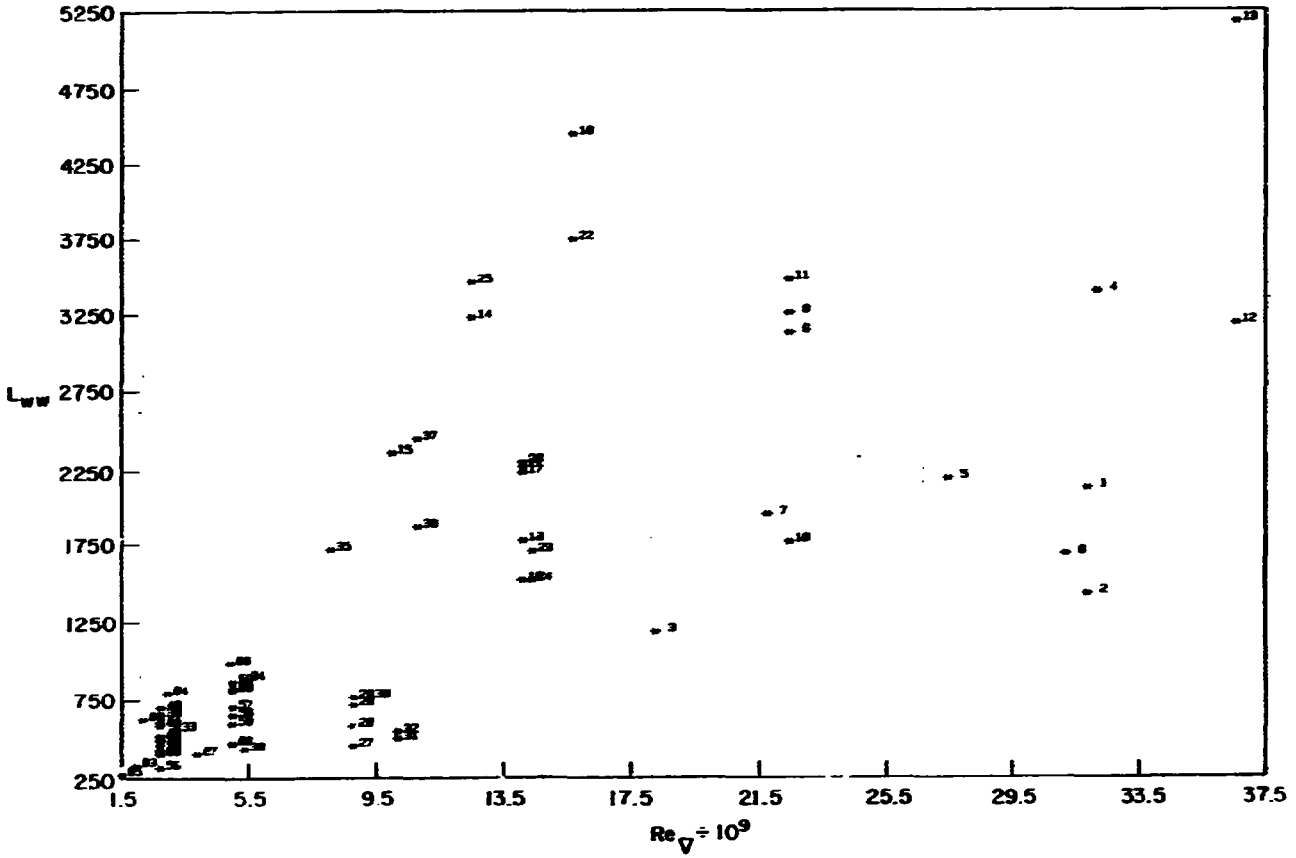

Figure 24 White-water wake length (L_{ww}) vs displacement Reynolds number (Re_V).

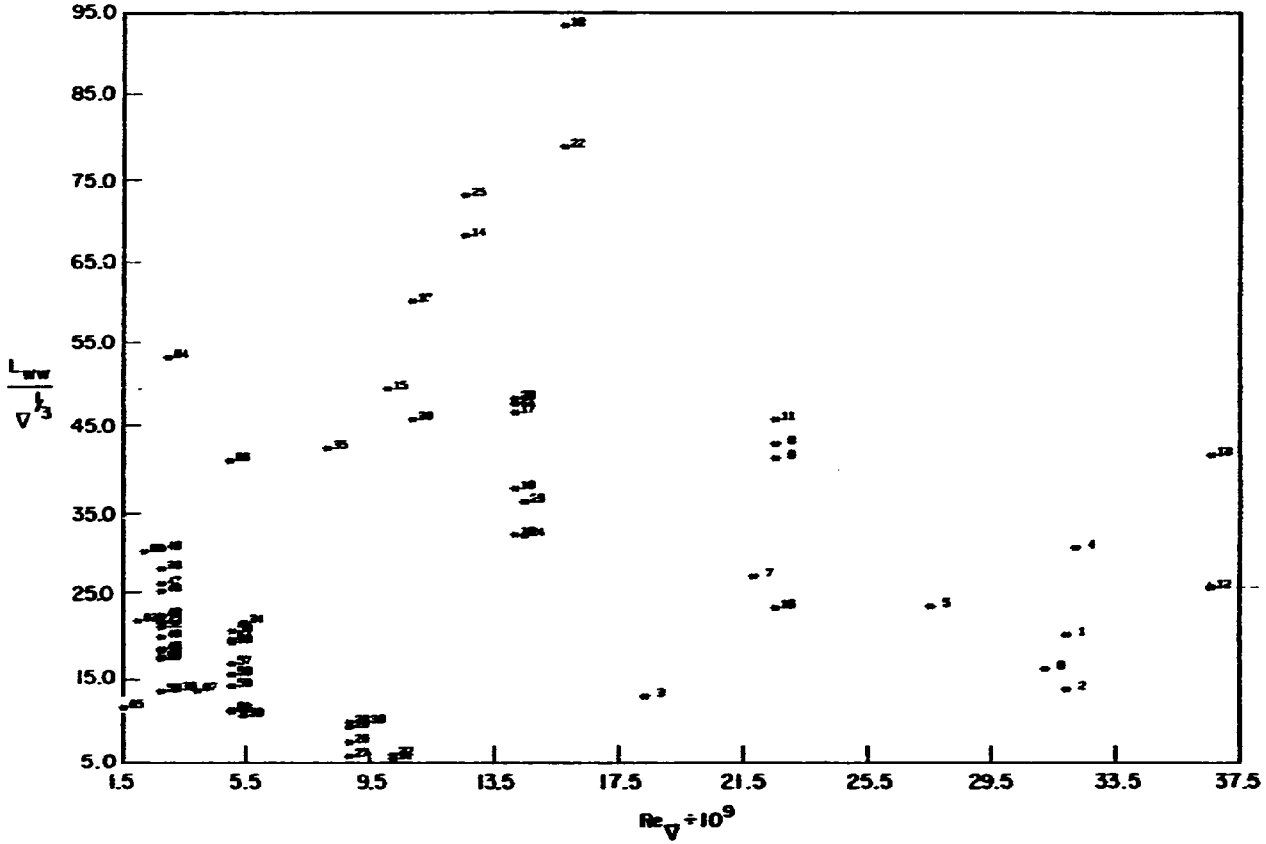

Figure 25 White-water wake length divided by vessel displacement ($L_{ww}/\nabla^{1/3}$) vs displacement Reynolds number (Re_{∇}).

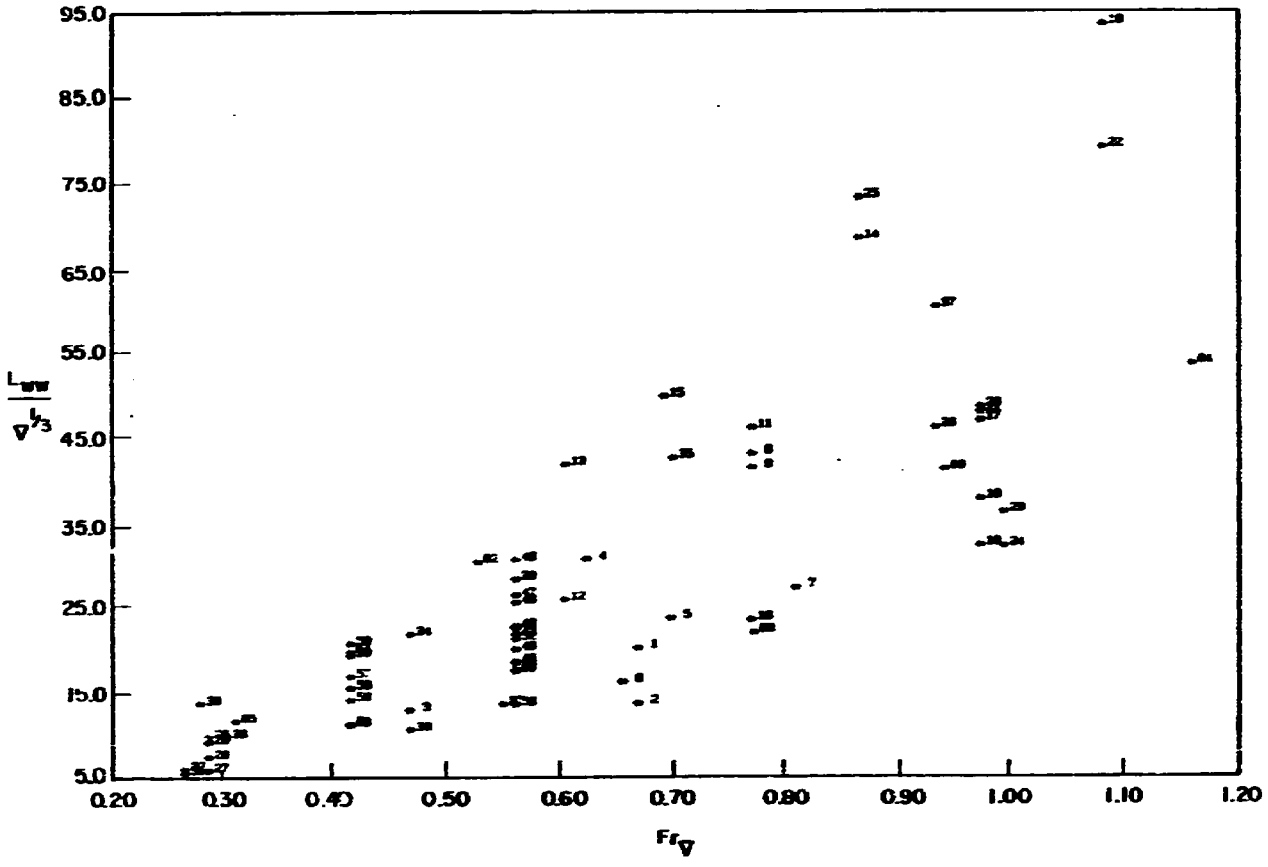

Figure 26 White-water wake length divided by vessel displacement ($L_{ww}/\nabla^{1/3}$) vs displacement Froude number (Fr_∇).

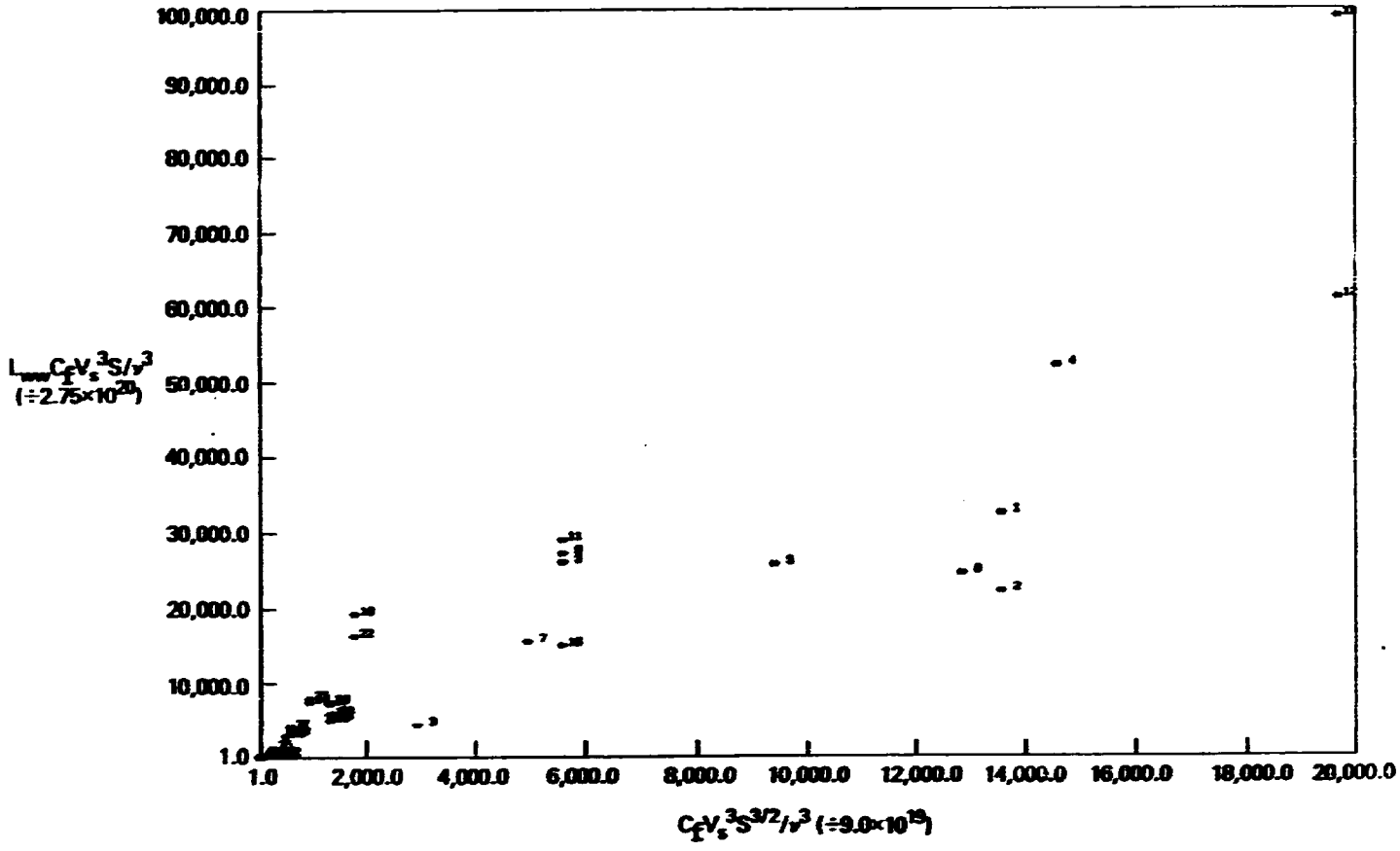

Figure 27 $L_{ww}C_fV_s^3S/\nu^3$ vs $C_fV_s^3S^{3/2}/\nu^3$

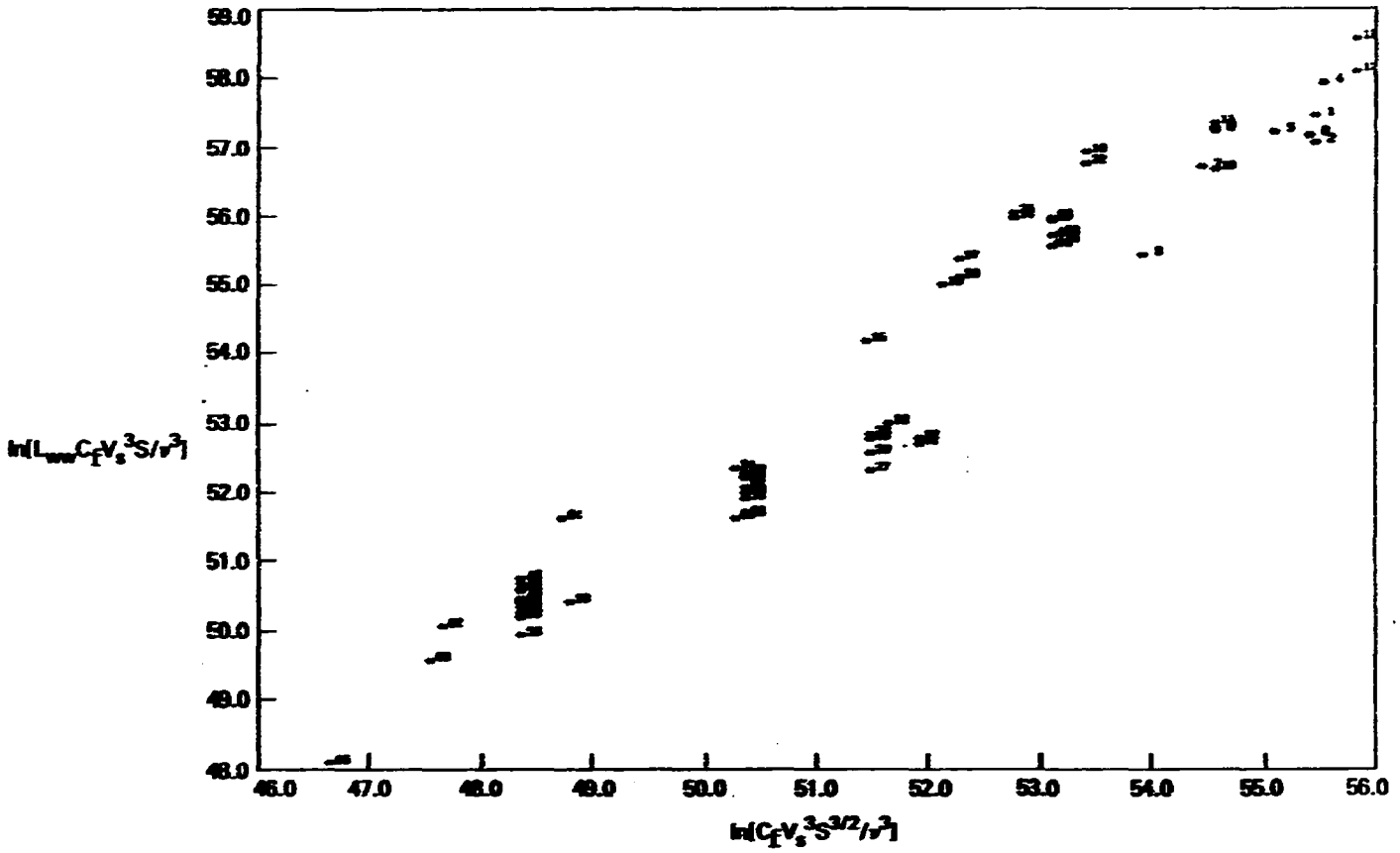

Figure 28 $\ln [L_{ww} C_f V_s^3 S/\nu^3]$ vs $\ln [C_f V_s^3 S^{3/2}/\nu^3]$

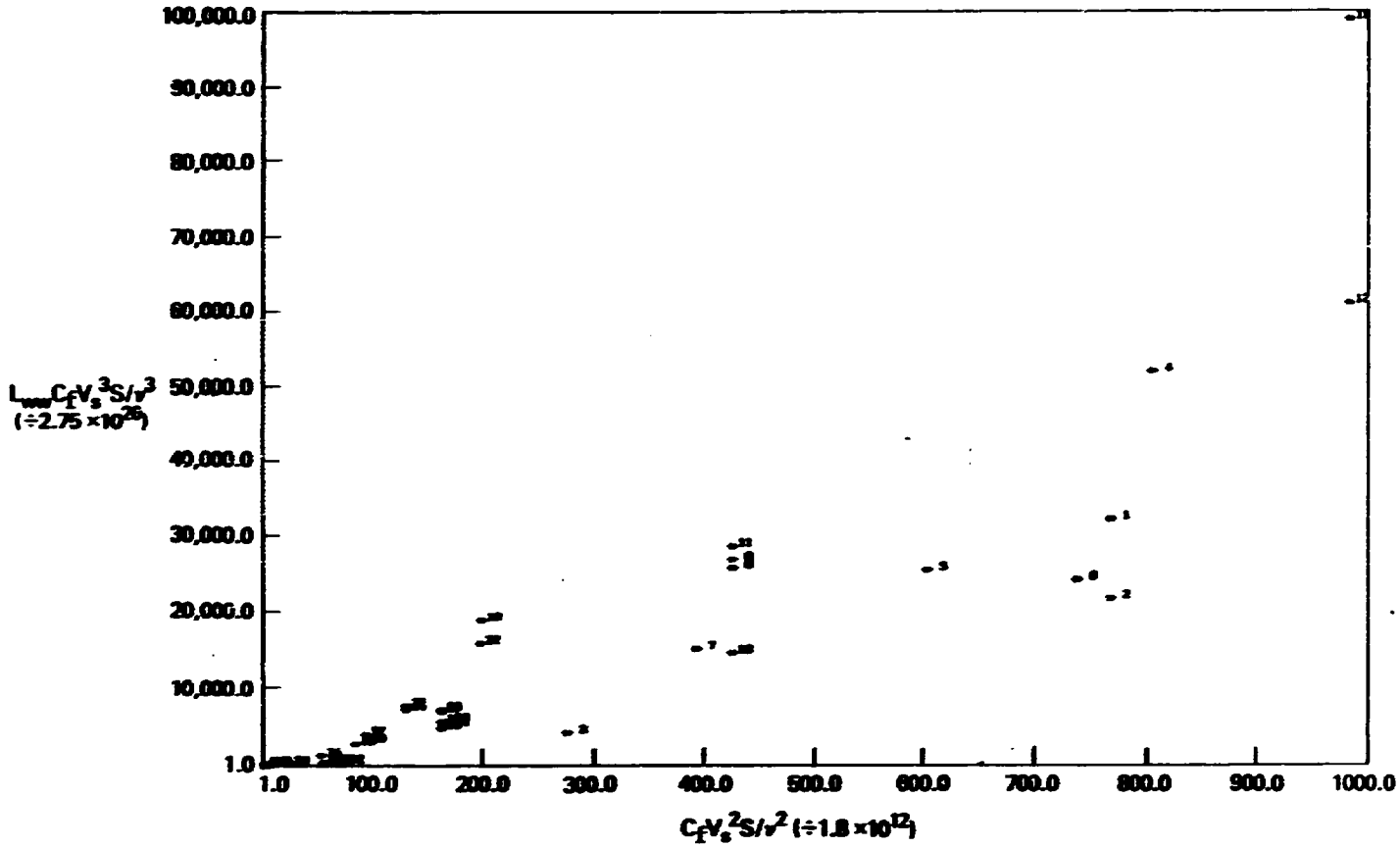

Figure 29 $L_{ww}C_fV_s^3S/v^3$ vs $C_fV_s^2S/v^2$

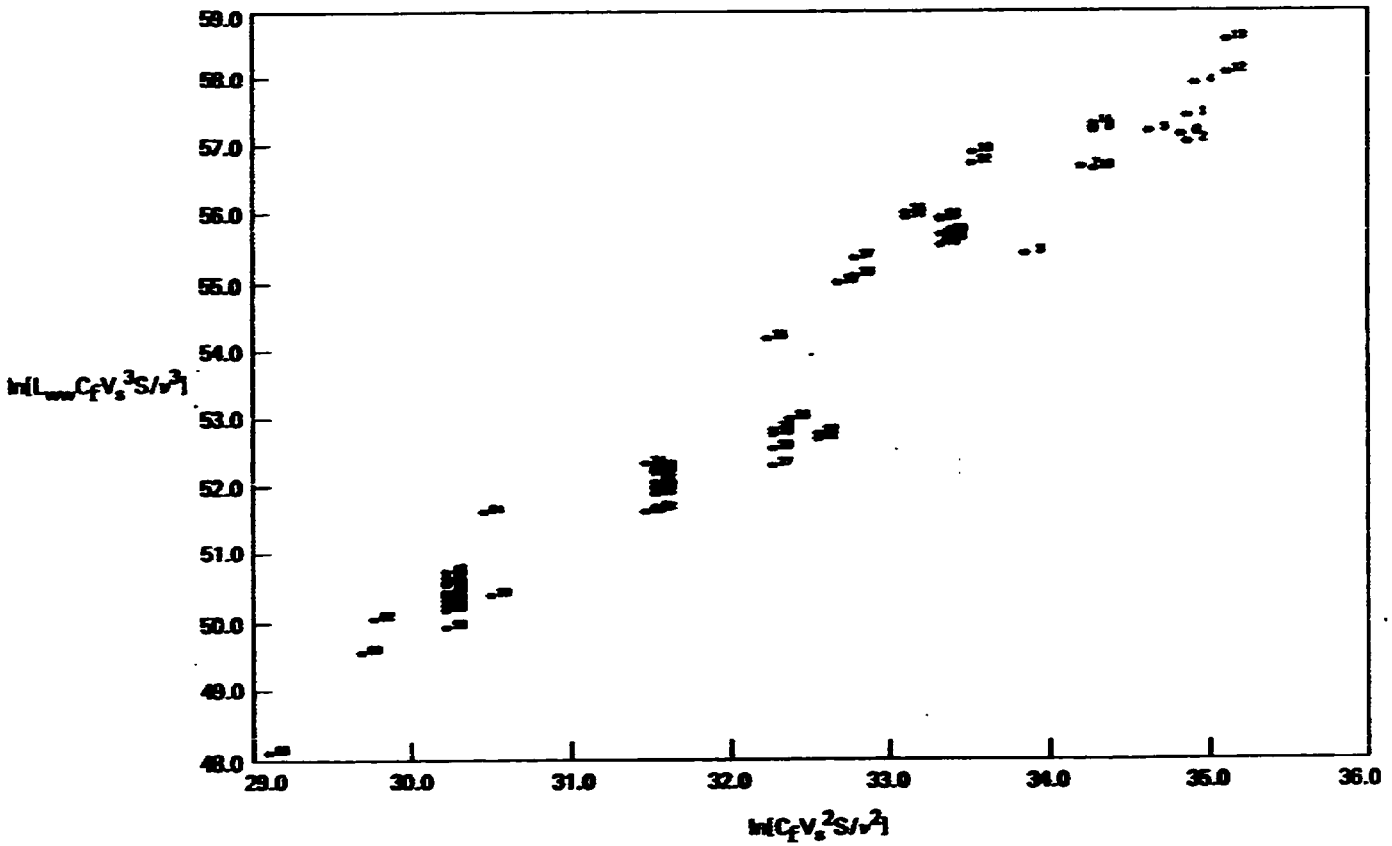

Figure 30 $\ln [L_{ww} C_f V_s^3 S/\nu^3]$ vs $\ln [C_f V_s^2 S/\nu^2]$

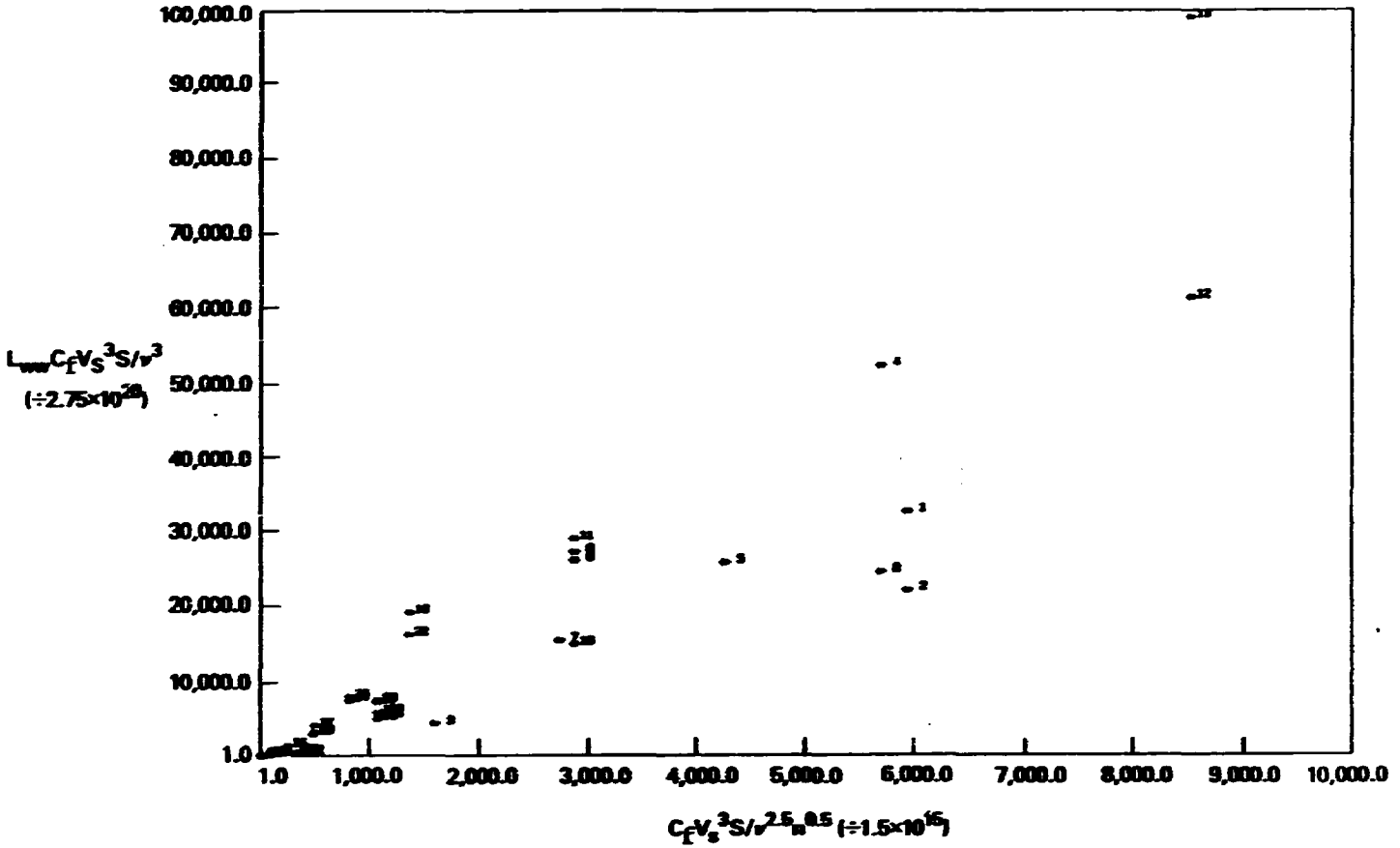

Figure 31 $L_{ww}C_fV_s^3S/\nu^3$ vs $C_fV_s^3S/\nu^{2.5}n^{0.5}$

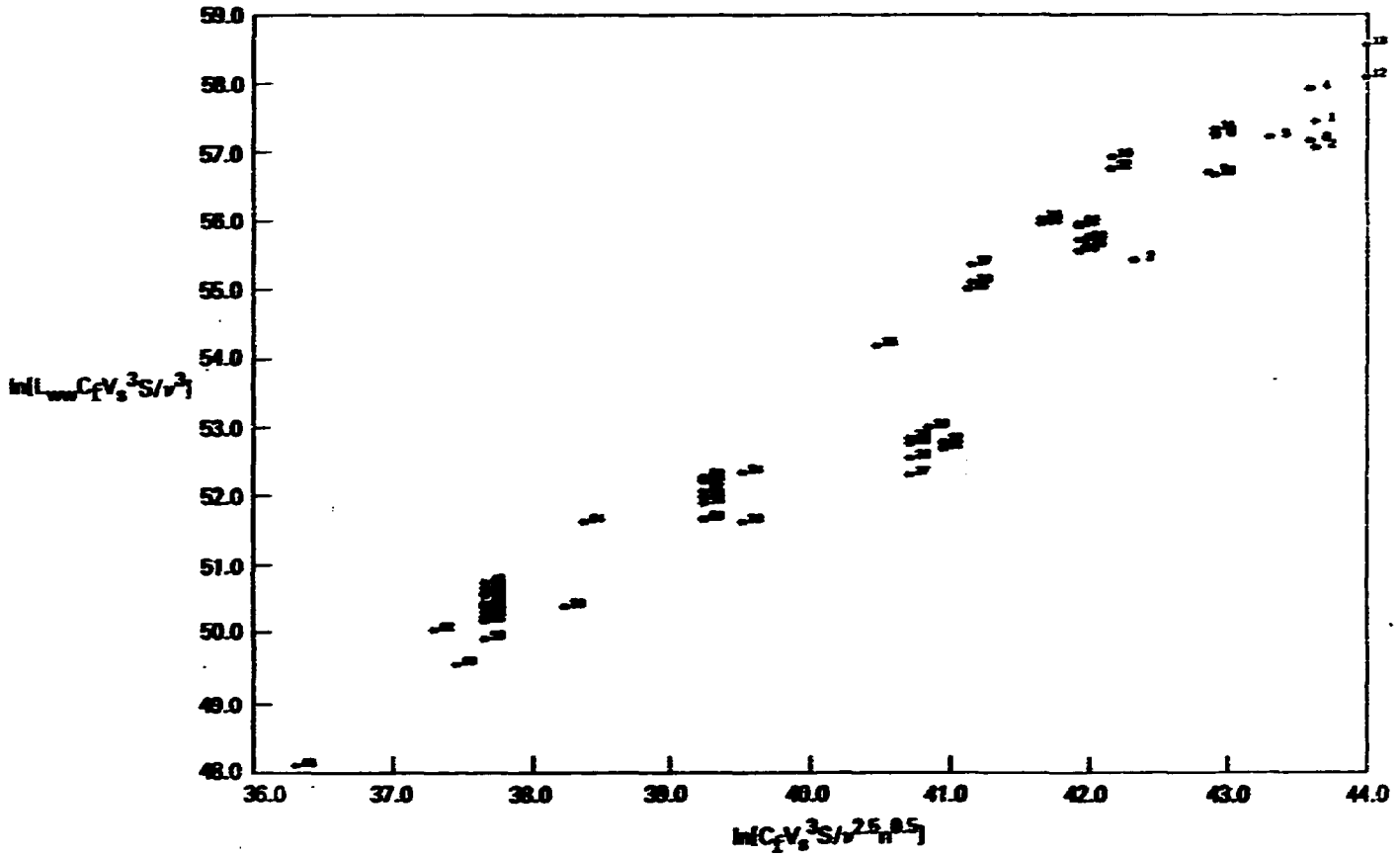

Figure 32 ln $[L_{ww} C_f V_s^3 S/\nu^3]$ vs ln $[C_f V_s^3 S/\nu^{2.5} n^{0.5}]$

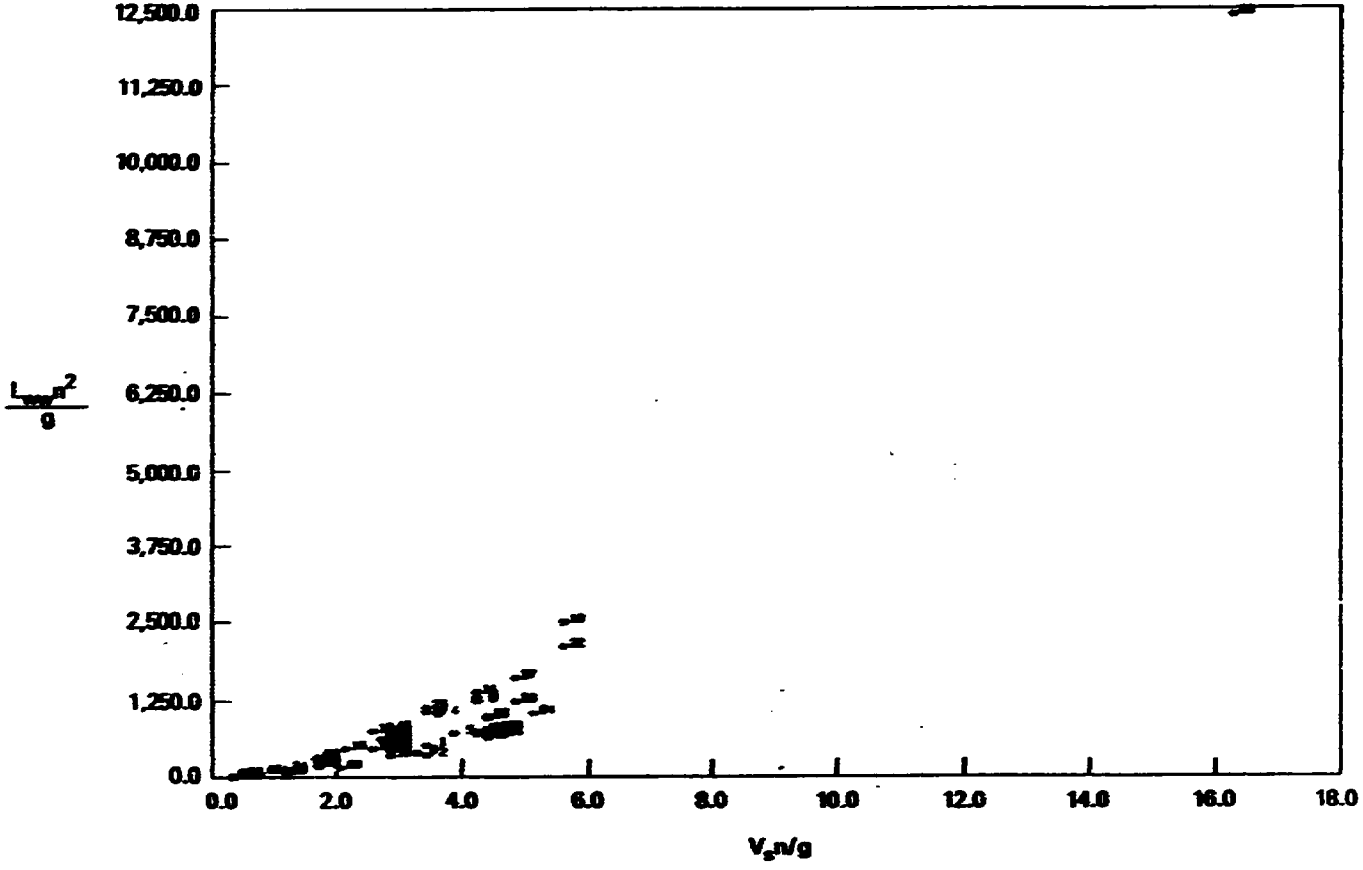

Figure 33 $L_{ww}n^2/g$ vs $V_s n/g$

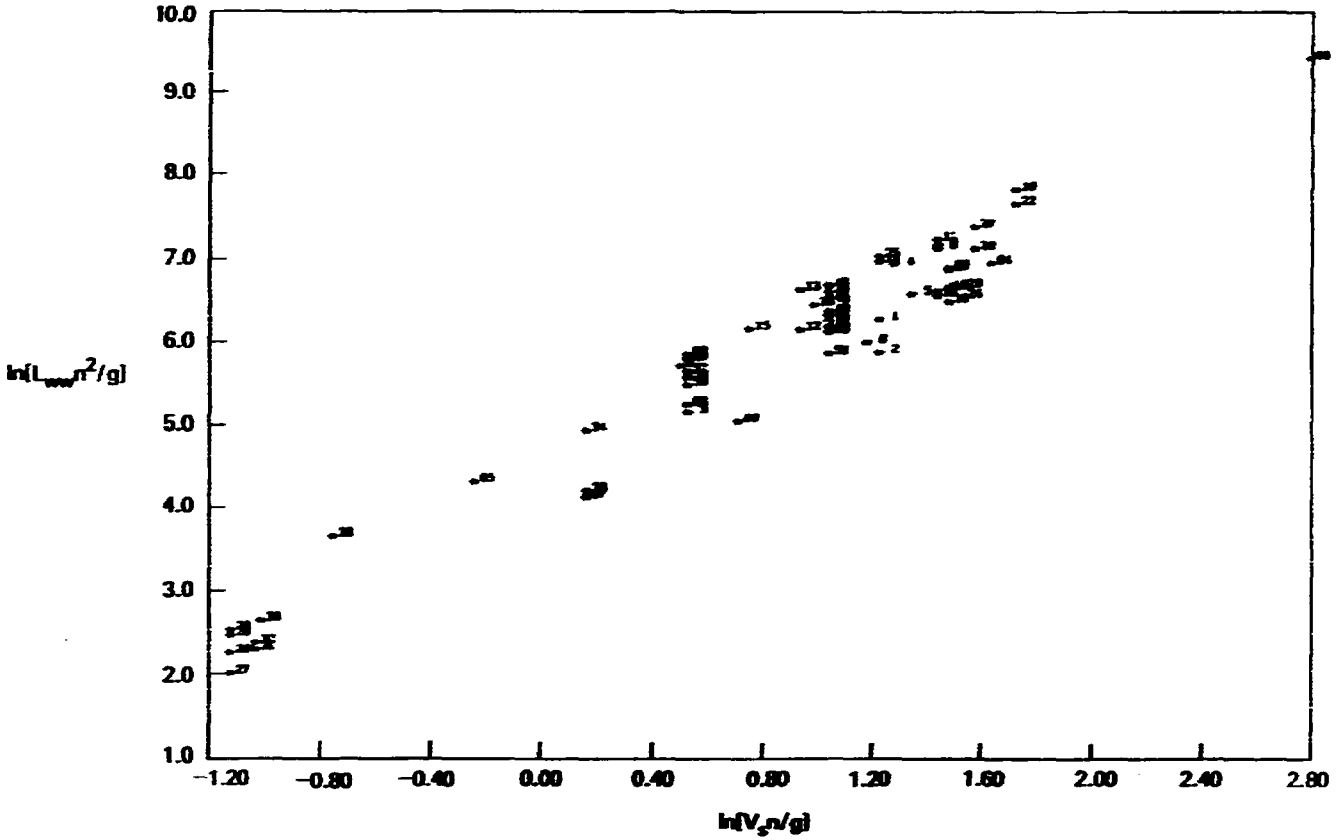

Figure 34 $\ln[L_{ww} n^2/g]$ vs $\ln[V_s n/g]$

R-1060(B)

Figure 35 Closeup aerial photograph of the white-water wake generated by the USS Moale.

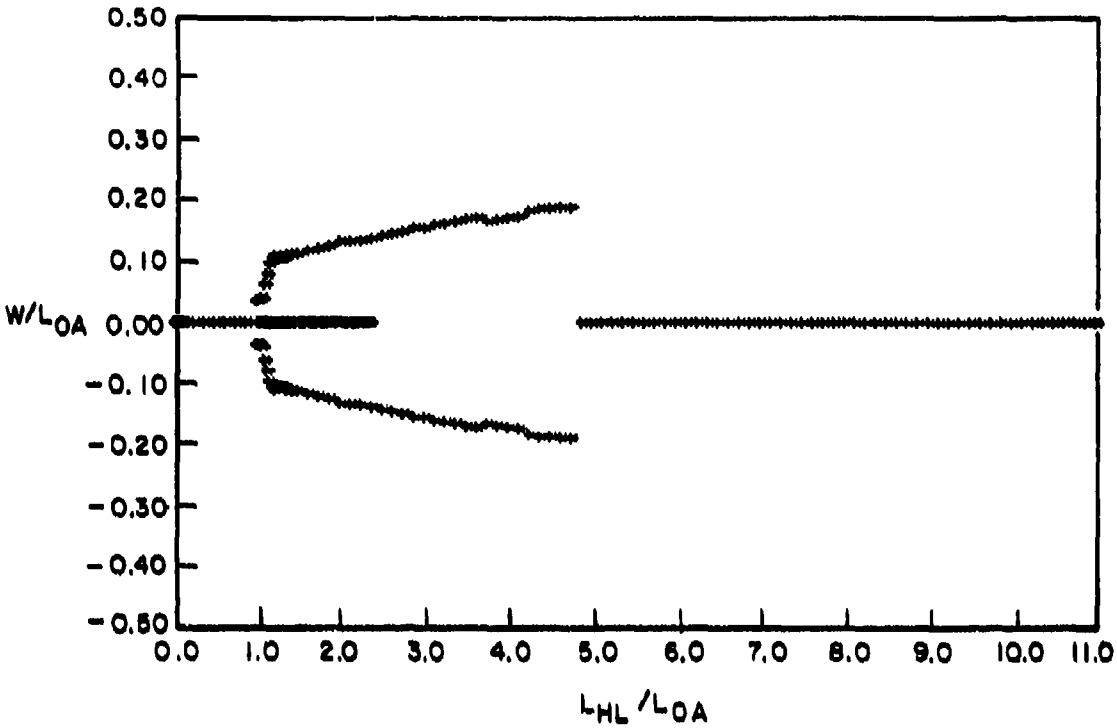

R-1067

Figure 36 Photograph and plot of the white-water wake generated by the USS Moale at 16 knots.

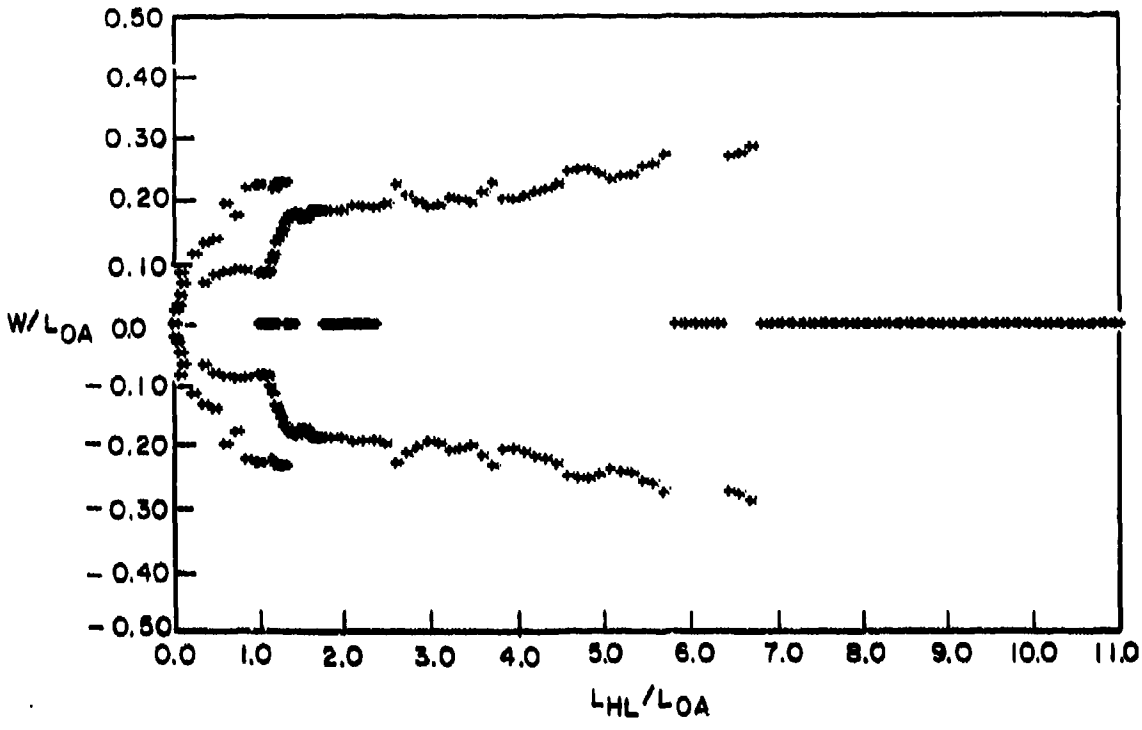

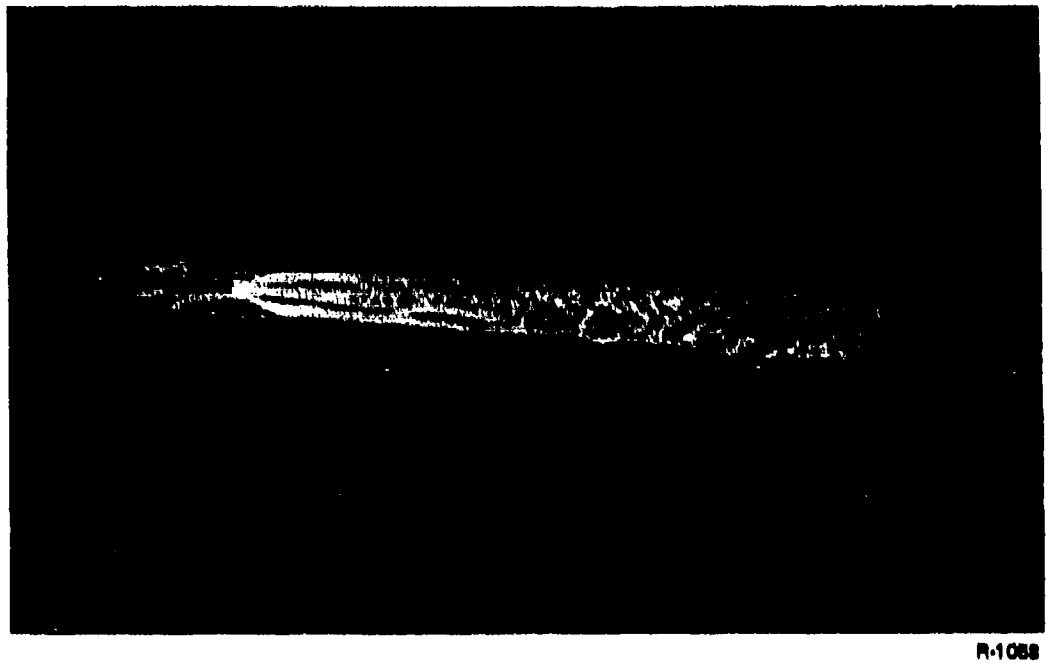

R-1088

Figure 37 Photograph and plot of the white-water wake generated by the USS Moale at 20 knots.

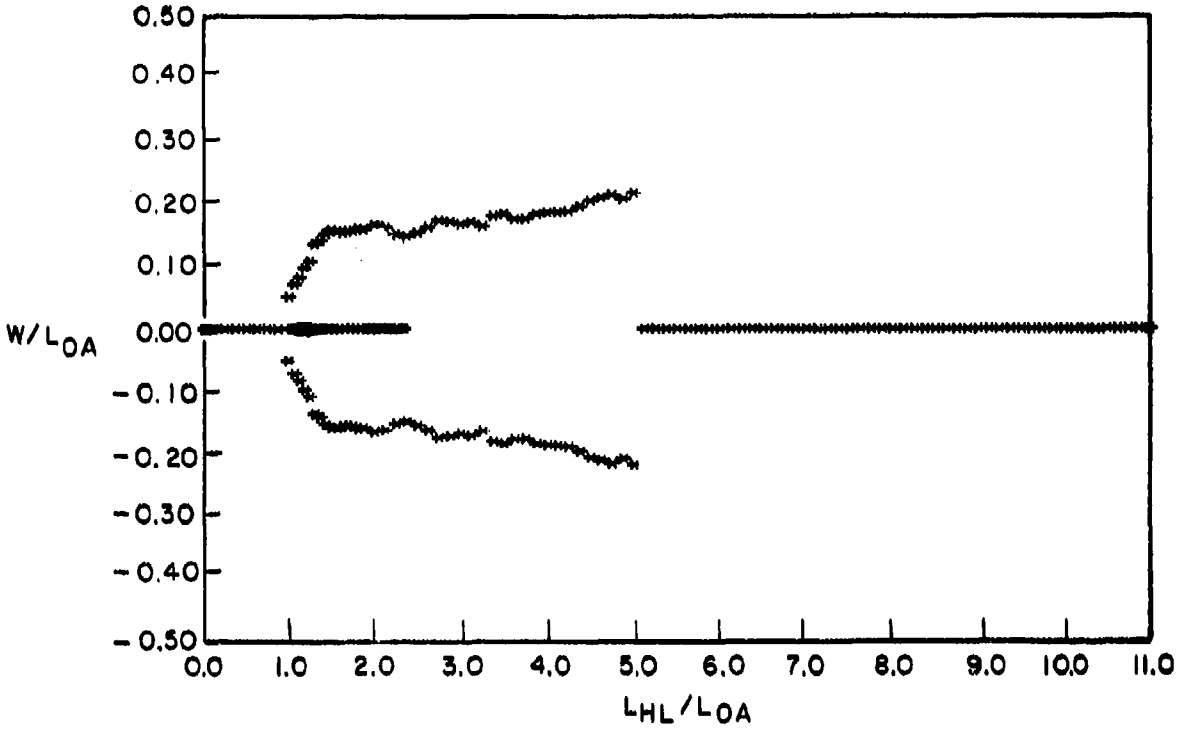

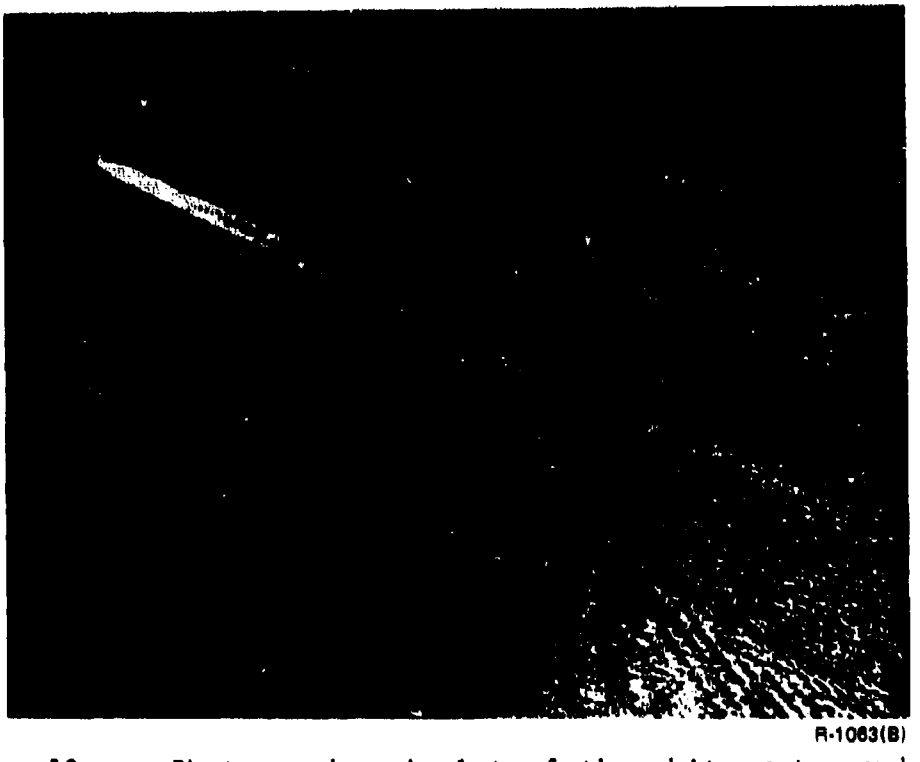

Figure 38 Photograph and plot of the white-water wake generated by an American destroyer at 20 knots.

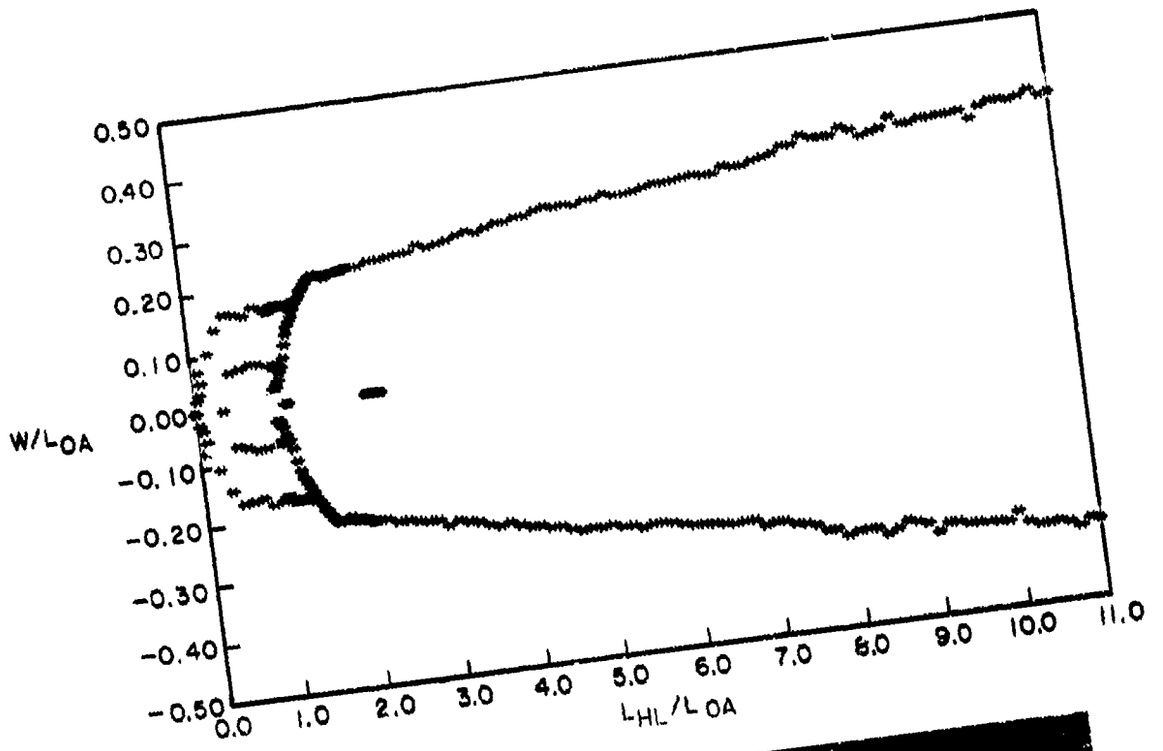

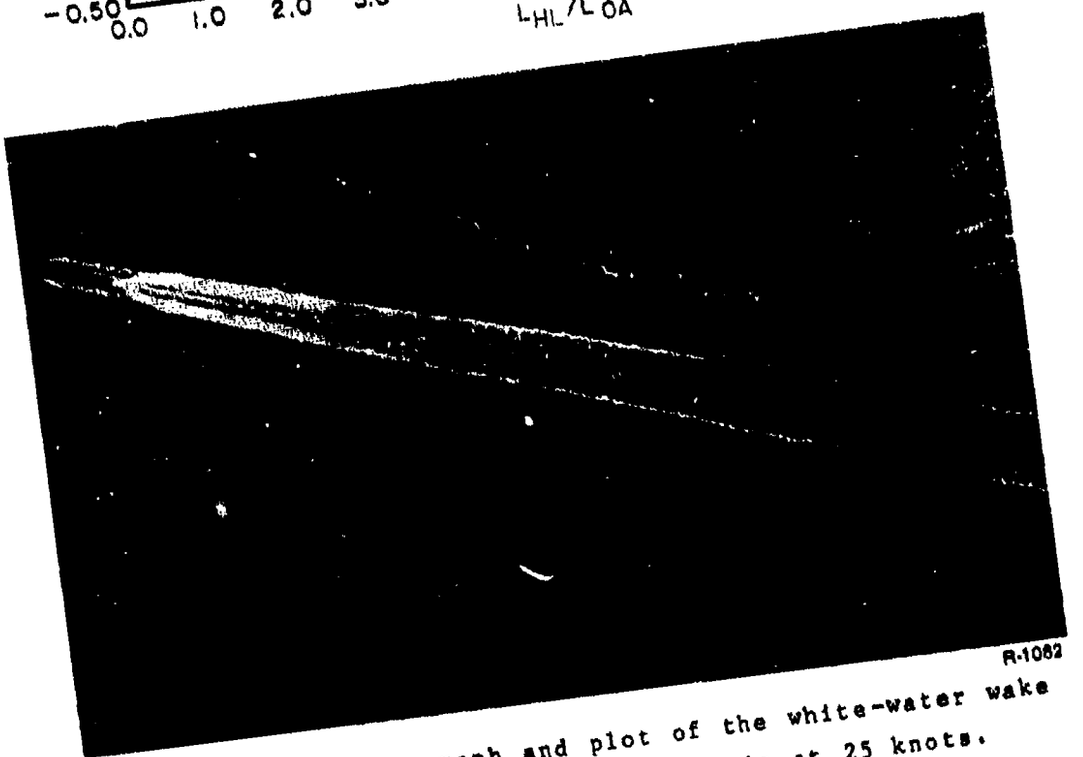

Figure 39 Photograph and plot of the white-water wake generated by the USS Moale at 25 knots.

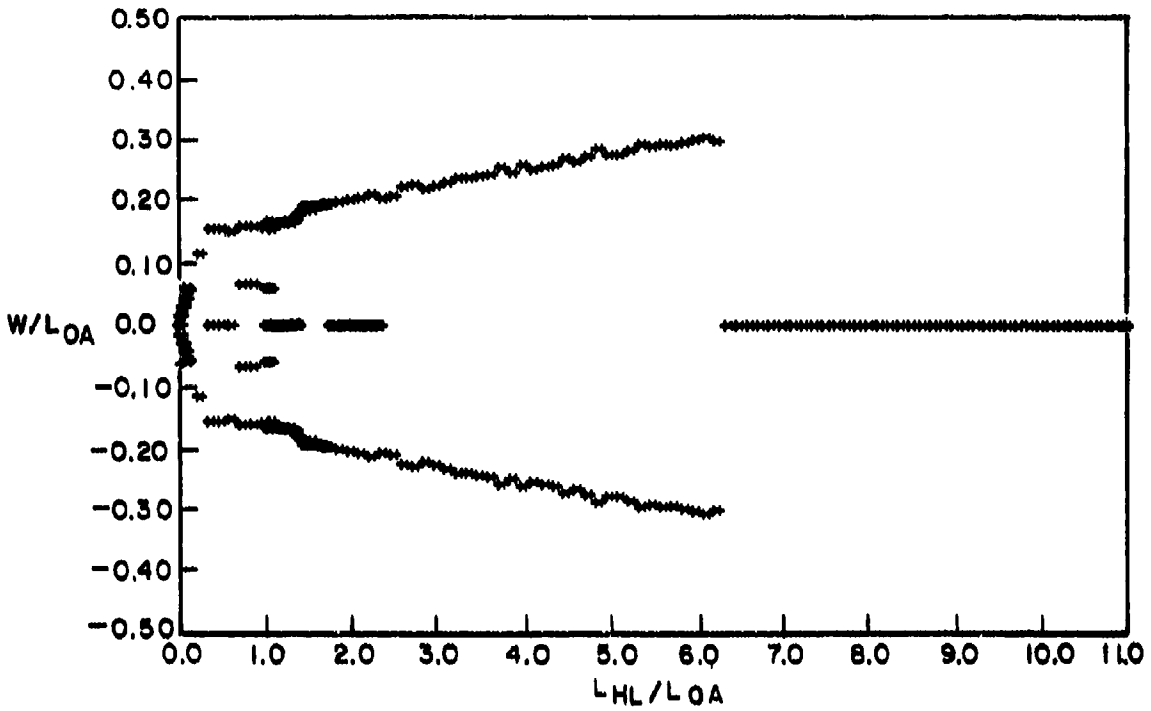

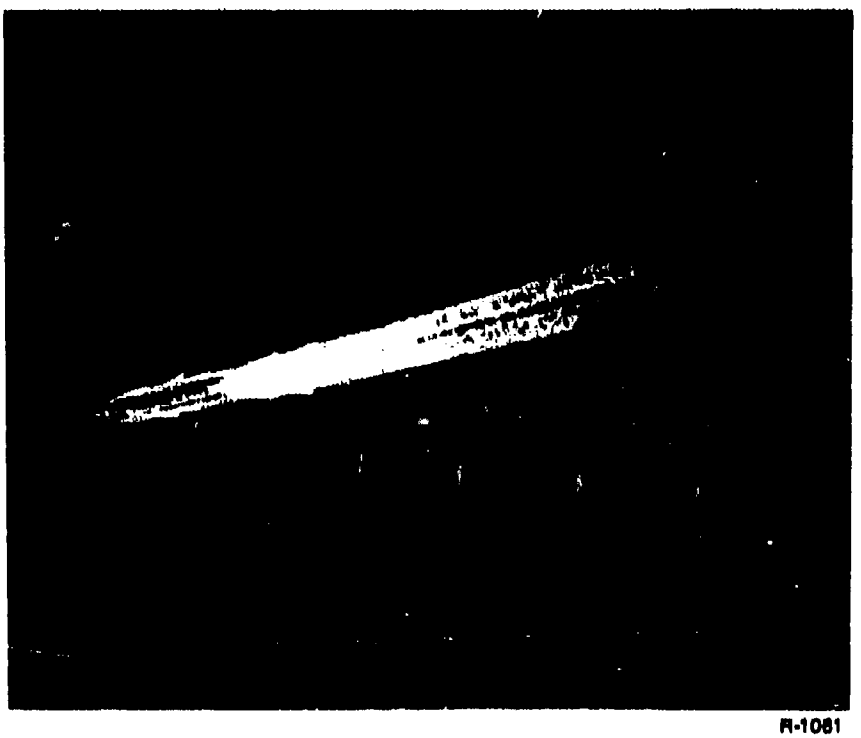

Figure 40 Photograph and plot of the white-water wake generated by a German Narvik class destroyer at 25 knots.

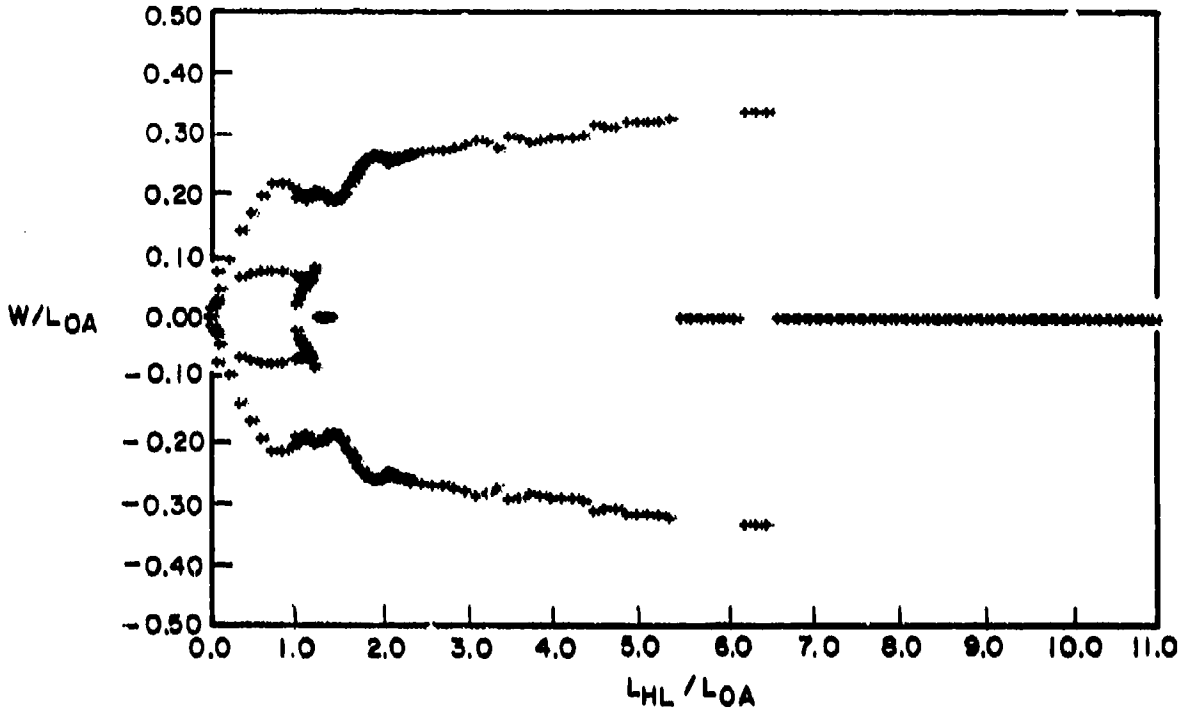

R-1084

Figure 41 Photograph and plot of the white-water wake generated by the USS Moale at 33 knots.

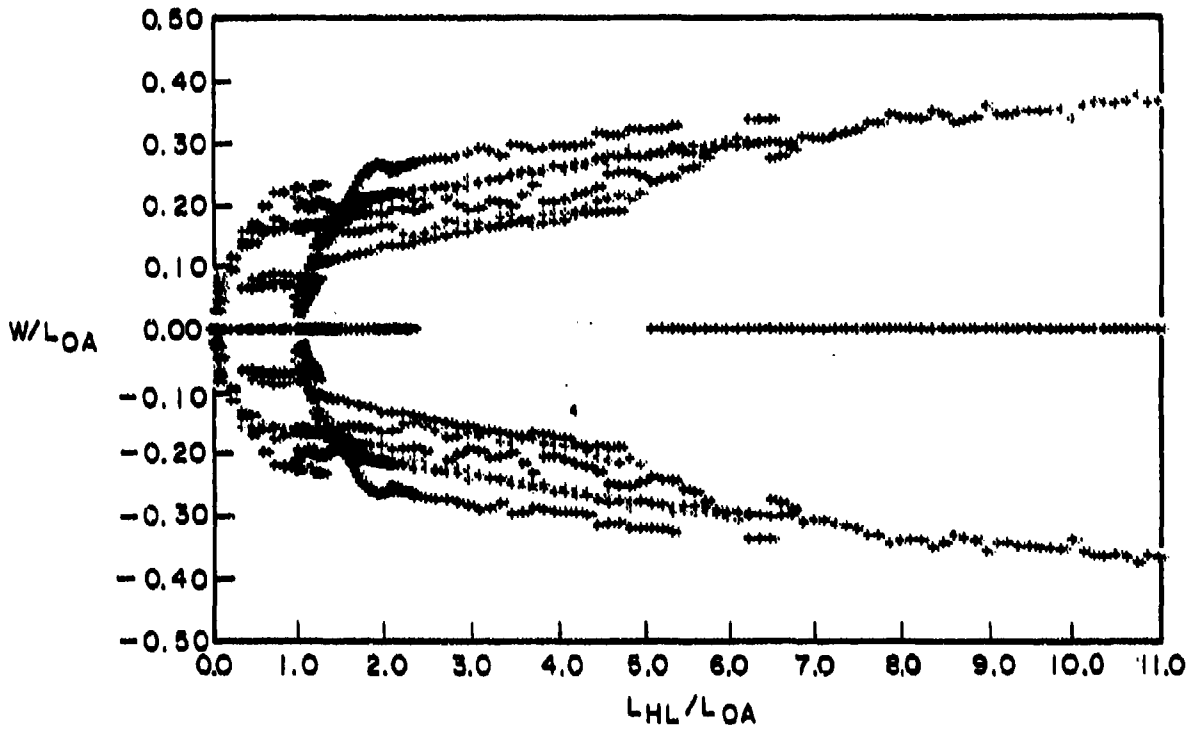

Figure 42 Superposition of the white-water wakes generated by the Moale at 16, 20, 25 and 33 knots, the Narvik class destroyer at 25 knots and the American destroyer at 20 knots.

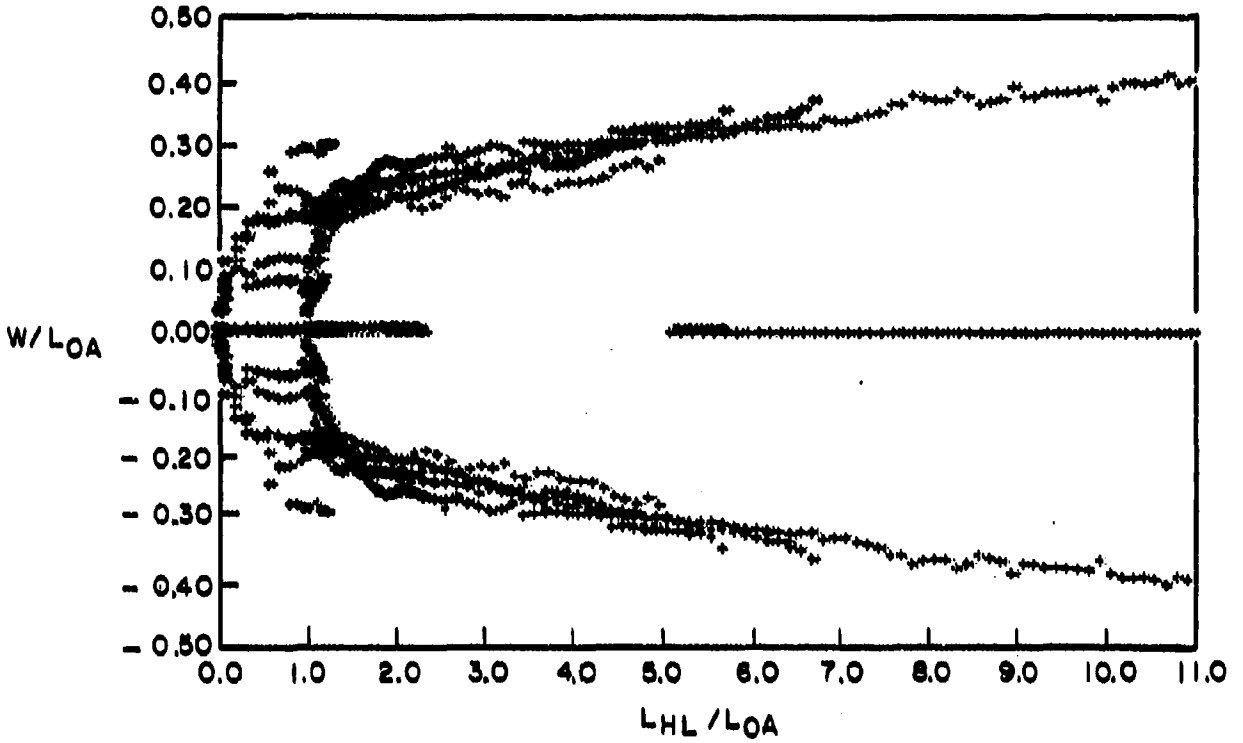

Figure 43 Superposition of the six destroyer wakes multiplied by constants (based on the velocity differences) to demonstrate the possible existence of a similarity solution for far wake spreading.

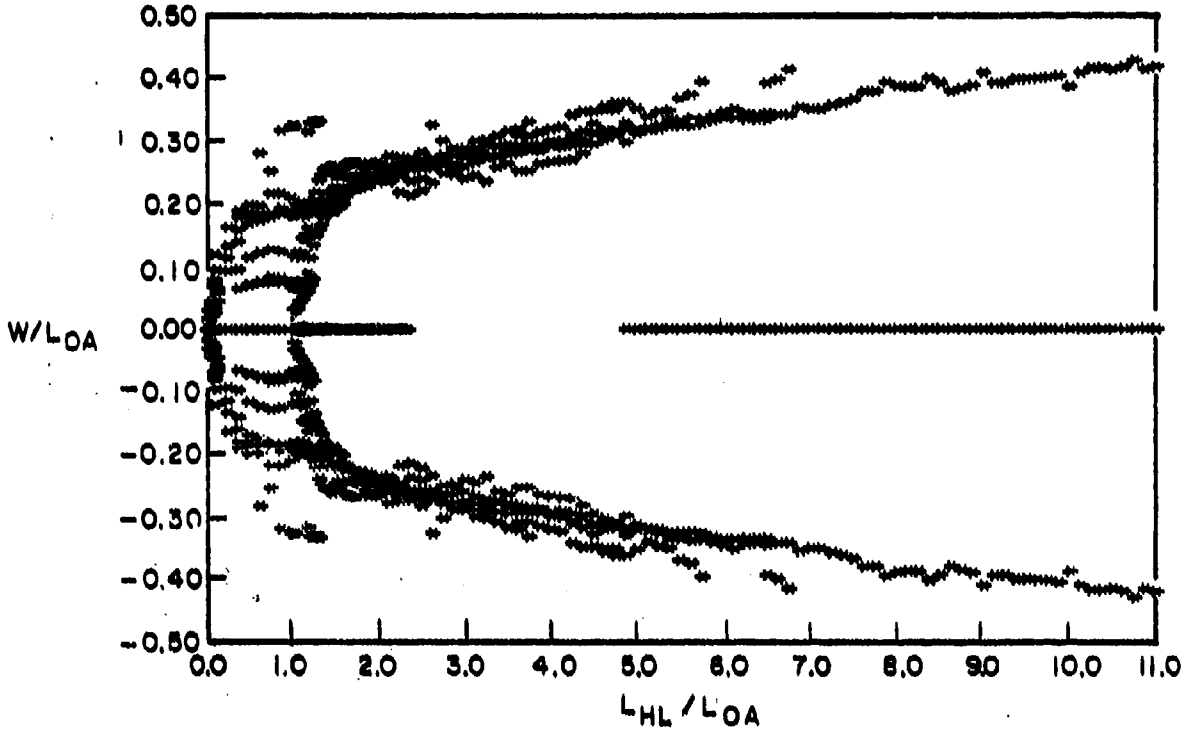

Figure 44 Superposition of the six destroyer wakes multiplied by constants (based on the propeller rpm differences) to demonstrate the possible existence of a similarity solution for far wake spreading.

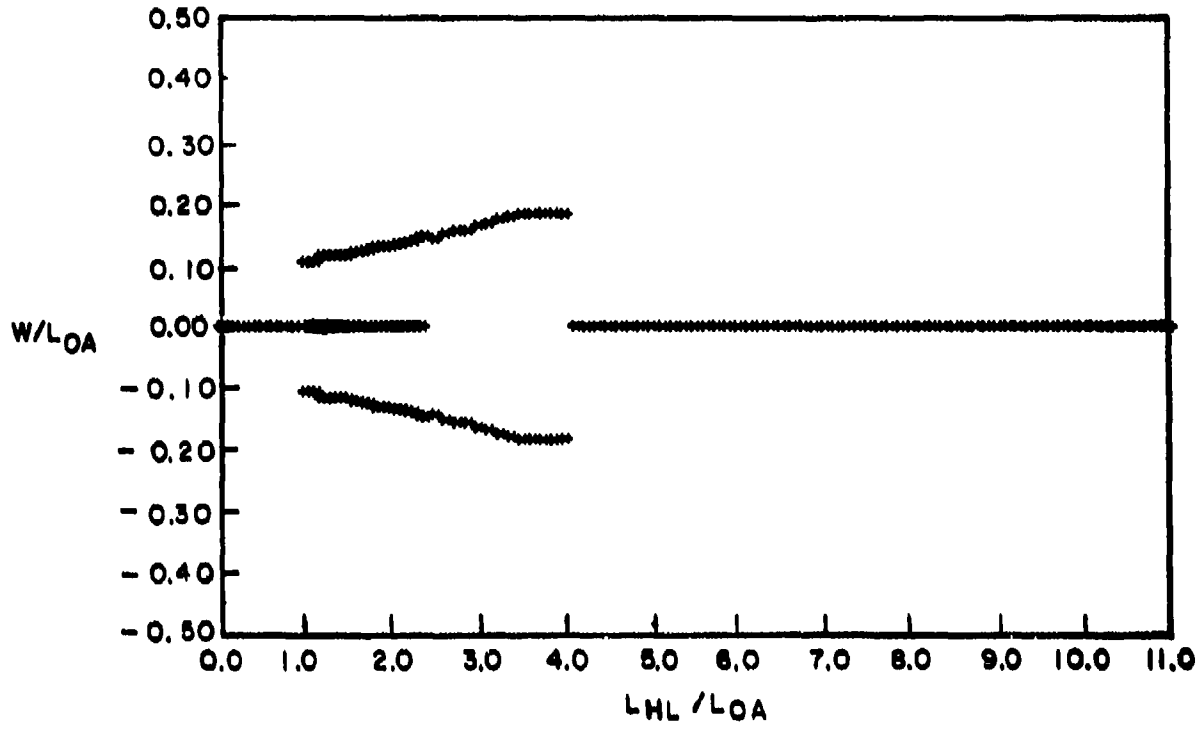

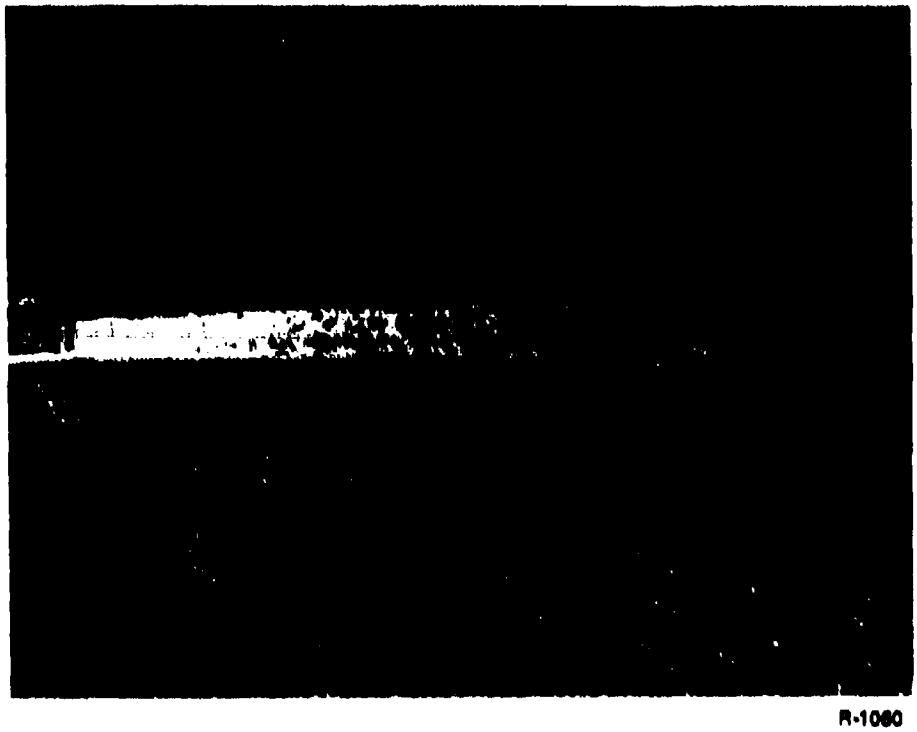

R-1060

Figure 45 Photograph and plot of the white-water wake generated by the USS Saratoga at 22 knots.

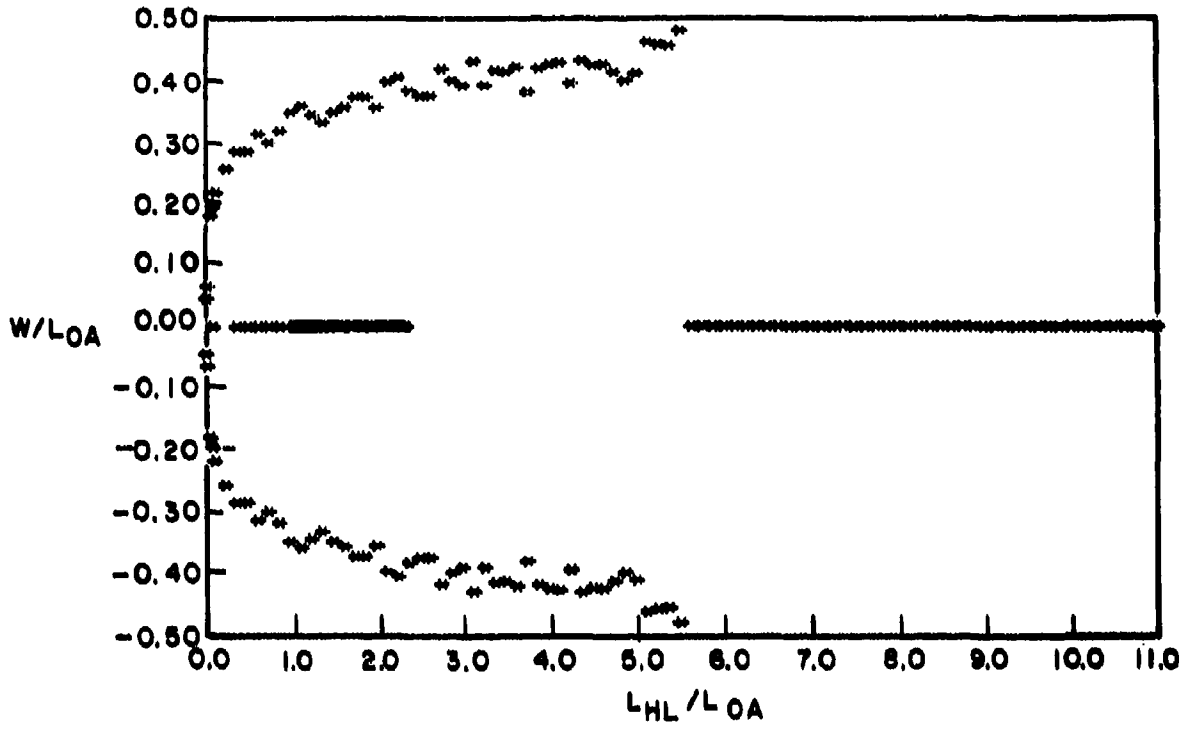

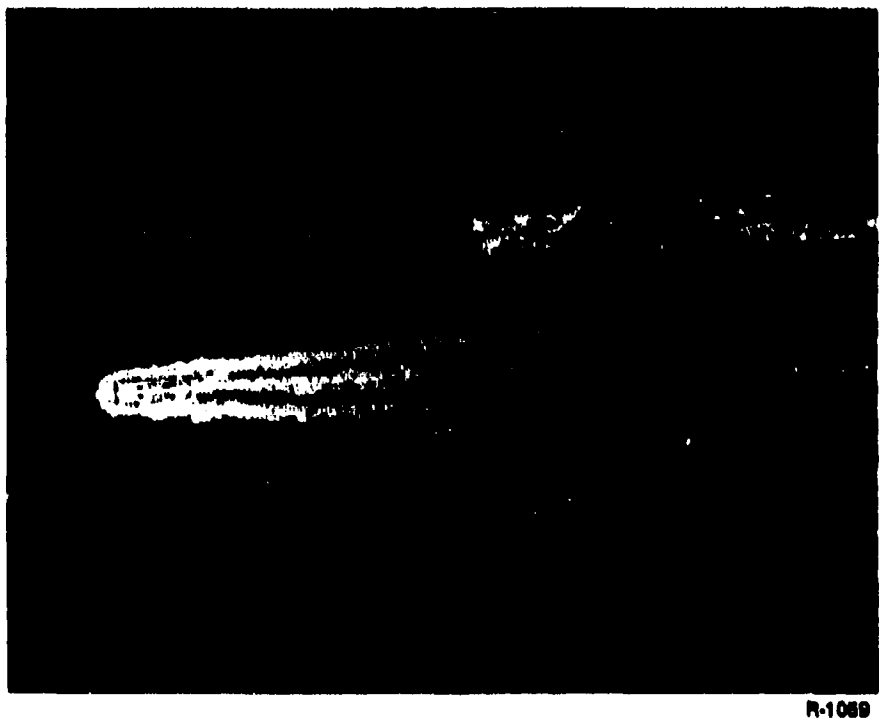

Figure 46 Photograph and plot of the white-water wake generated by the ferry boat, Uncatena, at 15.5 knots.

Appendix A

Dimensionless Groups

Before listing the eighteen groups of functional relationships, an array titled $\underline{L}$ will be defined, where $\underline{L}$ represents any one of the geometric length scales [L_{wl}, B_{wl}, D_{wl}, $S^{1/2}$, $\Delta^{1/3}$, D_p, D_T]. The first of the eighteen groups [$L_{ww}/\underline{L}$], is a function of the following 51 products of individual variables:

1) $V_s \underline{L}/\nu$ — Reynolds number

2) $V_s/n\ \underline{L}$ — Advance ratio

3) $V_s^2/g\ \underline{L}$ — Froude number

4) $(g^{1/2}/\nu)\ \underline{L}^{3/2}$

5) $n^2\underline{L}/g$

6) $n\underline{L}^2/\nu$

7) $V_s n/g$

8) $V_s^2/\nu n$

9) $V_s^3/\nu g$

10) $n^3\nu/g^2$

11) $EHP/V_s^2 \mu \underline{L} = (2\nu 550)^{-1}\ [C_T V_s S/\underline{L}]$

12) $EHP/V_s^3 \rho \underline{L}^2 = (2 \cdot 550)^{-1}\ [C_T S/\underline{L}^2]$

13) $R_T/V_s \mu \underline{L} = (2\nu)^{-1}\ [C_T V_s S/\underline{L}]$

14) $R_T/V_s^2 \rho \underline{L}^2 = (2)^{-1}\ [C_T S/\underline{L}^2]$

15) $EHP/\mu n^2 \underline{L}^3 = (2\nu 550)^{-1}\ [C_T V_s^3 S/n^2 \underline{L}^3]$

16) $EHP/\rho n^3 \underline{L}^5 = (2 \cdot 550)^{-1}\ [C_T V_s^3 S/n^3 \underline{L}^5]$

17) $EHP/R_T n\underline{L} = [V_s/n\underline{L}]$

18) $R_T/\mu n\underline{L}^2 = (2\nu)^{-1}\ [C_T V_s^2 S/\underline{L}^2 n]$

19) $EHP/\mu n^2 \underline{L}^3 = (2 \cdot 550\nu)^{-1}\ [C_T V_s^3 S/\underline{L}^3 n^2]$

20) $R_T/\rho n^2 \underline{L}^4 = (2)^{-1}\ [C_T V_s^2 S/n^2 \underline{L}^4]$

21) $EHP/R_T L^{1/2} g^{1/2} = (550)^{-1} [V_s/gL)^{1/2}$

22) $[R_T^2/EHPL\mu]^{1/2} = (550/2\nu)^{1/2} [C_T V_s S/L]^{1/2}$

23) $[R_T^3/\rho L^2 EHP^2]^{1/3} = (550^2/2)^{1/3} [C_T S/L^2]^{1/3}$

24) $R_T^2/\mu LEHP = (550/2\nu) [C_T V_s S/L]$

25) $R_T/(\mu^2 g L^3)^{1/2} = (2\nu g^{1/2})^{-1} [C_T V_s^2 S/L^{3/2}]$

26) $R_T\rho/\mu^2 = (2\nu^2)^{-1} [C_T V_s^2 S]$

27) $R_T^{3/2}/EHP\rho^{1/2} L = (550/2^{1/2}) [C_T^{1/2} S^{1/2}/L]$

28) $R_T/\rho L^3 g = (2g)^{-1} [C_T V_s^2 S/L^3]$

29) $EHP/\mu L^2 g = (2\nu 550g)^{-1} [C_T V_s^3 S/L^2]$

30) $[EHP\rho^2 L/\mu^3]^{1/2} = (2\nu^3 550)^{-1/2} [C_T V_s^3 SL]^{1/2}$

31) $EHP/\rho L^{7/2} g^{3/2} = (2g^{3/2} 550)^{-1} [C_T V_s^3 S/L^{7/2}]$

32) $EHPn/V_s^3\mu = (2\nu 550)^{-1} [C_T Sn]$

33) $EHPn^2/V_s^5\rho = (2 \cdot 550)^{-1} [C_T Sn^2/V_s^2]$

34) $R_T n/V_s^2 \mu = (2\nu)^{-1} [C_T Sn]$

35) $R_T n^2/V_s^4 \rho = (2)^{-1} [C_T Sn^2/V_s^2]$

36) $EHPg/\mu V_s^4 = (g/2\nu 550) [C_T S/V_s]$

37) $EHP\rho/\mu^2 V_s = (2\nu^2 550)^{-1} [C_T V_s^2 S]$

38) $EHPg^2/\rho V_s^7 = (g^2/2 \cdot 550) [C_T S/V_s^4]$

39) $R_T g/\mu V_s^3 = (g/2\nu) [C_T S/V_s]$

40) $R_T g^2/\rho V_s^6 = (g^2/2) [C_T S/V_s^4]$

41) $EHPn/R_T g = (550)^{-1} [V_s n/g]$

42) $[R_T^3 n/EHP^2\mu]^{1/2} = (550^2/2\nu)^{1/2} [C_T Sn]^{1/2}$

43) $[EHP^2\rho^3/\mu^5 n]^{1/2} = (2\nu^{5/2} 550)^{-1} [C_T V_s^3 S/n^{1/2}]$

44) $R_T^{5/4} n^{1/2}/EHP\rho^{1/4} = (550/2^{1/4}) [C_T Sn^2/V_s^2]^{1/4}$

45) $EHPn^4/\mu g^3 = (2\nu 550g^3)^{-1} [C_T V_s^3 Sn^4]$

46) $EHPn^7/\rho g^5 = (2g^5 550)^{-1} [C_T V_s^3 Sn^7]$

47) $R_T n^3/\mu g^2 = (2g^2\nu)^{-1} [C_T V_s^2 Sn^3]$

48) $R_T n^6/g^4\rho = (2g^4)^{-1}\ [C_T V_s^2 S n^6]$

49) $[R_T^4 g/EHP^3\mu]^{1/3} = 550(g/2\nu)^{1/3}\ [C_T S/V_s]^{1/3}$

50) $[R_T^7 g^2/EHP^6\rho]^{1/7} = (550^6 g^2/2)^{1/7}\ [C_T S/V_s^4]^{1/7}$

51) $[EHP^3\rho^4/\mu^7 g]^{1/4} = (2^3\nu^7 g 550^3)^{-1/4}\ [C_T^3 V_s^9 S^3]^{1/4}$.

The second of the groups, $[L_{ww} n^2/g]$, is a function of the following eight products:

1) $[n^2 \underline{L}/g]$

2) $EHPn/R_T g = [V_s n/g]$

3) $V_s n/g$

4) $EHPn^4/\mu g^3 = (\nu g^3)^{-1}\ [C_T V_s^3 S n^4]$

5) $EHPn^7/\rho g^5 = (g^5)^{-1}\ [C_T V_s^3 S n^7]$

6) $R_T n^6/g^4\rho = (g^4)^{-1}\ [C_T V_s^2 S n^6]$

7) $R_T n^3/\mu g^2 = (g^2\nu)^{-1}\ [C_T V_s^2 S n^3]$

8) $n^3\nu/g^2$.

The third group, $[L_{ww} n/V_s]$, is a function of the following eleven products:

1) $\underline{L}n/V_s$

2) $V_s n/g$

3) $EHPn/R_T g = [V_s n/g]$

4) $EHPn/\mu V_s^3 = (\nu)^{-1}\ [C_T S n]$

5) $R_T \underline{L} n/EHP = [V_s/n\underline{L}]$

6) $EHPn^2/\rho V_s^5 = [C_T S n^2/V_s^2]$

7) $EHP\mu^{1/2}/(nR_T^3)^{1/2} = (\nu)^{-1}\ [C_T S n]$

8) $R_T n/\mu V_s^2 = (\nu)^{-1}\ [C_T S n]$

9) $R_T n^2/\rho V_s^4 = [C_T S n^2/V_s^2]$

10) $V_s^2\nu/n$

11) $EHP\rho^{1/4}/R_T^{5/4} n^{1/2} = [C_T S n^2/V_s^2]$.

The fourth group, $[L_{ww}g/V_s^2]$, is a function of the following eleven products:

1) $\underline{L}g/V_s^2$
2) $V_s n/g$
3) $V_s^3/\nu g$
4) $EHPg/\mu V_s^4 = (g/\nu)\,[C_T S/V_s]$
5) $EHPg^2/\rho V_s^7 = (g^2)\,[C_T S/V_s^4]$
6) $R_T g/\mu V_s^3 = (g/\nu)\,[C_T S/V_s]$
7) $R_T g^2/\rho V_s^6 = (g^2)\,[C_T S/V_s^4]$
8) $EHP/\underline{L}^{1/2} g^{1/2} R_T = [V_s/(g\underline{L})^{1/2}]$
9) $EHPn/R_T g = [V_s n/g]$
10) $[EHP^3\mu/gR_T^4]^{1/3} = (g/\nu)^{1/3}\,[C_T S/V_s]^{1/3}$
11) $[R_T^7 g^2/EHP^6\rho]^{1/7} = (g^2)^{1/7}\,[C_T S/V_s^4]^{1/7}$.

The fifth group, $[L_{ww}V_s/\nu]$, is a function of the following five products:

1) $V_s\underline{L}/\nu$
2) $R_T\rho/\mu^2 = (\nu^2)^{-1}\,[C_T V_s^2 S]$
3) $EHP\rho/\mu^2 V_s = (\nu^2)^{-1}\,[C_T V_s^2 S]$
4) $V_s^3/\nu g$
5) $V_s^2/\nu n$.

The sixth group, $[L_{ww}^2 n/\nu]$, is a function of the following five products:

1) $\underline{L}^2 n/\nu$
2) $V_s^2/\nu n$
3) $R_T\rho/\mu^2 = (\nu^2)^{-1}\,[C_T V_s^2 S]$

4) $[EHP^2\rho^3/\mu^5 n]^{1/2} = (\nu^{5/2})^{-1} [C_T V_s^3 S/n^{1/2}]$

5) $n^3\nu/g^2$.

The seventh group, $[L_{ww}^2/C_T S]$, is a function of the following eleven products:

1) $[R_T^3/\rho \underline{L}^2 EHP]^{1/3} = [\underline{L}^2/C_T S]$
2) $EHP\rho^{1/4}/R_T^{5/4} n^{1/2} = [C_T S n^2/V_s^2]^{1/4}$
3) $[R_T^7 g^2/EHP^6\rho]^{1/7} = (g^2)^{1/7} [C_T S/V_s^4]^{1/7}$
4) $EHP/V_s^3 \rho \underline{L}^2 = [C_T S/\underline{L}^2]$
5) $EHPn^2/\rho V_s^5 = [C_T S n^2/V_s^2]$
6) $EHPg^2/\rho V_s^7 = (g^2) [C_T S/V_s^4]$
7) $EHP\rho/\mu^2 V_s = (\nu^2)^{-1} [C_T V_s^2 S]$
8) $V_s^2 \rho \underline{L}^2/R_T = [\underline{L}^2/C_T S]$
9) $R_T n^2/\rho V_s^4 = [C_T S n^2/V_s^2]$
10) $R_T g^2/\rho V_s^6 = (g^2) [C_T S/V_s^4]$
11) $R_T \rho/\mu^2 = (\nu^2)^{-1} [C_T V_s^2 S]$.

The eighth group, $[L_{ww}\nu/C_T V_s S]$, is a function of the following eleven products:

1) $EHP/V_s^2 \mu \underline{L} = (\nu)^{-1} [C_T V_s S/\underline{L}]$
2) $EHPn/\mu V_s^3 = (\nu)^{-1} [C_T S n]$
3) $EHPg/\mu V_s^4 = (g/\nu) [C_T S/V_s]$
4) $EHP\rho/\mu^2 V_s = (\nu^2)^{-1} [C_T V_s^2 S]$
5) $V_s \mu \underline{L}/R_T = (\nu)^{-1} [C_T V_s S/\underline{L}]$
6) $EHP\mu^{1/2}/(nR_T^3)^{1/2} = (\nu^{-1})^{1/2} [C_T S n]^{1/2}$
7) $R_T n/\mu V_s^2 = (\nu)^{-1} [C_T S n]$
8) $[EHP^3\mu/gR_T^4]^{1/3} = (g/\nu)^{1/3} [C_T S/V_s]^{1/3}$

9) $R_T g/\mu V_s^3 = (g/\nu)\ [C_T S/V_s]$

10) $EHPL\mu/R_T^2 = (\nu)^{-1}\ [C_T V_s S/\underline{L}]$

11) $R_T \rho/\mu^2 = (\nu^2)^{-1}\ [C_T V_s^2 S]$.

The ninth group, $[L_{ww}^{3/2} g^{1/2}/\nu]$, is a function of the following five products:

1) $\underline{L}^{3/2} g^{1/2}/\nu$

2) $V_s^3/\nu g$

3) $n^3\nu/g^2$

4) $R_T \rho/\mu^2 = (\nu^2)^{-1}\ [C_T V_s^2 S]$

5) $[EHP^3 \rho^4/\mu^7 g]^{1/4} = (\nu^7 g)^{-1/4} [C_T^3 V_s^9 S^3]^{1/4}$.

The tenth group, $[L_{ww}^3 n^2 \nu/C_T V_s^3 S]$, is a function of the following five products:

1) $EHP/\mu \underline{L}^3 n^2 = (\nu)^{-1}\ [C_T V_s^3 S/\underline{L}^3 n^2]$

2) $EHP\mu^{1/2}/(nR_T^3)^{1/2} = (\nu)^{-1/2} [C_T Sn]^{1/2}$

3) $EHPn/\mu V_s^3 = (\nu)^{-1}\ [C_T Sn]$

4) $EHPn^4/\mu g^3 = (\nu g^3)^{-1}\ [C_T V_s^3 Sn^4]$

5) $[EHP^2 \rho^3/\mu^5 n]^{1/2} = (\nu^{-5/2})\ [C_T V_s^3 S/n^{1/2}]$.

The eleventh group, $[L_{ww}^5 n^3/C_T V_s^3 S]$, is a function of the following five products:

1) $EHP/\rho n^3 \underline{L}^5 = [C_T V_s^3 S/\underline{L}^5 n^3]$

2) $EHP\rho^{1/4}/R_T^{5/4} n^{1/2} = [C_T Sn^2/V_s^2]^{1/4}$

3) $EHPn^2/\rho V_s^5 = [C_T Sn^2/V_s^2]$

4) $EHPn^7/\rho g^5 = (g^{-5})\ [C_T V_s^3 Sn^7]$

5) $[EHP^2 \rho^3/\mu^5 n]^{1/2} = (\nu^{-5/2})\ [C_T V_s^3 S/n^{1/2}]$.

The twelfth group, $[L_{ww}{}^{2}n\upsilon/C_T V_s{}^{2}S]$, is a function of the following five products:

1) $R_T/\underline{L}^2\mu n = (\upsilon^{-1})\ [C_T V_s{}^{2}S/\underline{L}^2 n]$
2) $R_T n/\mu V_s{}^{2} = (\upsilon^{-1})\ [C_T Sn]$
3) $R_T\rho/\mu^{2} = (\upsilon^{-2})\ [C_T V_s{}^{2}S]$
4) $EHP\mu^{1/2}/(nR_T{}^{3})^{1/2} = (\upsilon^{-1/2})\ [C_T Sn]^{1/2}$
5) $R_T n^{3}/\mu g^{2} = (g^{2}\upsilon)^{-1}\ [C_T V_s{}^{2}Sn^{3}]$.

The thirteenth group, $[L_{ww}{}^{4}n^{2}/C_T V_s{}^{2}S]$, is a function of the following five products:

1) $R_T/\underline{L}^4 n^2\rho = [C_T V_s{}^{2}S/\underline{L}^4 n^2]$
2) $R_T n^{2}/\rho V_s{}^{4} = [C_T Sn^{2}/V_s{}^{2}]$
3) $[EHP\rho^{1/4}/R_T{}^{5/4}n^{1/2}] = [C_T Sn^{2}/V_s{}^{2}]^{1/4}$
4) $R_T\rho/\mu^{2} = (\upsilon^{-2})\ [C_T V_s{}^{2}S]$
5) $R_T n^{6}/g^{4}\rho = (g^{-4})\ [C_T V_s{}^{2}Sn^{6}]$.

The fourteenth group, $[\upsilon g^{1/2} L_{ww}{}^{3/2}/C_T V_s{}^{2}S]$, is a function of the following five products:

1) $R_T/(\mu^{2}\underline{L}^3 g)^{1/2} = (\upsilon g^{1/2})^{-1}\ [C_T V_s{}^{2}S/\underline{L}^{3/2}]$
2) $R_T g/\mu V_s{}^{3} = (g/\upsilon)\ [C_T S/V_s]$
3) $R_T n^{3}/\mu g^{2} = (g^{2}\upsilon)^{-1}\ [C_T V_s{}^{2}Sn^{3}]$
4) $[EHP^{3}\mu/gR_T{}^{4}]^{1/3} = (g/\upsilon)^{1/3}\ [C_T S/V_s]^{1/3}$
5) $R_T\rho/\mu^{2} = (\upsilon^{-2})\ [C_T V_s{}^{2}S]$.

The fifteenth group, $[L_{ww}{}^3g/C_TV_s{}^2S]$, is a function of the following five products:

1) $R_T/\underline{L}^3\rho g = (g^{-1})\ [C_TV_s{}^2S/\underline{L}^3]$
2) $R_Tg^2/\rho V_s{}^6 = (g^2)\ [C_TS/V_s{}^4]$
3) $R_Tn^6/g^4\rho = (g^{-4})\ [C_TV_s{}^2Sn^6]$
4) $R_T\rho/\mu^2 = (\nu^{-2})\ [C_TV_s{}^2S]$
5) $[R_T{}^7g^2/EHP^6\rho]^{1/7} = (g^2)^{1/7}\ [C_TS/V_s{}^4]^{1/7}$.

The sixteenth group, $[L_{ww}{}^2g\nu/C_TV_s{}^3S]$, is a function of the following five products:

1) $EHP/\mu\underline{L}^2g = (\nu g)^{-1}\ [C_TV_s{}^3S/\underline{L}^2]$
2) $EHPg/\mu V_s{}^4 = (g/2\nu)\ [C_TS/V_s]$
3) $EHPn^4/\mu g^3 = (\nu g^3)^{-1}\ [C_TV_s{}^3Sn^4]$
4) $[EHP^3\rho^4/\mu^7g]^{1/4} = (\nu^7g)^{-1/4}[C_T{}^3V_s{}^9S^3]^{1/4}$
5) $[EHP^3\mu/gR_T{}^4]^{1/3} = (g/2\nu)^{1/3}\ [C_TS/V_s]^{1/3}$.

The seventeenth group, $[L_{ww}C_TV_s{}^3S/\nu^3]$, is a function of the following four products:

1) $EHP\rho^2\underline{L}/\mu^3 = (\nu^{-3})\ [\underline{L}C_TV_s{}^3S]$
2) $EHP\rho/\mu^2V_s = (\nu^{-2})\ [C_TV_s{}^2S]$
3) $[EHP^2\rho^3/\mu^5n]^{1/2} = (\nu^{-5/2})\ [C_TV_s{}^3Sn^{1/2}]$
4) $[\rho^4EHP^3/\mu^7g]^{1/4} = (\nu^7g)^{-1/4}[C_T{}^3V_s{}^9S^3]^{1/4}$.

The eighteenth group, $[L_{ww}^{7/2} g^{3/2} / C_T V_s^3 S]$, is a function of the following five products:

1) $\rho \underline{L}^{7/2} g^{3/2} / EHP = (g^{-3/2}) [C_T V_s^3 S / \underline{L}^{7/2}]$

2) $EHP g^2 / \rho V_s^7 = (g^2) [C_T S / V_s^4]$

3) $EHP n^7 / \rho g^5 = (g^{-5}) [C_T V_s^3 S n^7]$

4) $[R_T^7 g^2 / EHP b]^{1/7} = (g^2)^{1/7} [C_T S / V_s^4]^{1/7}$.

Appendix B

Dimensional Analysis

It was assumed that the length of the white-water wake generated by a vessel moving through the surface of a body of water could be related by some nondimensional product of unrelated variables. The significant variables that were available for the present analysis are listed and defined below (foot/pound/second system).

1)	L_{ww}	White-water wake length	(L)
2)	L_{wl}	Vessel waterline length	(L)
3)	B_{wl}	Vessel waterline beam	(L)
4)	D_{wl}	Midsection draft	(L)
5)	S	Wetted surface area	(L^2)
6)	∇	Displacement volume	(L^3)
7)	D_p	Propeller diameter	(L)
8)	D_T	Propeller tip to surface clearance	(L)
9)	V_s	Vessel Velocity	(L/T)
10)	n	Propeller revolutions per second	(L/T)
11)	EHP	Vessel effective horsepower	(ML^2/T^3)
12)	R_T	Total resistance	(ML/T^2)
13)	η_p	Propulsive efficiency	
14)	g	Gravitational acceleration	(L/T^2)
15)	μ	Absolute viscosity of seawater	(M/LT)
16)	ρ	Mass density of seawater	(M/L^3)

The complete dimensional analysis procedure will be outlined throughout the remainder of this Appendix. The variables L_{wl}, B_{wl}, D_{wl}, $S^{1/2}$, $\nabla^{1/3}$, D_p and D_T will be represented by L in the analysis. The fundamental dimensions that will be used are mass (M), length (L) and time (T). The maximum number of individual dimensionless parameters that could be formed with the given variables are listed below.

1) EHP V_s n $\underline{L}$

$$[ML^2T^{-3}]^a \quad [LT^{-1}]^b \quad [T^{-1}]^c \quad L = M^oL^oT^o$$

$a = 0 \qquad b = -1 \qquad c = 1$

$[\underline{L}n/V_s]$ Dimensionless group 1

2) EHP V_s g $\underline{L}$

$$[ML^2T^{-3}]^a \quad [LT^{-1}]^b \quad [LT^{-2}]^c \quad L = M^oL^oT^o$$

$a = 0 \qquad b = -2 \qquad c = 1$

$[\underline{L}\, g/V_s^2]$ Dimensionless group 2

3) EHP V_s μ $\underline{L}$

$$[ML^2T^{-3}]^a \quad [LT^{-1}]^b \quad [ML^{-1}T^{-1}]^c \quad L = M^oL^oT^o$$

$a = -1 \qquad b = 2 \qquad c = 1$

$[V_s^2 \mu\ \underline{L}\ /EHP]$ Dimensionless group 3

or

$(2\nu 550)^{-1}\ [C_T\ V_s\ S/\underline{L}]$

4) EHP V_s $\underline{L}$ ρ

$$[ML^2T^{-3}]^a \quad [LT^{-1}]^b \quad [L]^c \quad ML^{-3} = M^oL^oT^o$$

$a = -1 \qquad b = 3 \qquad c = 2$

$[V_s\ \rho\ \underline{L}^2/EHP]$ Dimensionless group 4

or

$(2(550))^{-1}\ [C_T\ S/\underline{L}^2]$

5) R_T V_s n $\underline{L}$ same as 1

6) R_T V_s g $\underline{L}$ same as 2

7) $R_T\ V_s\ \mu\ \underline{L}$

$$[MLT^{-2}]^a\ [LT^{-1}]^b\ [ML^{-1}T^{-1}]^c\ L = 0$$

$a = -1 \quad b = 1 \quad c = 1$

$[V_s\ \mu\ \underline{L}/R_T]$ dimensionless group 7

or

$(2\nu)^{-1}[C_T\ S\ V_s/\underline{L}]$

8) $R_T\ V_s\ \underline{L}\ \rho$

$$[MLT^{-2}]^a\ [LT^{-1}]^b\ [\ \ \ L^{-3} = M^oL^oT^o$$

$a = -1 \quad b = 2 \quad c = 2$

$[V_s^2\ \rho\ \underline{L}^2/R_T]$ Dimensionless group 8

or

$(2)^{-1}[C_T\ S/\underline{L}^2]$

9) $\mu\ V_s\ n\ \underline{L}$ same as 1

10) $\mu V_s\ g\ \underline{L}$ same as 2

11) $\mu\ V_s\ \rho\ \underline{L}$

$$[ML^{-1}T^{-1}]^a\ [LT^{-1}]^b\ [ML^{-3}]^c\ L = M^oL^oT^o$$

$a = -1 \quad b = 1 \quad c = 1$

$[V_s\ \rho\ \underline{L}/\mu]$ Dimensionless group 11

or

$[V_s\ \underline{L}/\gamma]$ Reynolds number

12) $\rho\ V_s\ n\ \underline{L}$ same as 1

13) $\rho\ V_s\ \underline{L}\ g$ same as 2

14) EHP $\underline{L}\ n\ g$

$$[ML^2T^{-3}]^a\ [L]^b\ [T^{-1}]^c\ LT^{-2} = M^oL^oT^o$$

$a = 0 \quad b = -1 \quad c = -2$

$[g/n^2\underline{L}]$ Dimensionless group 14

15) EHP $\underline{L}$ n μ

$$[ML^2T^{-3}]^a \; [L]^b \; [T^{-1}]^c \; ML^{-1}T^{-1} = M^oL^oT^o$$

$a = -1 \quad b = 3 \quad c = 2$

$[\mu n^2 \underline{L}^3/EHP]$ Dimensionless group 15

or

$(2\nu 550)^{-1} \; [C_T \; V_s^3 S/n^2 \underline{L}^3]$

16) EHP $\underline{L}$ n ρ

$$[ML^2T^{-3}]^a \; [L]^b \; [T^{-1}]^c \; ML^{-3} = M^oL^oT^o$$

$a = -1 \quad b = 5 \quad c = 3$

$[\rho \; n^3 \; \underline{L}^5/EHP]$ Dimensionless group 16

or

$(2(550))^{-1} [C_T \; V_s^3 S/n^3 \; \underline{L}^5]$

17) R_T $\underline{L}$ n EHP

$$[MLT^{-2}]^a \; [L]^b \; [T^{-1}]^c \; ML^2T^{-3} = M^oL^oT^o$$

$a = -1 \quad b = -1 \quad c = -1$

$[EHP/R_T \; \underline{L} \; n]$ Dimensionless group 17

or

$(550)^{-1} [V_s/n \; \underline{L}]$

18) R_T L n g same as 14

19) R_T $\underline{L}$ n μ

$$[MLT^{-2}]^a \; [L]^b \; [T^{-1}]^c \; ML^{-1}T^{-1} = M^oL^oT^o$$

$a = -1 \quad b = 2 \quad c = 1$

$[\mu \; \underline{L}^2 n/R_T]$ Dimensionless group 19

or

$(2\nu)^{-1} [C_T \; V_s^2 S/\underline{L}^2 \; n]$

20) μ $\underline{L}$ n EHP

$$[ML^{-1}T^{-1}]^{a} \quad [L]^{b} \quad [T^{-1}]^{c} \quad ML^{2}T^{-3} = M^{o}L^{o}T^{o}$$

$a = -1 \quad b = -3 \quad c = -2$

$[EHP/\mu \underline{L}^{3} n^{2}]$ Dimensionless group 20

or

$(2\nu 550)^{-1}[C_{T} V_{s}^{3} S/\underline{L}^{3} n^{2}]$

21) μ $\underline{L}$ n g same as 14

22) μ $\underline{L}$ n ρ

$$[ML^{-1}T^{-1}]^{a} \quad [L]^{b} \quad [T^{-1}]^{c} \quad ML^{-3} = M^{o}L^{o}T^{o}$$

$a = -1 \quad b = 2 \quad c = 1$

$[\rho \; n \; \underline{L}^{2}/\mu]$ Dimensionless group 22

or

$(\nu)^{-1} \; [n \; \underline{L}^{2}]$

23) ρ $\underline{L}$ n R_{T}

$$[ML^{-3}]^{a} \quad [L]^{b} \quad [T^{-1}]^{C} \quad MLT^{-2} = M^{o}L^{o}T^{o}$$

$a = -1 \quad b = -4 \quad c = -2$

$[R_{T}/\rho \; n^{2} \; \underline{L}^{4}]$ Dimensionless group 23

or

$(2)^{-1}[C_{T} V_{s}^{2} S/n^{2} \; \underline{L}^{4}]$

24) ρ $\underline{L}$ n g Same as 14

25) EHP $\underline{L}$ g R_{T}

$$[ML^{2}T^{-3}]^{a} \quad [L]^{b} \quad [LT^{-2}]^{c} \quad MLT^{-2} = M^{o}L^{o}T^{o}$$

$a = -1 \quad b = 1/2 \quad c = 1/2$

$[R_{T} \; \underline{L}^{1/2} \; g^{1/2} \; /EHP]$ Dimensionless group 25

or

$(550)^{-1}[V_{s}/(g \; \underline{L})^{1/2}]$

26) EHP $\underline{L}$ μ R_T

$$[ML^2T^{-3}]^a \; [L]^b \; [ML^{-1}T^{-1}]^c \; MLT^{-2} = M^oL^oT^o$$

$a = -1/2 \quad b = -1/2 \quad c = -1/2$

$[R_T^2/(EHP\ \underline{L}\ \mu)]^{1/2}$ Dimensionless group 26

or

$(550/2\nu)^{1/2} \; [C_T \; V_s \; S/\underline{L}]^{1/2}$

27) EHP $\underline{L}$ ρ R_T

$$[ML^2T^{-3}]^a \; [L]^b \; [ML^{-3}]^c \; MLT^{-2} = M^oL^oT^o$$

$a = -2/3 \quad b = 2/3 \quad c = -1/3$

$[R_T^3/(\rho \; \underline{L}^2 \; EHP^2)]^{1/3}$ Dimensionless group 27

or $(550^2/2)^{1/3} \; [C_T \; S/\underline{L}^2]^{1/3}$

28) μ $\underline{L}$ R_T EHP

$$[ML^{-1}T^{-1}]^a \; [L]^b \; [MLT^{-2}]^c \; ML^{-2}T^{-3} = M^oL^oT^o$$

$a = 1 \quad b = 1 \quad c = -2$

$[\mu \; \underline{L} \; EHP/R_T^2]$ Dimensionless Ratio 28

or

$(550/2\nu) \; [C_T \; V_s \; S/\underline{L}]$

29) μ $\underline{L}$ g R_T

$$[ML^{-1}T^{-1}]^a \; [L]^b \; [LT^{-2}]^c \; MLT^{-2} = M^oL^oT^o$$

$a = -1 \quad b = -3/2 \quad c = -1/2$

$[R_T/(\mu^2 \; \underline{L}^3 \; g)^{1/2}]$ Dimensionless group 29

or

$(2\nu g^{1/2})^{-1} \; [C_T V_s^2 \; S/\underline{L}^{3/2}]$

30) μ $\underline{L}$ R_T ρ

$$[ML^{-1}T^{-1}]^{a} \quad [L]^{b} \quad [MLT^{-2}]^{c} \quad ML^{-3} = M^{o}L^{o}T^{o}$$

$a = -2 \quad b = 0 \quad c = 1$

$[R_T \rho / \mu^2]$ Dimensionless group 30

or

$(2\nu^2)^{-1} [C_T V_s^2 S]$

31) ρ $\underline{L}$ R_T EHP

$$[ML^{-3}]^{a} \quad [L]^{b} \quad [MLT^{-2}]^{c} \quad ML^{2}T^{-3} = M^{o}L^{o}T^{o}$$

$a = 1/2 \quad b = 1 \quad c = -3/2$

$[\rho^{1/2} \underline{L} \, EHP / R_T^{3/2}]$ Dimensionless group 31

or

$(550/2^{1/2}) [C_T^{1/2} S^{1/2} / \underline{L}]$

32) ρ $\underline{L}$ g R_T

$$[ML^{-3}]^{a} \quad [L]^{b} \quad [LT^{-2}]^{c} \quad MLT^{-2} = M^{o}L^{o}T^{o}$$

$a = -1 \quad b = -3 \quad c = -1$

$[R_T / \rho \underline{L}^3 g]$ Dimensionless group 32

or

$(2g)^{-1} [C_T V_s^2 S / \underline{L}^3]$

33) μ $\underline{L}$ g EHP

$$[ML^{-1}T^{-1}]^{a} \quad [L]^{b} \quad [LT^{-2}]^{c} \quad ML^{2}T^{-3} = M^{o}L^{o}T^{o}$$

$a = -1 \quad b = -2 \quad c = -1$

$[EHP / \mu \underline{L}^2 g]$ Dimensionless group 33

or

$(2(550) g \nu)^{-1} [V_s^3 S C_T / \underline{L}^2]$

34) μ $\underline{L}$ EHP ρ

$$[ML^{-1}T^{-1}]^{a} \quad [L]^{b} \quad [ML^{2}T^{-3}]^{c} \quad ML^{-3} = M^{o}L^{o}T^{o}$$

$a = -3/2 \quad b = 1/2 \quad c = 1/2$

$$[\rho^{2}\underline{L}\ EHP/\ \mu^{3}]^{1/2}$$ Dimensionless group 34

or

$$(2(550)\nu^{3})^{-1/2}\ [C_{T}S\ V_{s}^{3}\ \underline{L}]^{1/2}$$

35) ρ $\underline{L}$ g EHP

$$[ML^{-3}]^{a} \quad [L]^{b} \quad [LT^{-2}]^{c} \quad ML^{2}T^{-3} = M^{o}L^{o}T^{o}$$

$a = -1 \quad b = -7/2 \quad c = -3/2$

$$[EHP/\rho\ \underline{L}^{7/2}\ g^{3/2}]$$ Dimensionless group 35

or

$$(2(550)g^{3/2})^{-1}\ [C_{T}\ V_{s}^{3}S/L^{7/2}]$$

36) μ $\underline{L}$ g ρ

$$[ML^{-1}T^{-1}]^{a} \quad [L]^{b} \quad [LT^{-2}]^{c} \quad ML^{-3} = M^{o}L^{o}T^{o}$$

$a = -1 \quad b = 3/2 \quad c = 1/2$

$$[\rho\ \underline{L}^{3/2}\ g^{1/2}/\mu\ ]$$ Dimensionless group 36

or

$$(g^{1/2}/\nu)\ \ [\underline{L}^{3/2}]$$

37) EHP V_s n g

$$[ML^{2}T^{-3}]^{a} \quad [LT^{-1}]^{b} \quad [T^{-1}]^{c} \quad LT^{-2} = M^{o}L^{o}T^{o}$$

$a = 0 \quad b = -1 \quad c = -1$

$$[g/V_{s}\ n]$$ Dimensionless group 37

38) EHP V_s n μ

$$[ML^2T^{-3}]^a \quad [LT^{-1}]^b \quad [T^{-1}]^c \quad ML^{-1}T^{-1} = M^oL^oT^o$$

$$a = -1 \qquad b = 3 \qquad c = -1$$

$[\mu \; V_s^3/EHP \; n]$ Dimensionless group 38

or

$(2(550)\nu)^{-1}[C_T \; S \; n]$

39) EHP V_s n ρ

$$[ML^2T^{-3}]^a \quad [LT^{-1}]^b \quad [T^{-1}]^c \quad ML^{-3} = M^oL^oT^o$$

$$a = -1 \qquad b = 5 \qquad c = -2$$

$[\rho \; V_s^5/EHP \; n^2]$ Dimensionless group 39

or

$(2(550))^{-1} \; [C_T \; S \; n^2/V_s^2]$

40) R_T V_s n g same as 37

41) R_T V_s n μ

$$[MLT^{-2}]^a \quad [LT^{-1}]^b \quad [T^{-1}]^c \quad ML^{-1}T^{-1} = M^oL^oT^o$$

$$a = -1 \qquad b = 2 \qquad c = -1$$

$[\mu \; V_s^2/R_T \; n]$ Dimensionless group 41

or

$(2\nu)^{-1}[C_T \; S \; n]$

42) R_T V_s n ρ

$$[MLT^{-2}]^a \quad [LT^{-1}]^b \quad [T^{-1}]^c \quad ML^{-3} = M^oL^oT^o$$

$$a = -1 \qquad b = 4 \qquad c = -2$$

$[\rho \; V_s^4/R_T \; n^2]$ Dimensionless group 42

or

$(2)^{-1}[C_T \; S \; r^2/V_s^2]$

43) g V_s n ρ same as 37

44) $\rho\ V_s\ n\ \mu$

$$[ML^{-3}]^{a}\quad [LT^{-1}]^{b}\quad [T^{-1}]^{c}\quad ML^{-1}T^{-1} = M^{o}L^{o}T^{o}$$

$a = -1 \quad b = -2 \quad c = 1$

$[\mu\ n/V_s^{2}\ \rho]$ Dimensionless group 44

or

$\nu[n/V_s^{2}]$

45) $g\ V_s\ n\ \mu$ same as 37

46) $\mu\ V_s\ g$ EHP

$$[ML^{-1}T^{-1}]^{a}\quad [LT^{-1}]^{b}\quad [LT^{-2}]^{c}\quad ML^{2}T^{-3} = M^{o}L^{o}T^{o}$$

$a = -1 \quad b = -4 \quad c = 1$

$[EHP\ g/\mu\ V_s^{4}]$ Dimensionless group 46

or

$(g/2\ \nu\ 550)\ [C_T\ S/V_s]$

47) $\mu\ V_s\ \rho$ EHP

$$[ML^{-1}T^{-1}]^{a}\quad [LT^{-1}]^{b}\quad [ML^{-3}]^{c}\quad ML^{2}T^{-3} = M^{o}L^{o}T^{o}$$

$a = -2 \quad b = -1 \quad c = 1$

$[EHP\ \rho/\mu^{2}\ V_s]$ Dimensionless group 47

or

$(2(550)\nu^{2})^{-1}\ [C_T\ V_s^{2}\ S]$

48) EHP $g\ V_s\ \rho$

$$[ML^{2}T^{-3}]^{a}\quad [LT^{-2}]^{b}\quad [LT^{-1}]^{c}\quad ML^{-3} = M^{o}L^{o}T^{o}$$

$a = -1 \quad b = -2 \quad c = 7$

$[\rho\ V_s^{7}/EHP\ g^{2}]$ Dimensionless group 48

or

$(g^{2}/2(550))\ [C_T\ S/V_s^{4}]$

49) $\mu\ V_s\ g\ R_T$

$[ML^{-1}T^{-1}]^a \quad [LT^{-1}]^b \quad [LT^{-2}]^c \quad MLT^{-2} = M^oL^oT^o$

$a = -1 \quad b = -3 \quad c = 1$

$[R_T\ g/\mu\ V_s^3]$ Dimensionless group 49

or

$(g/2\nu)\ [C_T\ S/V_s]$

50) $\mu\ V_s\ \rho\ R_T$ Same as 30

51) $\rho\ V_s\ g\ R_T$

$[ML^{-3}]^a \quad [LT^{-1}]^b \quad [LT^{-2}]^c \quad MLT^{-2} = M^oL^oT^o$

$a = -1 \quad b = -6 \quad c = 2$

$[R_T\ g^2/\rho\ V_s^6]$ Dimensionless group 51

or

$(g^2/2)\ [C_T\ S/V_s^4]$

52) $\rho\ V_s\ g\ \mu$

$[ML^{-3}]^a \quad [LT^{-1}]^b \quad [LT^{-2}]^c \quad ML^{-1}T^{-1} = M^oL^oT^o$

$a = -1 \quad b = -3 \quad c = 1$

$[\mu\ g/\rho\ V_s^3]$ Dimensionless group 52

or

$(\nu g)^{-1}\ [V_s^3]$

53) $R_T\ n\ g\ EHP$

$[MLT^{-2}]^a \quad [T^{-1}]^b \quad [LT^{-2}]^c \quad ML^2T^{-3} = M^oL^oT^o$

$a = -1 \quad b = 1 \quad c = -1$

$[EHP\ n/R_T\ g]$ Dimensionless group 53

or

$(550)^{-1}\ [V_s\ n/g]$

54) R_T n μ EHP

$$[MLT^{-2}]^{a} \quad [T^{-1}]^{b} \quad [ML^{-1}T^{-1}]^{c} \quad ML^2T^{-3} = M^oL^oT^o$$

$a = -3/2 \quad b = -1/2 \quad c = 1/2$

$$[EHP\ \mu^{1/2}/(n\ R_T^3)^{1/2}] \qquad \text{Dimensionless group 54}$$

or

$$(550/(2\nu)^{1/2})\ [n\ C_T\ S]^{1/2}$$

55) μ n ρ EHP

$$[ML^{-1}T^{-1}]^{a} \quad [T^{-1}]^{b} \quad [ML^{-3}]^{c} \quad ML^2T^{-3} = M^oL^oT^o$$

$a = -5/2 \quad b = -1/2 \quad c = 3/2$

$$[EHP^2\rho^3/\mu^5 n]^{1/2} \qquad \text{Dimensionless group 55}$$

or

$$(\nu^{5/2}(550)2)^{-1}\ [C_T\ V_s^3 S/n^{1/2}]$$

56) R_T n ρ EHP

$$[MLT^{-2}]^{a} \quad [T^{-1}]^{b} \quad [ML^{-3}]^{c} \quad ML^2T^{-3} = M^oL^oT^o$$

$a = -5/4 \quad b = -2/4 \quad c = 1/4$

$$[EHP\ \rho^{1/4}/R_T^{5/4}\ n^{1/2}] \qquad \text{Dimensionless group 56}$$

or

$$550\ [C_T\ S\ n/2V_s^2]^{1/4}$$

57) μ n g EHP

$$[ML^{-1}T^{-1}]^{a} \quad [T^{-1}]^{b} \quad [LT^{-2}]^{c} \quad ML^2T^{-3} = M^oL^oT^o$$

$a = -1 \quad b = 4 \quad c = -3$

$$[EHP\ n^4/\mu\ g^3] \qquad \text{Dimensionless group 57}$$

or

$$(2\nu(550)g^3)^{-1}\ [C_T\ V_s^3\ S\ n^4]$$

58) ρ n g EHP

$$[ML^{-3}]^{a} \quad [T^{-1}]^{b} \quad [LT^{-2}]^{c} \quad ML^{2}T^{-3} = M^{o}L^{o}T^{o}$$

a = -1 b = 7 c = -5

$[EHP\ n^{7}/\rho\ g^{5}]$ Dimensionless group 58

or

$$(2(55)g^{5})^{-1} \quad [C_T\ V_s^{3}\ S\ n^{7}]$$

59) μ n g R_T

$$[ML^{-1}T^{-1}]^{a} \quad [T^{-1}]^{b} \quad [LT^{-2}]^{c} \quad MLT^{-2} = M^{o}L^{o}T^{o}$$

a = -1 b = 3 c = -2

$[R_T\ n^{3}/\mu\ g^{2}]$ Dimensionless group 59

or

$$(2g^{2}\nu)^{-1} \quad [C_T\ S\ V_s^{2}\ n^{3}]$$

60) μ n ρ R_T Sames as 30

61) ρ n g R_T

$$[ML^{-3}]^{a} \quad [T^{-1}]^{b} \quad [LT^{-2}]^{c} \quad MLT^{-2} = M^{o}L^{o}T^{o}$$

a = -1 b = 6 c = -4

$[R_T\ n^{6}/g^{4}\ \rho]$ Dimensionless group 61

or

$$(2g^{4})^{-1} \quad [C_T\ S\ V_s^{2}\ n^{6}]$$

62) ρ n g μ

$$[ML^{-3}]^{a} \quad [T^{-1}]^{b} \quad [LT^{-2}]^{c} \quad ML^{-1}T^{-1} = M^{o}L^{o}T^{o}$$

a = -1 b = 3 c = -2

$[\mu\ n^{3}/\rho^{2}\ g\ ]$ Dimensionless group 62

or

$$(\nu/g^{2}) \quad [n^{3}]$$

63) μ g R_T EHP

$$[ML^{-1}T^{-1}]^{a} \quad [LT^{-2}]^{b} \quad [MLT^{-2}]^{c} \quad ML^{2}T^{-3} = M^{o}L^{o}T^{o}$$

$a = 1/3 \quad b = -1/3 \quad c = -4/3$

$$[EHP^{3}\,\mu/g\,R_T^{4}]^{1/3}$$ Dimensionless group 63

or

$$550\,(g/2\nu)^{1/3}\,[C_T\,S/V_s]^{1/3}$$

64) ρ g EHP R_T

$$[ML^{-3}]^{a} \quad [LT^{-2}]^{b} \quad [ML^{2}T^{-3}]^{c} \quad MLT^{-2} = M^{o}L^{o}T^{o}$$

$a = -1/7 \quad b = 2/7 \quad c = -6/7$

$$[R_T^{7}\,g^{2}/EHP^{6}\,\rho]^{1/7}$$ Dimensionless group 64

or

$$((550)^{6}\,g^{2}/2)^{1/7}\,[C_T\,S/V_s^{4}]^{1/7}$$

65) μ g EHP ρ

$$[ML^{-1}T^{-1}]^{a} \quad [LT^{-2}]^{b} \quad [ML^{2}T^{-3}]^{c} \quad ML^{-3} = M^{o}L^{o}T^{o}$$

$a = -7/4 \quad b = -1/4 \quad c = 3/4$

$$[\rho^{4}\,EHP^{3}/\mu^{7}\,g]^{1/4}$$ Dimensionless group 65

or

$$((2)^{3}(550)^{3}\,\nu^{7}\,g)^{-1/4}\,[V_s^{9}\,S^{3}\,C_T^{3}]^{1/4}$$

66) μ g R_T ρ Same as 30

APPENDIX C — Individual Data Sets

DATA POINT NUMBER	SHIP CLASS	[illegible]	[illegible]	[illegible]	[illegible]	[illegible]	[illegible]	[illegible]	[illegible]	[illegible]	[illegible]	[illegible]	SHP	C_p	C_f	[illegible]	[illegible]	[illegible]
1	CV18	214E+04	214E+04	[illegible]	[illegible]	[illegible]	[illegible]	[illegible]	[illegible]	[illegible]	[illegible]	[illegible]	[illegible]	177E-02	250E-02	[illegible]	227E+05	[illegible]
2	CV16	[illegible]	[illegible]	[illegible]	[illegible]	[illegible]	[illegible]	[illegible]	[illegible]	[illegible]	[illegible]	[illegible]	[illegible]	177E-02	[illegible]	[illegible]	227E+05	[illegible]
3	CV6	[illegible]	[illegible]	770E+03	[illegible]	[illegible]	[illegible]	[illegible]	133E+02	[illegible]	[illegible]	[illegible]	[illegible]	[illegible]	[illegible]	[illegible]	[illegible]	[illegible]
4	CV3	342E+04	342E+04	[illegible]	[illegible]	[illegible]	342E+03	.111E+03	[illegible]	[illegible]	371E+02	312E+01	[illegible]	177E-02	[illegible]	[illegible]	[illegible]	[illegible]
5	CV6	[illegible]	[illegible]	770E+03	[illegible]	[illegible]	[illegible]	[illegible]	.130E+02	[illegible]	[illegible]	325E+01	[illegible]	[illegible]	[illegible]	[illegible]	177E+05	[illegible]
6	CV	.177E+04	[illegible]	[illegible]	[illegible]	[illegible]	[illegible]	[illegible]	[illegible]	[illegible]	[illegible]	270E+01	205E+05	[illegible]	[illegible]	[illegible]	.217E+05	[illegible]
7	CA	[illegible]	[illegible]	[illegible]	[illegible]	[illegible]	[illegible]	.718E+02	[illegible]	[illegible]	[illegible]	[illegible]	114E+05	[illegible]	[illegible]	[illegible]	.115E+05	[illegible]
8	CL	[illegible]	[illegible]	[illegible]	[illegible]	.227E+02	219E+03	[illegible]	[illegible]	[illegible]	[illegible]	[illegible]	[illegible]	[illegible]	[illegible]	[illegible]	125E+05	[illegible]
9	CL	.315E+04	315E+04	[illegible]	[illegible]	227E+02	[illegible]	[illegible]	[illegible]	[illegible]	[illegible]	[illegible]	[illegible]	[illegible]	[illegible]	[illegible]	125E+05	[illegible]
10	CL	178E+04	178E+04	[illegible]	[illegible]	227E+02	[illegible]	[illegible]	[illegible]	[illegible]	[illegible]	[illegible]	[illegible]	[illegible]	[illegible]	[illegible]	[illegible]	[illegible]
11	CL	[illegible]	[illegible]	[illegible]	[illegible]	.227E+02	[illegible]	[illegible]	[illegible]	[illegible]	[illegible]	[illegible]	[illegible]	[illegible]	[illegible]	[illegible]	125E+05	[illegible]
12	[illegible]	.321E+04	[illegible]	[illegible]	[illegible]	[illegible]	[illegible]	.124E+03	[illegible]	.130E+02	[illegible]	.217E+01	[illegible]	.177E-02	[illegible]	[illegible]	[illegible]	[illegible]
13	[illegible]	[illegible]	[illegible]	[illegible]	[illegible]	345E+02	[illegible]	124E+03	[illegible]	.130E+02	[illegible]	[illegible]	[illegible]	.177E-02	[illegible]	[illegible]	[illegible]	[illegible]
14	DD	.325E+04	325E+04	[illegible]	[illegible]	143E+02	[illegible]	[illegible]	.115E+02	[illegible]	330E+02	[illegible]	[illegible]	[illegible]	[illegible]	625E+00	[illegible]	754E+05
15	DD	[illegible]	[illegible]	[illegible]	[illegible]	143E+02	[illegible]	[illegible]	[illegible]	[illegible]	270E+02	[illegible]	[illegible]	[illegible]	375E-02	[illegible]	[illegible]	477E+05
16	DD	[illegible]	[illegible]	[illegible]	[illegible]	143E+02	[illegible]	[illegible]	.115E+02	[illegible]	.422E+02	427E+01	[illegible]	[illegible]	[illegible]	[illegible]	[illegible]	[illegible]
17	DD	[illegible]	[illegible]	[illegible]	[illegible]	142E+02	132E+03	[illegible]	.115E+02	[illegible]	[illegible]	[illegible]	[illegible]	[illegible]	[illegible]	[illegible]	[illegible]	[illegible]
18	DD	[illegible]	[illegible]	[illegible]	[illegible]	143E+02	[illegible]	[illegible]	.115E+02	[illegible]	[illegible]	[illegible]	[illegible]	[illegible]	[illegible]	[illegible]	[illegible]	[illegible]
19	DD	[illegible]	154E+04	[illegible]	[illegible]	143E+02	[illegible]	[illegible]	.115E+02	[illegible]	[illegible]	[illegible]	[illegible]	[illegible]	[illegible]	[illegible]	[illegible]	[illegible]
20	DD	[illegible]	[illegible]	[illegible]	[illegible]	143E+02	[illegible]	[illegible]	115E+02	[illegible]	[illegible]	[illegible]	[illegible]	[illegible]	[illegible]	[illegible]	[illegible]	[illegible]
21	DD	[illegible]	[illegible]	[illegible]	[illegible]	143E+02	[illegible]	[illegible]	.115E+02	[illegible]	[illegible]	[illegible]	[illegible]	[illegible]	[illegible]	[illegible]	[illegible]	[illegible]
22	DD	[illegible]	[illegible]	[illegible]	[illegible]	[illegible]	[illegible]	[illegible]	.115E+02	[illegible]	.422E+02	[illegible]	[illegible]	[illegible]	[illegible]	[illegible]	[illegible]	[illegible]
23	DD	173E+04	[illegible]	[illegible]	[illegible]	[illegible]	[illegible]	[illegible]	.115E+02	[illegible]	[illegible]	[illegible]	[illegible]	[illegible]	[illegible]	[illegible]	[illegible]	[illegible]
24	DD	164E+04	[illegible]	[illegible]	[illegible]	[illegible]	[illegible]	[illegible]	[illegible]	[illegible]	[illegible]	[illegible]	[illegible]	[illegible]	[illegible]	[illegible]	[illegible]	[illegible]
25	DD	[illegible]	[illegible]	[illegible]	[illegible]	[illegible]	[illegible]	[illegible]	[illegible]	[illegible]	[illegible]	325E+01	[illegible]	[illegible]	[illegible]	[illegible]	[illegible]	754E+05
26	AKA	[illegible]	[illegible]	[illegible]	[illegible]	[illegible]	[illegible]	[illegible]	[illegible]	[illegible]	[illegible]	[illegible]	[illegible]	[illegible]	[illegible]	[illegible]	[illegible]	[illegible]
27	AKA	[illegible]	[illegible]	[illegible]	[illegible]	[illegible]	[illegible]	[illegible]	[illegible]	[illegible]	[illegible]	[illegible]	[illegible]	[illegible]	[illegible]	[illegible]	[illegible]	[illegible]
28	AKA	770E+03	.770E+03	[illegible]	[illegible]	[illegible]	[illegible]	[illegible]	[illegible]	[illegible]	[illegible]	[illegible]	[illegible]	[illegible]	[illegible]	[illegible]	[illegible]	[illegible]
29	AKA	[illegible]	[illegible]	[illegible]	[illegible]	[illegible]	[illegible]	[illegible]	[illegible]	[illegible]	[illegible]	[illegible]	[illegible]	[illegible]	[illegible]	[illegible]	[illegible]	[illegible]
30	AE	777E+03	[illegible]	[illegible]	[illegible]	[illegible]	[illegible]	[illegible]	[illegible]	[illegible]	[illegible]	[illegible]	[illegible]	[illegible]	[illegible]	[illegible]	[illegible]	[illegible]
31	AO	[illegible]	[illegible]	[illegible]	[illegible]	[illegible]	[illegible]	[illegible]	[illegible]	[illegible]	[illegible]	[illegible]	[illegible]	[illegible]	275E-02	[illegible]	[illegible]	[illegible]
32	AO	[illegible]	[illegible]	[illegible]	[illegible]	[illegible]	[illegible]	[illegible]	[illegible]	[illegible]	[illegible]	[illegible]	[illegible]	[illegible]	[illegible]	[illegible]	[illegible]	[illegible]
33	SS	[illegible]	[illegible]	[illegible]	270E+02	[illegible]	.112E+03	[illegible]	[illegible]	[illegible]	[illegible]	[illegible]	[illegible]	[illegible]	[illegible]	[illegible]	[illegible]	[illegible]
34	SS	[illegible]	[illegible]	[illegible]	270E+02	[illegible]	.112E+03	[illegible]	[illegible]	[illegible]	[illegible]	[illegible]	[illegible]	[illegible]	[illegible]	[illegible]	[illegible]	[illegible]

DATA POINT NUMBER	SHIP CLASS	L	L	L	B	D	S	V	B	B	V	RPS	EHP	C	C	[illegible]	R	R
35	SS	[illegible]	[illegible]	[illegible]	[illegible]	[illegible]	[illegible]	[illegible]	[illegible]	[illegible]	[illegible]	[illegible]	[illegible]	[illegible]	[illegible]	[illegible]	[illegible]	[illegible]
36	SS	[illegible]	[illegible]	[illegible]	[illegible]	[illegible]	[illegible]	[illegible]	[illegible]	[illegible]	[illegible]	[illegible]	[illegible]	[illegible]	[illegible]	[illegible]	[illegible]	[illegible]
37	SS	[illegible]	[illegible]	[illegible]	[illegible]	[illegible]	[illegible]	[illegible]	[illegible]	[illegible]	[illegible]	[illegible]	[illegible]	[illegible]	[illegible]	[illegible]	[illegible]	[illegible]
38	SS	[illegible]	[illegible]	[illegible]	[illegible]	[illegible]	[illegible]	[illegible]	[illegible]	[illegible]	[illegible]	[illegible]	[illegible]	[illegible]	[illegible]	[illegible]	[illegible]	[illegible]
39	LO	[illegible]	[illegible]	[illegible]	[illegible]	[illegible]	[illegible]	[illegible]	[illegible]	[illegible]	[illegible]	[illegible]	[illegible]	[illegible]	[illegible]	[illegible]	[illegible]	[illegible]
40	LO	[illegible]	[illegible]	[illegible]	[illegible]	[illegible]	[illegible]	[illegible]	[illegible]	[illegible]	[illegible]	[illegible]	[illegible]	[illegible]	[illegible]	[illegible]	[illegible]	[illegible]
41	LO	[illegible]	[illegible]	[illegible]	[illegible]	[illegible]	[illegible]	[illegible]	[illegible]	[illegible]	[illegible]	[illegible]	[illegible]	[illegible]	[illegible]	[illegible]	[illegible]	[illegible]
42	LO	[illegible]	[illegible]	[illegible]	[illegible]	[illegible]	[illegible]	[illegible]	[illegible]	[illegible]	[illegible]	[illegible]	[illegible]	[illegible]	[illegible]	[illegible]	[illegible]	[illegible]
43	LO	[illegible]	[illegible]	[illegible]	[illegible]	[illegible]	[illegible]	[illegible]	[illegible]	[illegible]	[illegible]	[illegible]	[illegible]	[illegible]	[illegible]	[illegible]	[illegible]	[illegible]
44	LO	[illegible]	[illegible]	[illegible]	[illegible]	[illegible]	[illegible]	[illegible]	[illegible]	[illegible]	[illegible]	[illegible]	[illegible]	[illegible]	[illegible]	[illegible]	[illegible]	[illegible]
45	LO	[illegible]	[illegible]	[illegible]	[illegible]	[illegible]	[illegible]	[illegible]	[illegible]	[illegible]	[illegible]	[illegible]	[illegible]	[illegible]	[illegible]	[illegible]	[illegible]	[illegible]
46	LO	[illegible]	[illegible]	[illegible]	[illegible]	[illegible]	[illegible]	[illegible]	[illegible]	[illegible]	[illegible]	[illegible]	[illegible]	[illegible]	[illegible]	[illegible]	[illegible]	[illegible]
47	LO	[illegible]	[illegible]	[illegible]	[illegible]	[illegible]	[illegible]	[illegible]	[illegible]	[illegible]	[illegible]	[illegible]	[illegible]	[illegible]	[illegible]	[illegible]	[illegible]	[illegible]
48	LO	[illegible]	[illegible]	[illegible]	[illegible]	[illegible]	[illegible]	[illegible]	[illegible]	[illegible]	[illegible]	[illegible]	[illegible]	[illegible]	[illegible]	[illegible]	[illegible]	[illegible]
49	LO	[illegible]	[illegible]	[illegible]	[illegible]	[illegible]	[illegible]	[illegible]	[illegible]	[illegible]	[illegible]	[illegible]	[illegible]	[illegible]	[illegible]	[illegible]	[illegible]	[illegible]
50	LO	[illegible]	[illegible]	[illegible]	[illegible]	[illegible]	[illegible]	[illegible]	[illegible]	[illegible]	[illegible]	[illegible]	[illegible]	[illegible]	[illegible]	[illegible]	[illegible]	[illegible]
51	LO	[illegible]	[illegible]	[illegible]	[illegible]	[illegible]	[illegible]	[illegible]	[illegible]	[illegible]	[illegible]	[illegible]	[illegible]	[illegible]	[illegible]	[illegible]	[illegible]	[illegible]
52	LO	[illegible]	[illegible]	[illegible]	[illegible]	[illegible]	[illegible]	[illegible]	[illegible]	[illegible]	[illegible]	[illegible]	[illegible]	[illegible]	[illegible]	[illegible]	[illegible]	[illegible]
53	LST	[illegible]	[illegible]	[illegible]	[illegible]	[illegible]	[illegible]	[illegible]	[illegible]	[illegible]	[illegible]	[illegible]	[illegible]	[illegible]	[illegible]	[illegible]	[illegible]	[illegible]
54	LST	[illegible]	[illegible]	[illegible]	[illegible]	[illegible]	[illegible]	[illegible]	[illegible]	[illegible]	[illegible]	[illegible]	[illegible]	[illegible]	[illegible]	[illegible]	[illegible]	[illegible]
55	LST	[illegible]	[illegible]	[illegible]	[illegible]	[illegible]	[illegible]	[illegible]	[illegible]	[illegible]	[illegible]	[illegible]	[illegible]	[illegible]	[illegible]	[illegible]	[illegible]	[illegible]
56	LST	[illegible]	[illegible]	[illegible]	[illegible]	[illegible]	[illegible]	[illegible]	[illegible]	[illegible]	[illegible]	[illegible]	[illegible]	[illegible]	[illegible]	[illegible]	[illegible]	[illegible]
57	LST	[illegible]	[illegible]	[illegible]	[illegible]	[illegible]	[illegible]	[illegible]	[illegible]	[illegible]	[illegible]	[illegible]	[illegible]	[illegible]	[illegible]	[illegible]	[illegible]	[illegible]
58	LST	[illegible]	[illegible]	[illegible]	[illegible]	[illegible]	[illegible]	[illegible]	[illegible]	[illegible]	[illegible]	[illegible]	[illegible]	[illegible]	[illegible]	[illegible]	[illegible]	[illegible]
59	LST	[illegible]	[illegible]	[illegible]	[illegible]	[illegible]	[illegible]	[illegible]	[illegible]	[illegible]	[illegible]	[illegible]	[illegible]	[illegible]	[illegible]	[illegible]	[illegible]	[illegible]
60	LST	[illegible]	[illegible]	[illegible]	[illegible]	[illegible]	[illegible]	[illegible]	[illegible]	[illegible]	[illegible]	[illegible]	[illegible]	[illegible]	[illegible]	[illegible]	[illegible]	[illegible]
61	LST	[illegible]	[illegible]	[illegible]	[illegible]	[illegible]	[illegible]	[illegible]	[illegible]	[illegible]	[illegible]	[illegible]	[illegible]	[illegible]	[illegible]	[illegible]	[illegible]	[illegible]
62	YMS	[illegible]	[illegible]	[illegible]	[illegible]	[illegible]	[illegible]	[illegible]	[illegible]	[illegible]	[illegible]	[illegible]	[illegible]	[illegible]	[illegible]	[illegible]	[illegible]	[illegible]
63	SC	[illegible]	[illegible]	[illegible]	[illegible]	[illegible]	[illegible]	[illegible]	[illegible]	[illegible]	[illegible]	[illegible]	[illegible]	[illegible]	[illegible]	[illegible]	[illegible]	[illegible]
64	SC	[illegible]	[illegible]	[illegible]	[illegible]	[illegible]	[illegible]	[illegible]	[illegible]	[illegible]	[illegible]	[illegible]	[illegible]	[illegible]	[illegible]	[illegible]	[illegible]	[illegible]
65	LCU	[illegible]	[illegible]	[illegible]	[illegible]	[illegible]	[illegible]	[illegible]	[illegible]	[illegible]	[illegible]	[illegible]	[illegible]	[illegible]	[illegible]	[illegible]	[illegible]	[illegible]
66	FER	[illegible]	[illegible]	[illegible]	[illegible]	[illegible]	[illegible]	[illegible]	[illegible]	[illegible]	[illegible]	[illegible]	[illegible]	[illegible]	[illegible]	[illegible]	[illegible]	[illegible]
67	GSS	[illegible]	[illegible]	[illegible]	[illegible]	[illegible]	[illegible]	[illegible]	[illegible]	[illegible]	[illegible]	[illegible]	[illegible]	[illegible]	[illegible]	[illegible]	[illegible]	[illegible]

Naval Research Laboratory
Technical Library
Research Reports Section

DATE: February 9, 2004

FROM: **Mary Templeman**, Code 5596.3

TO: **Code 7200 Lee Rickard**

C: Tina Smallwood, Code 1221.1 ts 2/11/04

SUBJ: Review of NRL Report

Dear Sir/Madam:

Please review NRL Memo Report 5335 for:

☑ Possible Distribution Statement change To "A"
☐ Possible Change in Classification

Thank you,

Mary Templeman
(202)767-3425
maryt@library.nrl.navy.mil

The subject report can be:

☑ Changed to Distribution A (Unlimited)
☐ Changed to Classification _____
☐ Other:

L Rickard 2/9/04
Signature Date